ABSTRACT

CHATTOPADHYAY, SRINJOY. Optimizing and Controlling Spreading Processes in Multilayer Networks. (Under the direction of Dr. Huaiyu Dai and Dr. Do Young Eun.)

Networks have received considerable attention as a mathematical tool for modeling both cyber and physical systems. The diverse application domains range from classical fields such as evolutionary dynamics and infectious disease spreading to recent topics such as online social networks, infrastructure networks and neuroscience. Technological progress in recent years has brought the perhaps intuitive fact to the attention of researchers that networks are rarely (if ever) isolated in nature. A deeper look into many application areas have revealed that more sophisticated models, comprising distinct network layers interacting with each other, provide a much better abstraction for analysis of practical systems. Researchers have revisited many classical problems from a multi-layered perspective, leading to interesting theoretical results and practical engineering strategies.

In this dissertation, we study the propagation of diverse spreading processes through multi-layer networks and devise network design strategies to control the spread of these processes. We consider several distinct types of multi-layer spreading processes, namely, failure of network components cascading through the inter-connected networks, redistribution of load in multi-layer infrastructure networks, and the propagation of infectious diseases through multi-layer contact networks. The fundamental theme in these different problems is that the topologies of the network layers and the propagation parameters of the processes are assumed to be known to us. Under this setting, we explore the possibility of manipulating the inter-layer network structure between the different network layers to optimize the spreading of these diverse processes through the multi-layer network.

In the initial part of this dissertation, we focus on scenarios where the topology of the network layers follow various theoretical graph generation models. For such theoretical models, we develop network design strategies to optimize the spreading of these processes, subject to certain constraints limiting the total number of inter-layer connections that can be added to the multi-layer network. In later parts of our dissertation, we move to the more realistic setting of arbitrary network topologies, where the constituent network layers are not guaranteed to follow well-behaved theoretical models. In addition to facilitating the spreading of the processes, we also study some more sophisticated problems, wherein our objective is to devise strategies to control the process spreading to a desired amount.

We believe that the study of spreading processes on multi-layer networks is important from a practical perspective as well, on top of being vital towards developing a deeper theoretical understanding. We present various real-world scenarios, where the problems discussed herein are relevant and the proposed strategies can provide crucial network design guidelines. We hope that our dissertation can motivate further development in the area of network science, from the perspectives of both academic research and real-world innovations.

Optimizing and Controlling Spreading Processes in Multilayer Networks

by
Srinjoy Chattopadhyay

A dissertation submitted to the Graduate Faculty of
North Carolina State University
in partial fulfillment of the
requirements for the Degree of
Doctor of Philosophy

Electrical Engineering

Raleigh, North Carolina

2020

APPROVED BY:

Dr. Huaiyu Dai Co-chair of Advisory Committee	Dr. Do Young Eun Co-chair of Advisory Committee
Dr. Dror Baron	Dr. Keith Townsend

Dr. Irina Kogan

BIOGRAPHY

Srinjoy Chattopadhyay received his Bachelor of Technology degree in Electronics and Electrical Communication Engineering in 2012 and his Master of Technology degree with specialization in Telecommunication Systems Engineering in 2013 from Indian Institute of Technology, Kharagpur. He worked on his Ph.D. degree in Electrical Engineering with a minor in Mathematics at North Carolina State University, Raleigh, NC, under the guidance of Prof. Huaiyu Dai. His doctoral research mainly focuses on network science and applied mathematics.

ACKNOWLEDGEMENTS

Firstly, I would like to extend a heartfelt gratitude to my advisor Professor Huaiyu Dai for his guidance and continuous support of my Ph.D study and related research. His deep and broad knowledge, in addition to his humility and patience has been a continuous source of motivation for me. It has truly been an honor to work with him and learn from him over these last years. Additionally, I sincerely thank my co-advisor Professor Do Young Eun for providing his insightful suggestions and encouragement throughout the course of my doctoral research.

I would also like to thank Professor Dror Baron, Professor Keith Townsend and Professor Irina Kogan for their illuminating instructions and advice. Moreover, I would also like to take this opportunity to express my indebtedness to all other professors and teachers whose courses provided the strong foundations upon which I based my research. I am also deeply indebted to the National Science Foundation (grants ECCS-1444009 and CNS-1824518) and the Army Research Office (Grant W911NF-17-1-0087) for supporting me financially throughout the duration of my doctoral degree.

Additionally, I thank all my fellow labmates and friends, Xiaofan, Yufan, Richeng, Ali A, Ali R, Jung Hoon Lee, Nhan, Sandeep, Gaurav, Sanjeev, Rohit, Pranav, Aravind and Shreyas. The stimulating discussions with them, about both academic and non-academic topics, have been a constant source of encouragement for me.

Last but far from the least, I am extremely grateful to my parents for their unconditional love and support, not just for the duration of my doctoral degree but throughout my life. They were my first teachers and undoubtedly play the pivotal role for everything I achieve in life. Finally, a special thanks to my dearest Rashmi. I cannot imagine having made this long journey without her unwavering love and support.

TABLE OF CONTENTS

LIST OF FIGURES . . . . . **vi**

Chapter 1 Introduction **1**
1.1 Objectives 1
1.2 Problems Studied 2

Chapter 2 Estimation of Robustness **4**
2.1 System Model and Problem Statement 4
2.2 System Equations 6
2.2.1 Factors for survival 6
2.2.2 Interdependent Self-referencing Equations 6
2.2.3 Robustness in terms of edge percolation probability 8
2.3 Analysis 8
2.4 Erdos-Renyi (ER) Graph Models 10
2.4.1 Completely Interdependent Networks 10
2.4.2 Partially Interdependent Networks: Identically Distributed Layers 11
2.5 Scale Free (SF) Graph Models 12
2.5.1 Completely Interdependent Networks: Identically Distributed Layers 12
2.5.2 Completely Interdependent Networks: Non-Identically Distributed Layers . . 14
2.5.3 Partially Interdependent Networks: Identically Distributed Layers 14
2.6 Targeted Attack Scenario 14
2.6.1 Completely Interdependent Networks: Identically Distributed Layers 15
2.7 Results and Discussion 17

Chapter 3 Optimal Interlink Design **22**
3.1 State of the Art 22
3.2 System Model 23
3.3 Summary of Results 26
3.4 Analysis: Complete Interdependence 27
3.4.1 One-to-one structure 27
3.4.2 One-to-Many Structure 30
3.5 Analysis: Partial Interdependence 32
3.5.1 Description of Nash Bargaining Problem 35
3.6 Analysis: Targeted Attack Model 38
3.6.1 Double-Layer Targeted Attack model 38
3.6.2 Single-Layer Targeted Attack model 40
3.7 Simulation Results 40
3.8 Conclusion and Future Work 44

Chapter 4 Interlinks with cost **45**
4.1 Background 45
4.2 Our Approach 46
4.3 Contributions 47
4.4 System Model 48
4.5 Studying a Simple Metric 50
4.6 Process Dependent Metrics 52

4.6.1 Cascading Failure in Interdependent Networks . . . 53
4.6.2 Load Distribution in Interdependent Networks . . . 56
4.6.3 Connectivity in Demand-Supply Networks . . . 58
4.7 Distributed Implementation . . . 60
4.8 Simulation Results . . . 62
4.8.1 Implementation of Processes . . . 62
4.8.2 Performance gain variation with total available budget . . . 67
4.9 Conclusion and Future Work . . . 67
4.10 Mathematical Details . . . 68
4.10.1 Convexity of Optimization Problem . . . 68
4.10.2 Analysis for general metric . . . 69
4.10.3 Analysis for Effective Degree . . . 70
4.10.4 Analysis for load distribution . . . 71
4.10.5 Analysis for connectivity in demand-supply networks . . . 72

Chapter 5 Controlled Infection Spreading . . . 73
5.1 Background . . . 73
5.1.1 Related Works . . . 74
5.1.2 Motivation . . . 75
5.1.3 Our contribution . . . 76
5.2 System Model and Problem Statement . . . 77
5.3 Analysis of Epidemic Dynamics . . . 79
5.3.1 Epidemics in interlink subgraphs . . . 83
5.3.2 Estimation of infection size . . . 87
5.4 Optimizing the Interlinking structure . . . 89
5.4.1 Interlinking structure for identical hub degrees . . . 89
5.4.2 Interlinking structure for the general case . . . 92
5.5 Engineering the metastable state . . . 95
5.5.1 The core and supplementary groups . . . 95
5.5.2 Augmenting the metastable state . . . 97
5.5.3 Algorithms for interlinking design . . . 98
5.5.4 Estimating the hub sets . . . 100
5.5.5 Limits of achievable infection densities . . . 104
5.6 Simulation Results . . . 105
5.6.1 Details of the Simulation Framework . . . 106
5.6.2 Verification of the Lemmas . . . 106
5.6.3 Comparison of different strategies . . . 108
5.6.4 Case Studies . . . 111
5.7 Conclusion . . . 114

Chapter 6 Conclusion . . . 116
6.1 Contributions . . . 116
6.2 Future directions of research . . . 117

BIBLIOGRAPHY . . . 119

LIST OF FIGURES

Figure 2.1 System model for partially interdependent network. 5
Figure 2.2 Convergence of robustness vs attack strength for completely Interdependent i.i.d. networks. 18
Figure 2.3 Simulation vs analytical results for interdependent networks under randomized attack model with layers generated by the ER model. 18
Figure 2.4 Comparison of simulation results to analytical approximations for critical node fraction (η_c) for completely interdependent generated by the ER model. 19
Figure 2.5 Comparison of simulation results to analytical approximations for random attack on interdependent Scale Free (SF) networks generated by the Barabasi-Albert model. 21
Figure 2.6 Comparison of simulation results to analytical approximations for targeted attack 21

Figure 3.1 Interdependent system model with one-to-one structure. Solid lines give intra-layer topology and dotted arrows showing inter-layer topology. 24
Figure 3.2 Interdependent system model: one-to-one structure with partial interdependence. Hexagonal nodes are autonomous, while the rest are interdependent. 33
Figure 3.3 Completely interdependent networks with one-to-one interdependence. The individual layers have been generated by the Barabasi-Albert model with $m = 3$. '$\diamond$', '$\square$', and 'o' markers represent the random, monotonic, and anti-monotonic arrangement of interdependent nodes, respectively, on the basis of their intra-layer degrees. The left and right figures correspond to the cases of double-layer and single-layer randomized attacks, respectively. . . . 41
Figure 3.4 Completely interdependent networks with one-to-many interdependence under randomized attack. The individual layers have been generated by the Barabasi-Albert model with $m = 3$, and the allocation of interlinks is regular. '$\diamond$', '$\square$', and 'o' markers represent the random, monotonic, and anti-monotonic arrangement of interdependent nodes on the basis of their intra-layer degrees, respectively. The left and right figures correspond to the cases of double-layer and single-layer attacks, respectively. 42
Figure 3.5 Partially interdependent networks with one-to-one interdependence. The individual layers have been generated by the Barabasi-Albert model with $m = 3$ and 75% of nodes in the network are autonomous. '$\diamond$', '$\square$', and 'o' markers represent the cases of random, low-low, and high-high, respectively, which are strategies of decoupling of nodes. The left and right figures correspond to the cases of double-layer and single-layer randomized attacks, respectively. 43
Figure 3.6 Completely interdependent networks with one-to-one interdependence under perfect targeted attack. The individual layers have been generated by the Barabasi-Albert model with $m = 3$. '$\diamond$', '$\square$', and 'o' markers represent the random, monotonic, and anti-monotonic arrangement of interdependent nodes, respectively, on the basis of their intra-layer degrees. The left and right figures correspond to the cases of double-layer and single-layer attacks, respectively. 43

Figure 3.7 Completely interdependent networks with one-to-one interdependence under perfect targeted attack. The individual layers have been generated by the Barabasi-Albert model with $m = 3$. '$\diamond$', '$\square$', and 'o' markers represent the random, monotonic, and anti-monotonic arrangement of interdependent nodes, respectively, on the basis of their intra-layer betweenness (left) and closeness (right). 44

Figure 4.1 Plot of metric versus network robustness values for the connectivity based cascading failure process under node degree based targeted model. 55
Figure 4.2 Plot of metric versus network robustness values for the load distribution process under random attack model. 57
Figure 4.3 Plot of metric versus network robustness values for the connectivity process in demand-supply networks under a random attack model. 58
Figure 4.4 Connected component based cascading failure under stringent (top) and sufficient (bottom) budget constraints. 63
Figure 4.5 Load distribution in interdependent networks under stringent (top) and sufficient (bottom) budget constraints. 64
Figure 4.6 Connectivity in demand-supply networks under stringent (top) and sufficient (bottom) budget constraints. 65
Figure 4.7 Variation of performance gain w.r.t. random resource allocation for different interlink construction strategies. The three figures correspond to processes: i) connected component based cascading failure (top), ii) load distribution (middle), and iii) connectivity in demand supply networks (bottom). 66

Figure 5.1 Instances of the microscopic subgraphs: a) Interlink subgraph with 1 interlink, b) Interlink subgraph with k interlinks. 84
Figure 5.2 Extended star topology with infected centre with attached line graphs of length L. 86
Figure 5.3 Instance of interlinking structure between two subsets of the core group, with $H_a^0 = \{1,2,3\}$ and $H_b^0 = \{1,2,3,4,5\}$. The maximally uniform interlink allocation to H_a^0 following Algorithm 4 is 3, 2, 2, respectively 100
Figure 5.4 Variation of extinction time in interlink subgraphs with the intra-layer degrees of the constituent hubs. 107
Figure 5.5 Variation of η_i with hub degree k_i for different infection propagation rates. . 108
Figure 5.6 Variation of average size of localized infection around hubs with infection propagation rate. 109
Figure 5.7 Comparison of infection sizes under the following interlinking strategies: i) one-to-one interlinking, ii) one-to-many interlinking, iii) Skewed interlink allocation, and iv) Uniform interlink allocation. 110
Figure 5.8 Comparison of infection sizes under the following interlinking strategies: i) one-to-one interlinking, ii) one-to-many interlinking, iii) Uniform interlink allocation following monotonic structure, and iv) Uniform interlink allocation following anti-monotonic arrangement. 110
Figure 5.9 Predicted vs simulated infection size in the two network layers, D_a (top) and D_b (bottom), with varying infection propagation rate for Case 1. 112
Figure 5.10 Predicted vs simulated infection size in the two network layers, D_a (top) and D_b (bottom), with varying infection propagation rate for Case 2. 114

CHAPTER

1

INTRODUCTION

Multi-layer networks constitute the class of networks comprising multiple network layers interconnected to each other in some way. Across the domain of cyber and physical systems, we can observe a steadfast transition from modeling systems as isolated networks to a multi-layer interdependent modeling. Examples of such interdependent networks can arise in diverse areas, e.g. smart grid for power distribution comprising interdependent power and communication networks [Bul10], multi-modal transportation systems comprising networks of airports and train stations for a particular geographic region, financial modeling comprising networks of banks and their assets [Hua13a], etc. Due to the inherent inter-connectivity among different systems observed in the physical world, multilayer modeling has become a vital element in many areas. The Italy blackout of 2003 [Bul10], which happened due to recursive cascade of failures between the power and communication network, spreading out from the failure of a single power station, triggered research interest in this area. Multi-layer modeling of networks exhibit many interesting properties which are not observed in single layer networks. This makes their study appealing from both an engineering as well as a theoretical perspective.

1.1 Objectives

The goal of our dissertation is to develop a mathematical understanding of the propagation of spreading processes in interdependent multilayer networks. Although there exist many different propagation models in different multilayer applications, the recurrent theme among them is that a phenomenon in one layer of the network can propagate to the inter-connected components in other layers, promoting the propagation. It is important to note that due to the diversity of areas where

multilayer modeling can be applied, the specifics of spreading processes for different applications tend to vary significantly.

In the first part of our dissertation, we focus our attention on a particular spreading process, named connected component based cascading failure, which is the most widely studied process in interdependent networks. In the later part of this study, we extend our focus to other processes, i.e., load redistribution in multi-layer networks and the spreading of infectious diseases in multi-layer contact networks. In the initial parts of this thesis, our aim will be to optimize the design of the interlinking structure among the network layers so as to maximize (or minimize) the robustness of the multi-layer network to the failure of components. Later on, we shift our focus to more sophisticated problems, where instead of optimizing the propagation, our basic objective is to control this propagation via intelligent design of the interlinking structure between the interdependent network layers of the multi-layer network.

1.2 Problems Studied

With these objectives in mind, we give a brief description of the specific problems studied in this dissertation. We also introduce the structure of the dissertation along the way.

In our first problem, we estimate the robustness of multi-layer interdependent networks against the failure of network components, where the propagation of failures among the interdependent layers is modeled by the cascading failure process [Bul10]. Given the topology of different network layers and assuming the interlinking between them to be random in nature, we want to estimate the robustness of the corresponding interdependent network. Under certain constraints, mathematical equations modeling the cascading failure process have been developed by researchers. We introduce these equations in Chapter 2 and utilize them to characterize the robustness of the interdependent network in the steady state.

In our second problem, discussed in Chapter 3, we endeavor to design the interlink structure to optimize the steady state robustness of the multi-layer network. Given the isolated network layers, we want to design the interlinking structure between these network layers so that the robustness of the resulting interdependent network is maximized or minimized. The underlying mathematical framework of these two problems is the generating function based approach, which considers the degree distribution of the network components. This is applicable for random graphs having a locally tree-like structure implying that the local neighborhood of nodes do not contain any loops. Random graphs can be effective models to study many physical problems and we have also provided instances in the study of the first two problems, where algorithms developed for random graphs also worked well for real graphs in both estimation of robustness and optimization of the interlinks to maximize the robustness.

However, it has been established in many studies that the topology of networks encountered in practice can vary dramatically from that of random graphs. For networks with arbitrary topology, the generating function based framework is not applicable. Within this purview, we pose our third

problem in Chapter 4, where we aim to design interlinks for networks with arbitrary topology to optimize their robustness against various models of phenomena propagation. In the first two problems, there was no notion of cost of construction of the interlink or any constraint on which interlinks can (not) be constructed. However as we begin to apply theoretical ideas to practical problems various factors constraining the design of interlinks emerge. We endeavor to address the cost based constraint in this problem, where we want to optimize the interlink structure subject to different interlinks having different costs of construction.

The fundamental objective in the problems studied in the above chapters is to optimize the propagation of spreading processes in multi-layer networks. Extending our attention to more sophisticated problems, in Chapter 5 we explore the possibility of controlling the spread of infectious diseases in multi-layer networks by manipulation of the interlinking structure between the network layers. This controlled spreading of propagation, instead of a maximization or minimization, significantly complicates the problem in relationship to the others considered in this dissertation. However, we are able to show that an intelligent design of the inter-layer links can achieve the controlled propagation of infection, albeit under certain constraints. Finally we conclude our dissertation presented in this dissertation in Chapter 6.

CHAPTER

2

ESTIMATION OF ROBUSTNESS

In this chapter we develop mathematical equations to track the cascading failure process in interdependent networks. We adhere to the generating function approach utilizing the intra-layer degree distribution of the nodes comprising the network. Our aim in this chapter is to set up a mathematical framework to estimate the network robustness and to examine whether we can develop mathematical formulas to characterize robustness of networks so that we can estimate robustness without running computationally expensive simulations.

2.1 System Model and Problem Statement

We consider a general system of partially interdependent network comprising two layers A and B with M and N nodes respectively. The two layers are constructed as random graphs with small average degrees λ_A and λ_B respectively ($\lambda_A \ll M, \lambda_B \ll N$). This construction ensures the locally tree-like property [Bra07] of the network layers which would be utilized in the formulation of the system equations. The degree distribution of the nodes are taken to be general in nature. The nature of interdependency among the two layers of the network has been taken to be one-to-one and bidirectional. Thus all interdependency links correspond to an interdependent pair of nodes (a, b) with $a \in A$ and $b \in B$ such that these two nodes in the two layers of the interdependent network depend on each other for their survival. The construction of the interdependency links has been taken to be uncorrelated with respect to the intra-layer degrees of the nodes, i.e. inter-links are constructed without the knowledge of the intra-layer graph structure. We are considering the case of partially interdependent networks where the network comprises two types of nodes: autonomous nodes, which do not require support from nodes of other layer for their survival; and interdependent

node, which are dependent on nodes of other layer. Let the number of interdependent node pairs in the network be K. Imposing the condition $K \leq min(M,N)$, our network model yields the general partially interdependent network. We also assume that the selection of nodes of the constituent layers of the network to be interdependent or autonomous is random, i.e. all nodes have the same probability of being either an autonomous or an interdependent node. Thus the probability of a node in layer A to be interdependent is K/M, since layer A has M nodes of which K are interdependent.

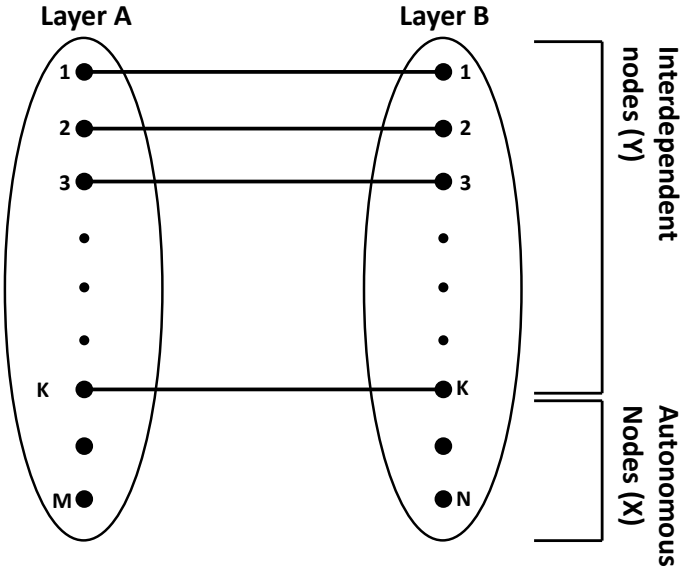

Figure 2.1 System model for partially interdependent network.

In this model of partially interdependent network, we are interested in studying the effect of failure of a fraction of nodes. Let a fraction $(1-\eta)$ of the nodes in both layers of the network be attacked. In this dissertation, we consider both the randomized attack case: where the attacker targets all nodes of the interdependent network with equal probability, and also the more realistic case of targeted attack: where the attacker targets nodes based on their intra-layer degrees.

We introduce two important notations which will form the basis of our formulation of the system equations to estimate the fractional size of the mutually connected component of the interdependent network which survives the cascade of failures. Let ψ_A and ψ_B denote the probability that a randomly chosen node, in layer A and B respectively, belongs to the mutually connected component which survives the cascading failure in the steady state. Thus ψ_A and ψ_B are the metrics of robustness of the interdependent network as they measure the probabilistic size of the component of the interdependent network which survives the cascading failure. Our aim in this dissertation is to estimate ψ_A and ψ_B based on the architectural parameters of the constituent layers of the

interdependent network.

2.2 System Equations

We would be formulating our system equations on the basis of the steady state probability of a randomly selected edge to be percolated. Here percolated denotes the event that the edge connects to the surviving component in the steady state after the cascading failure phenomenon. Let p_A (or p_B) define the probability such that a randomly chosen edge in layer A (or B) of the interdependent network on traversal in any arbitrary direction leads to a node in the mutually connected surviving component of the network. We would be relating the network robustness measured by ψ_A and ψ_B to this p_A and p_B. Furthermore, we would be defining p_A and p_B are *interdependent self-referencing* expressions.

2.2.1 Factors for survival

The survival of any node in the network depends on three conditions, on the basis of which we would be formulating the system equations:

- The node survives the initial attack.
- The node belongs to surviving connected component in its own layer, i.e. only nodes belonging to the largest connected component in each layer survive.
- If the node is interdependent in nature, its support node in the other layer should also satisfy the above two conditions.

2.2.2 Interdependent Self-referencing Equations

The first set of system equations expresses p_A and p_B by a self-consistent equation. We derive the expression for layer A of the network which can be symmetrically interchanged to obtain the expression for layer B. Let a randomly chosen edge in layer A upon traversal in any arbitrary direction connects to some node $a \in A$. The probability that the node a is interdependent is K/M. If a is interdependent, let its supporting node in the other layer be denoted by $b \in B$. Thus the three conditions can be quantified as:

- In this section, we assume that the node attack model is random in nature, i.e. the probability of a node to survive the initial attack is constant for all nodes and is equal to η, where $(1-\eta)$ is the fraction of nodes initially attacked. We would also be considering the case of targeted attack.
$$C1 \triangleq \eta. \tag{2.1}$$
- As we are choosing the edge in layer A randomly, the probability that the node it connects to ($a \in A$) has a degree of k_A is given by $P[k_A]k_A/\lambda_A$, where $P[k_A]$ denotes the degree distribution

of the nodes, i.e. $P[k_A]$ is the probability that a node $a \in A$ has degree k_A. Now according to the definition of p_A, for the node $a \in A$ to belong to the surviving component, at least one of its remaining $(k-1)$ edges should connect to the surviving component. Thus this condition can be quantified as :

$$C2 \triangleq \sum_{k_A} \frac{P[k_A]k_A}{\lambda_A}[1-(1-p_A^{k_A-1})]. \tag{2.2}$$

- For the third condition, we can observe that the node $b \in B$ is a randomly chosen node due to the randomized construction of the interdependency links. Thus the probability that the node $b \in B$ has a degree of k_B is $P[k_B]$. If $b \in B$ is not attacked initially, the condition for it to survive is that at least one of its edges should connect to the surviving component. Thus this condition can be quantified as:

$$C3 \triangleq \sum_{k_B} \eta P[k_B][1-(1-p_B^{k_B})]. \tag{2.3}$$

Now if a is an autonomous node, its survival is dependent only on the first two conditions, whereas interdependent nodes would require all three conditions to be simultaneously fulfilled to ensure its survival. Due to the randomized selection of nodes as autonomous and interdependent, we can write the self-consistent equation for p_A as :

$$\begin{aligned} p_A = &\frac{M-K}{M}\sum_{k_A}\eta P[k_A]\frac{k_A}{\lambda_A}[1-(1-p_A)^{k_A-1}]+ \\ &\frac{K}{M}\sum_{k_A}\eta\frac{k_A P[k_A]}{\lambda_A}[1-(1-p_A)^{k_A-1}]\cdot\sum_{k_B}\eta P[k_B][1-(1-p_B)^{k_B}]. \end{aligned} \tag{2.4}$$

Similarly for layer B we can write:

$$\begin{aligned} p_B = &\frac{N-K}{N}\sum_{k_B}\eta P[k_B]\frac{k_B}{\lambda_B}[1-(1-p_B)^{k_B-1}]+ \\ &\frac{K}{N}\sum_{k_B}\eta\frac{k_B P[k_B]}{\lambda_B}[1-(1-p_B)^{k_B-1}]\cdot\sum_{k_A}\eta P[k_A][1-(1-p_A)^{k_A}]. \end{aligned} \tag{2.5}$$

Thus it can be seen that at the heart of our system equations lies the interdependence whose study is the ultimate aim of this dissertation. It can clearly be observed that the self-consistent equation described above always has the trivial solution of $p_A = p_B = 0$, which corresponds to the case where the entire interdependent network breaks down and the fractional size of the mutually connected component is 0. However our main point of interest is the existence of a non-trivial solution for p_A and p_B.

2.2.3 Robustness in terms of edge percolation probability

In the next set of equations, we would express ψ_A and ψ_B as a function of p_A, p_B and the degree distribution of the nodes in each layer. Similar to the previous case, we only describe the formulation of the equation for layer A and the corresponding equation for layer B can be symmetrically obtained. Let us consider a randomly selected node $a \in A$ which can either be autonomous or interdependent. If a is interdependent, its corresponding support node is denoted by $b \in B$ as before. For this case, the only difference lies in the second condition due to the inherent difference between the definition of ψ and p. In the previous case, we randomly selected an edge and obtained the probability of the node connected to this edge to belong to the connected component through the remaining edges. As ψ is defined as the probability of a node to belong to the surviving component after the cascading failure, the second condition is defined as the probability that any one of its k_A edges traverses to the connected component. Thus we can write:

$$C2 \triangleq \sum_{k_A} \eta P[k_A][1-(1-p_A^{k_A})]. \tag{2.6}$$

Thus the expression for ψ_A can be written as:

$$\begin{aligned}\psi_A = &\frac{M-K}{M}\sum_{k_A}\eta P[k_A][1-(1-p_A)^{k_A}]+ \\ &\frac{K}{M}\sum_{k_A}\eta P[k_A][1-(1-p_A)^{k_A}]\cdot\sum_{k_B}\eta P[k_B][1-(1-p_B)^{k_B}].\end{aligned} \tag{2.7}$$

Similarly for layer B we can write:

$$\begin{aligned}\psi_B = &\frac{N-K}{N}\sum_{k_B}\eta P[k_B][1-(1-p_B)^{k_B}]+ \\ &\frac{K}{N}\sum_{k_A}\eta P[k_A][1-(1-p_A)^{k_A}]\cdot\sum_{k_B}\eta P[k_B][1-(1-p_B)^{k_B}].\end{aligned} \tag{2.8}$$

These four set of equations (2.10)-(2.5) and (2.9)-(2.8) are the system equations which form the basis of our dissertation. Similar equations have also been described in works like [Val13] and used to explain various other phenomena in interdependent networks.

2.3 Analysis

Here we will analyze the system equations derived in the previous chapter to obtain theoretical estimations for the robustness of interdependent networks. As discussed previously, our aim is to obtain a better understanding of cascading failure and derive mathematical relationships between network robustness and network structural parameters. Such relationships would be obtained by assuming specific random network generators like Erdos-Renyi (ER) model, Scale-Free (SF) model, etc., and simplifying the system equations by taking the node degree distributions of these network

generators. We would also we presenting simulation results for these different random networks in this chapter. We re-iterate the system equation for layer A here under the assumption that the sizes of both layers of the network is the same. We impose this condition on the interdependent system to simplify our analysis. The fraction K/N, where K is the number of interdependent nodes pairs in the network and N is the size of each layer of the network, is denoted by q, i.e. $q \triangleq K/N$. We would however be providing simulation results for both scenarios: networks of same and different sizes. It should be remembered that equations for layer B can be obtained just by mirroring the symbols A and B.

$$\begin{aligned}\psi_A =&(1-q)\sum_{k_A}\eta P[k_A][1-(1-p_A)^{k_A}]+\\ &q\sum_{k_A}\eta P[k_A][1-(1-p_A)^{k_A}]\cdot\sum_{k_B}\eta P[k_B][1-(1-p_B)^{k_B}].\end{aligned} \tag{2.9}$$

$$\begin{aligned}p_A =&(1-q)\sum_{k_A}\eta P[k_A]\frac{k_A}{\lambda_A}[1-(1-p_A)^{k_A-1}]+\\ &q\sum_{k_A}\eta\frac{k_A P[k_A]}{\lambda_A}[1-(1-p_A)^{k_A-1}]\cdot\sum_{k_B}\eta P[k_B][1-(1-p_B)^{k_B}].\end{aligned} \tag{2.10}$$

We analyze the system equations in parts by grouping the individual summation terms. We define F_1 as:

$$\begin{aligned}F_1 &\triangleq \sum_{k_A}\eta P[k_A]\frac{k_A}{\lambda_A}[1-(1-p_A)^{k_A-1}]\\ &= \eta\sum_{k_A}\left(\frac{P[k_A]}{\lambda_A}[k_A+\frac{\partial}{\partial p_A}(1-p_A)^{k_A}]\right)\\ &= \eta\left(1+\frac{1}{\lambda_A}\frac{\partial}{\partial p_A}\sum_{k_A}P[k_A](1-p_A)^{k_A}\right),\end{aligned}$$

since $\lambda_A=\sum_{k_A}k_A P[k_A]$ and partial derivative is a linear operator. Similarly:

$$\begin{aligned}F_2 &\triangleq \sum_{k_A}\eta P[k_A][1-(1-p_A)^{k_A}]\\ &= \eta\left(1-\sum_{k_A}P[k_A](1-p_A)^{k_A}\right).\end{aligned}$$

It should be noted here that both (2.9) and (2.10) can be described by combinations of F_1 and F_2. It can also be seen that the term of interest here is the expression: $F_3 \triangleq (\sum_k P[k](1-p)^k)$. We would be obtaining our analytical results under the assumption that the network layers have been

constructed as Erdos-Renyi (ER) graphs. Application of our method of analysis to random networks with arbitrary degree distributions has also been discussed in Section 3.2.

2.4 Erdos-Renyi (ER) Graph Models

The intra-layer degree distribution of the nodes in an ER graph are Poisson distributed, i.e. $P[k] = e^{-\lambda}/\lambda^k k!$, where $P[k]$ denotes the probability of a node to have an intra-layer degree of k and λ denotes the mean intra-layer node degree. Thus, we can write F_3 as:

$$F_3(\lambda, p) = \sum_k \frac{e^{-\lambda}\lambda^k}{k!}(1-p)^k = e^{-\lambda p}. \tag{2.11}$$

Remark: It can be observed that $\partial F_3(\lambda, p)/\partial p = -\lambda e^{\lambda p}$, which implies $F_1(\lambda, p) = F_2(\lambda, p)$. Thus $\psi = p$ for ER graphs, which is a very interesting result that proves ψ and p can be used interchangeably as a metric for network robustness. This phenomenon is usually not observed for arbitrary degree distributions.

The system equations can thus be written as:

$$\begin{aligned} \psi_A &= \eta(1-q)\left(1-e^{-\lambda_A p_A}\right) \\ &\quad +\eta^2 q\left(1-e^{-\lambda_A p_A}\right)\left(1-e^{-\lambda_B p_B}\right) = p_A. \end{aligned} \tag{2.12}$$

Since both layers of the network are subjected to the initial attack, the system equations for layer B are symmetrical to the above equation and have been omitted for brevity. We present the analysis of two scenarios.

2.4.1 Completely Interdependent Networks

We consider the case where $q = 0$, all nodes are interdependent. The system equations for this case can be written as:

$$\psi = \eta^2\left(1-e^{-\lambda_A p}\right)\left(1-e^{-\lambda_B p}\right) = p. \tag{2.13}$$

We are interested in obtaining the critical threshold η_c which denotes the minimum value of η that results in a non-trivial solution of ψ and p in (2.13). At the critical point, the slopes of the two sides of (2.13) should be equal. Thus:

$$\eta_c^2 = \left[\lambda_A e^{-\lambda_A p_c}(1-e^{-\lambda_B p_c}) + \lambda_B e^{-\lambda_B p_c}(1-e^{-\lambda_A p_c})\right]^{-1}. \tag{2.14}$$

Defining $f_A \triangleq e^{-\lambda_A p_c}$, $f_B \triangleq e^{-\lambda_B p_c}$ and substituting η^2 in (2.13), we get:

$$\frac{f_A \log f_A}{f_A - 1} + \frac{f_B \log f_B}{f_B - 1} = 1 \tag{2.15}$$

We can obtain another relationship between f_A and f_B using the ratio of the two mean degrees (λ_A and λ_B). Thus by defining $r \triangleq \lambda_B/\lambda_A$, we get $f_B = f_A^r$. Although a closed form solution for the two sets of equations do not exist, numerical methods can be used to estimate the value of η_c and p_c. The comparison of these theoretical results with simulation has been presented in Section 3.5.

Remark: For identically distributed network layers ($\lambda_A = \lambda_B$), (2.15) simplifies to $f = exp[(f-1)/2f]$ which can be solved by numerically. Using the value of f we can obtain closed form expressions for η_c and ψ_c: $\eta_c^2 = 2.4554/\lambda$, $\psi_c = 1.2864/\lambda$. These results have been obtained previously in [Bul10], where a generating function based technique was used. Thus this result establishes the equivalence of our method of analysis with existing ones in literature.

2.4.2 Partially Interdependent Networks: Identically Distributed Layers

The analysis for partially interdependent networks is significantly more complicated due to the quadratic nature of the system equations. Thus we focus on the case $\lambda_A = \lambda_B$, i.e. identically distributed layers. Under these conditions the system equations can be written as :

$$\psi = (1-q)\eta(1-e^{-\lambda p}) + q\eta^2(1-e^{-\lambda p})^2 = p. \tag{2.16}$$

Similar to the previous case, our aim is to obtain expressions for η_c and ψ_c. It has been shown in [**change**] that partially interdependent exhibit a phase transition from first order to second order as the coupling fraction (q) decreases. Thus for lower values of q, ψ_c and p_c tend to zero. We will use this fact to derive the relationship between η_c, q and λ when the phase transition is second order. Let us re-write the system equation for the critical condition, $\eta = \eta_c$, $p = p_c$, as:

$$\lim_{p_c \to 0} \left[(1-q)\eta \frac{1-e^{-\lambda p_c}}{p_c} + q\eta^2 \frac{(1-e^{-\lambda p_c})^2}{p_c} \right] = 1. \tag{2.17}$$

Evaluating the above limit, we can obtain the following equation relating η_c, q and λ:

$$\eta_c = [\lambda(1-q)]^{-1}. \tag{2.18}$$

The above expression can further be utilized to estimate the phase transition point ($q = q_c$). Substituting the value of η_c in (2.16), we get:

$$p = \frac{1-e^{-\lambda p}}{\lambda} + \frac{q}{(1-q)^2}\left(\frac{1-e^{-\lambda p}}{\lambda}\right)^2. \tag{2.19}$$

The above equation cannot be solved in a closed form due to the mixture of linear and exponential terms. We have used numerical methods to obtain the minimum value of q ($q = q_c$) which leads to a non-zero solution of p which is not arbitrarily close to 0. The solution for (2.19) is very close to 0

for upto $q \leq q_c$. The value of q at which the solution to (2.19) jumps to a non-zero value is defined as the percolation phase transition point (q_c). The comparison between the theoretical estimate and the simulation results have been presented in Section 3.5.

The system equations (2.16) can also be used to obtain a general expression for η_c. Equating the slopes of the two sides of (2.16) at the critical point ($\eta = \eta_c, p = p_c$), we get:

$$(1-q)\eta_c \lambda e^{-\lambda p_c} + 2q\eta_c^2(1-e^{-\lambda p_c})\lambda e^{-\lambda p_c} = 1. \tag{2.20}$$

Only one of the roots of the equation has physical meaning; which under the substitution of $f \triangleq e^{-\lambda p_c}$ can be written as:

$$\eta_c = \frac{-(1-q)\lambda f + \sqrt{(1-q)^2\lambda^2 f^2 + 8q\lambda f(1-f)}}{4q\lambda f(1-f)}. \tag{2.21}$$

Writing the numerator of the above expression as $\Phi(q,\lambda,f)$ and substituting in (2.16) we can obtain the following equation

$$\log f = \frac{f-1}{2f} - \Phi(q,\lambda,f)\frac{(1-q)^2}{8fq}. \tag{2.22}$$

Due to the combination of exponential and linear terms in the above equation we have not been able to obtain closed form solutions for f. As done in the previous sections, we have used numerical methods to obtain solutions for f, which can be substituted in (2.21) to yield η_c. We would be comparing the accuracy of the estimate with simulations in Section 3.5.

2.5 Scale Free (SF) Graph Models

As shown in the previous section of analysis, the Erdos-Renyi Model of graph generation yields closed form equations which relate the metrics of robustness (ψ, p) in interdependent networks to the network generation parameters (λ). However an overwhelming volume of research works indicate that real world networks are modeled much more accurately by Scale-Free (SF) networks where the intra-layer degree distribution of the nodes follows the power law, i.e. $P[k] \sim k^{-\gamma}$, where γ is the parameter defining the distribution.

The derivation of closed form equations in the previous section were possible due to the simplification of the summation term $F_3(\gamma,p) = \sum_k P[k](1-p)^k$ when the intra-layer degrees are Poisson distributed resulting from the ER model. Unfortunately most degree distributions prevent such simplifications. Thus we resort to obtain mathematical inequalities for F_3 which can be utilized to obtain approximations for ψ and p.

2.5.1 Completely Interdependent Networks: Identically Distributed Layers

With respect to the definitions of F_1, F_2 and F_3, the system equations can be written as:

$$\psi = \eta^2(1-F_3(\gamma,p))^2, \tag{2.23}$$

$$p = \eta^2(1+\frac{1}{\lambda}\frac{\partial F_3(\gamma,p)}{\partial p})(1-F_3(\gamma,p)), \tag{2.24}$$

where λ is the mean degree of the SF network. Applying Cauchy-Schwarz inequality on F_3 we get,

$$F_3(\gamma,p) \triangleq \sum_k P[k](1-p)^k \tag{2.25}$$

$$\leq \left(\sum_k P[k]^2\right)^{1/2} \cdot \left(\sum_k (1-p)^{2k}\right)^{1/2}. \tag{2.26}$$

Simple simulation tests (excluded for brevity) show that the incurred error due to the above inequality is very low except for small values of p below $p = 0.5$. Almost all research results regarding Scale-Free networks indicate that they are very sensitive to node removal and critical node fraction for such networks is almost always greater than 0.5. Thus we can say that the approximation by the Cauchy-Schwarz inequality is quite accurate in our region of interest. Simulation results in later sections will corroborate this. The advantage of this approximation is that this inequality separates F_3 into two sequences whose summation can be readily obtained.

- For SF networks: $P[k] = C\,k^{-\gamma}$, where γ is a network parameter and C is the proportionality constant. This summation is similar to the Riemann zeta functions [Edw01]: $\zeta(s) = \sum_{n=1}^{\infty} 1/n^s$, where s is a complex number whose real part is greater than 1. For real positive values of s, the values of this function are available. However a few adjustments are required as the Riemann function sums in the range $[1,\infty\}$ whereas in our case the range is $[k_{min}, k_{max}]$. The right hand side discrepancy (k_{max},∞) would result in very little error for large networks due to the polynomial decay of the function. The left hand side discrepancy can be removed by simple arithmetic operations.

- The second summation term is the geometric series:

$$\sum_{i=k_{min}}^{k_{max}} r^i = r^{k_{min}} \frac{1-r^{k_{max}-k_{min}+1}}{(1-r)}. \tag{2.27}$$

Thus we can obtain an approximation for $F_3(\gamma,p)$ which as discussed is tight as long as $p \not< 0.5$. The approximation is also a explicit function of p and thus we can obtain partial derivative of F_3 with respect to p. From (2.23) and (2.24) we can clearly observe that once $F_3(\gamma,p)$ is known as an explicit function of γ and p, we can obtain approximation for ψ and p. As the approximation is an upper bound for $F_3(\lambda,p)$, we can conclude from (2.23) and (2.24) that the obtained solution to the system equations would be a lower bound to the actual system performance.

Let us represent the solution of the self-consistent equation obtained from the right hand side of (2.24) by $p^\star$. Thus $p \geq p^\star$. Since approximations and bounds are involved, we should resort to simulations to justify.

2.5.2 Completely Interdependent Networks: Non-Identically Distributed Layers

In a manner similar to the case of ER graphs, we can extend the concepts used in the previous section to networks with non-identically distributed layers. The inequalities governing the system robustness parameters ψ and p can be written as:

$$\psi_A = \eta^2(1-F_3(\gamma_A,p))(1-F_3(\gamma_B,p)) = \psi_B, \tag{2.28}$$

$$p_A = \eta^2(1+\frac{1}{\lambda_A}\frac{\partial F_3(\gamma_A,p)}{\partial p})(1-F_3(\gamma_B,p)), \tag{2.29}$$

$$p_B = \eta^2(1+\frac{1}{\lambda_B}\frac{\partial F_3(\gamma_B,p)}{\partial p})(1-F_3(\gamma_A,p)). \tag{2.30}$$

In the above equations λ_A, λ_B respectively denote the two mean degrees of layers A and B, and γ_A, γ_B denote the exponents for the power law degree distribution of the two layers.

2.5.3 Partially Interdependent Networks: Identically Distributed Layers

Extension to partially interdependent networks, where q fraction of the nodes are interdependent, is also straightforward:

$$\begin{aligned}\psi_A &= (1-q)\eta^2(1-F_3(\gamma_A,p))+ \\ &\quad q\eta^2(1-F_3(\gamma_A,p))(1-F_3(\gamma_B,p)),\end{aligned} \tag{2.31}$$

$$\begin{aligned}p_A &= (1-q)\eta^2(1+\frac{1}{\lambda_A}\frac{\partial F_3(\gamma_A,p)}{\partial p}+ \\ &\quad q\eta^2(1+\frac{1}{\lambda_A}\frac{\partial F_3(\gamma_A,p)}{\partial p})(1-F_3(\gamma_B,p)).\end{aligned} \tag{2.32}$$

System equations for layer B can be symmetrically obtained.

The verification of the system equations derived for the case of Scale-Free networks has been presented in Section 3.5.

2.6 Targeted Attack Scenario

The underlying assumption in the analysis presented above is that the attacker randomly attack the nodes in the interdependent network. However, attacks on the nodes of the network with high intra-layer connectivity would undoubtedly be a much more effective strategy from the view of disrupting the functioning of the network. In the previous sections, we have considered the case where the attacker has no knowledge about the node degrees of the constituent layers of the network and thus attacks nodes randomly. In this section we analyze the other extreme situation, where the attacker has complete degree information about the nodes and attacks nodes in the strict descending order

of their intra-layer degrees.

2.6.1 Completely Interdependent Networks: Identically Distributed Layers

We present the analysis of the case of perfect targeted attack on completely interdependent networks with identically distributed constituent layers. This method of analysis can also be applied to more general structures of interdependent networks which has been presented later. For a particular instance of network generation, we index the nodes in both layers A and B of the interdependent network in the increasing order of their intra-layer degrees. Let this index be represented by i: $1 \leq i \leq N$, where N is the number of nodes in each layer of the network. Let $k_{A,i}$ (or $k_{B,i}$) be the intra-layer degrees of the i^{th} node in the layer A (or B) of the network. Let sequence $\{\rho\}$ be a permutation of the number set $\{1,2,\cdots,N\}$ and ρ_i represent the i^{th} term of the sequence $\{\rho\}$. We design the sequence $\{\rho\}$ such that it captures the interdependency structure for this particular instance of network generation, i.e. $\{\rho\}$ is designed in such a way that the i^{th} node in layer A is connected via an interdependency link to the ρ_i^{th} node in layer B. As previously, the initial attack leads to the failure of a fraction $(1-\eta)$ of the nodes in the network. Due to the perfectly targeted attack model, all nodes represented by the top $(1-\eta)\cdot N$ indices fail due to the initial attack. It should be noted at this point that the metrics of network robustness ψ and p are defined in a mean sense over all instances of network generation with specified intra-layer degree distribution of the nodes. Thus for the purpose of obtaining system equations for ψ and p with respect to indexed nodes, we need to take an expectation over all instances of network generation. Due to the identical distribution of the two layers of the network and the simultaneous attack on both layers of the network, ψ and p would be the same for both layers of the network. Thus the system equations for the interdependent network in this scenario can be written as:

$$\psi = E\Bigg[\frac{1}{N}\sum_{i=1}^{N}\Big(\eta[1-(1-p)^{k_{A,i}}]I_\eta\Big)\Big(\eta[1-(1-p)^{k_{B,\rho_i}}]\Big)\Bigg], \tag{2.33}$$

$$\begin{aligned} p &= E\Bigg[\frac{1}{N}\sum_{i=1}^{\eta N}\Big(\frac{\eta k_{A,i}}{\lambda}[1-(1-p)^{k_{A,i}-1}]I_\eta\Big) \\ &\quad \Big(\eta[1-(1-p)^{k_{B,\rho_i}}]\Big)\Bigg]. \end{aligned} \tag{2.34}$$

Here $E[\cdot]$ represents the expectation over all instances of network generation and I_η is an indicator function representing the targeted removal of the top $(1-\eta)N$ fraction of the indices i, i.e. $I_\eta = 1$ if $i \in (1,\eta N)$. The factor η appears in the summation term for layer B as the attack model removes $(1-\eta)$ fraction of nodes from both layers. As the interdependency has been assumed to be random, from the point of view of any particular node $a \in A$, the probability that its supporting node in the other layer ($b \in B$) survives the initial attack is independent of the attack model. Thus the probability of survival of the supporting node $b \in B$ is η. We now present the analysis of the expression for p:

$$
\begin{aligned}
p &= \frac{1}{N}\sum_{i=1}^{\eta N} E\Big[\frac{\eta k_{A,i}}{\lambda}[1-(1-p)^{k_{A,i}-1}]I_\eta\Big]E\Big[[1-(1-p)^{k_{B,\rho_i}}]\Big] \\
&= \frac{\eta}{N\lambda}\sum_{i=1}^{\eta N} E\Big[(k_{A,i}-\frac{\partial(1-p)^{k_{A,i}}}{\partial p})I_\eta\Big]E\Big[[1-(1-p)^{k_{B,\rho_i}}]\Big].
\end{aligned}
$$

This follows from the fact that the two layers of the network have been generated independently of each other and thus the expectation of the product of the expressions corresponding to the two layers of the network can be written as the product of the individual expectations. Now the function $f(x)=1-(1-p)^x$ is concave in x and thus invoking the Jensen's inequality we have:

$$
E[1-(1-p)^k] \geq [1-(1-p)^{E[k]}]. \tag{2.35}
$$

Similarly convexity of the function $f(x)=(1-p)^x$, yields

$$
E\Big[\frac{\partial(1-p)^k}{\partial p}\Big] = \frac{\partial}{\partial p}E\big[(1-p)^k\big] \leq \frac{\partial}{\partial p}\big[(1-p)^{E[k]}\big]. \tag{2.36}
$$

Using (2.35) and (2.36), we can write (2.34) as:

$$
p \geq [1-(1-p)^\lambda]\frac{\eta}{N\lambda}\sum_{i=1}^{N}\Big(E\big[k_{A,i}\big]-\frac{\partial}{\partial p}E\big[(1-p)^{k_{A,i}}I_\eta\big]\Big) \tag{2.37}
$$

Let us define $\Lambda_i \triangleq E[k_i]$. Thus Λ_i represents the order statistics of the degrees of the i^{th} node in the layer of the interdependent network. Thus we can rewrite the above equation as

$$
\begin{aligned}
p &\geq [1-(1-p)^\lambda]\frac{\eta}{N}\sum_{i=1}^{N}\frac{1}{\lambda}\Big(\Lambda_i-\frac{\partial}{\partial p}(1-p)^{\Lambda_i}\Big)I_\eta \\
&= [1-(1-p)^\lambda]\frac{\eta}{N}\sum_{i=1}^{N}\frac{1}{\lambda}\Big(\Lambda_i-\Lambda_i(1-p)^{\Lambda_i-1}\Big)I_\eta \\
&= [1-(1-p)^\lambda]\frac{\eta}{N}\sum_{i=1}^{N}\frac{\Lambda_i}{\lambda}\Big(1-(1-p)^{\Lambda_i-1}\Big)I_\eta
\end{aligned}
$$

We can think of the terms $(1-(1-p)^{\Lambda_i-1})I_\eta$ as weights of the Λ_i/λ terms. Now by the Rearrangement Inequality [Har52] have, for two increasing sequences $\{a\}$ and $\{b\}$ of length l and any random permutation ρ of the l indices:

$$
\sum_{i=1}^{l} a_i b_i \geq \sum_{i=1}^{l} a_i b_{\rho_i}, \tag{2.38}
$$

where ρ_i is the i^{th} term of the permutation ρ. Taking the expectation of the above equation over all

possible permutations ρ, we have:

$$\sum_{i=1}^{l} a_i b_i \geq E[b] \sum_{i=1}^{l} a_i. \tag{2.39}$$

Now as Λ_i and $(1-(1-p)^{\Lambda_i - 1})$ are increasing sequences in i, we can use the above inequality in (2.38). Thus we have:

$$p \geq [1-(1-p)^{\lambda}] E[I_\eta (1-(1-p)^{\Lambda_i - 1})] \frac{\eta}{N} \sum_{i=1}^{\eta N} \frac{\Lambda_i}{\lambda}, \tag{2.40}$$

where $E[\cdot]$ is the expectation over all instances of network generation. Invoking the Jensen's Inequality for the convex function $(1-(1-p)^{\Lambda_i - 1})$ we get,

$$p \geq [1-(1-p)^{\lambda}][1-(1-p)^{\lambda_\eta - 1}] \frac{\eta}{N} \sum_{i=1}^{\eta N} \frac{\Lambda_i}{\lambda}, \tag{2.41}$$

where $\lambda_\eta \triangleq E[\Lambda_i I_\eta]$. We can simplify the expression for ψ (2.33) is a similar way.

$$\begin{aligned}
\psi &= \frac{1}{N} \sum_{i=1}^{N} \eta E\Big[(1-(1-p)^{k_{A,i}}) I_\eta\Big] E\Big[1-(1-p)^{k_{B,\rho_i}}\Big] \\
&\geq \frac{\eta}{N} \sum_{i=1}^{N} \Big[(1-(1-p)^{E[k_{A,i}]}) I_\eta\Big] \Big[1-(1-p)^{E[k_{B,\rho_i}]}\Big] \\
&= \frac{\eta}{N} [1-(1-p)^{\lambda}] \sum_{i=1}^{N} [1-(1-p)^{\Lambda_i}] I_\eta \\
&= [1-(1-p)^{\lambda}] E[(1-(1-p)^{\Lambda_i}) I_\eta] \frac{\eta}{N} \sum_{i=1}^{\eta N} 1.
\end{aligned}$$

Thus the inequality for ψ can be written as:

$$\psi \geq \eta^2 [1-(1-p)^{\lambda}][1-(1-p)^{\lambda_\eta}] \tag{2.42}$$

We have used (2.41,2.42) to design a numerical method based algorithm to estimate the value of ψ and p for particular η and λ.

2.7 Results and Discussion

We have designed a test bench to simulate the mechanism of cascading failure in interdependent networks. The algorithm obtains the largest connected component in each layer of the interdependent network in each stage of the cascading failure. The steady state size of the mutually connected

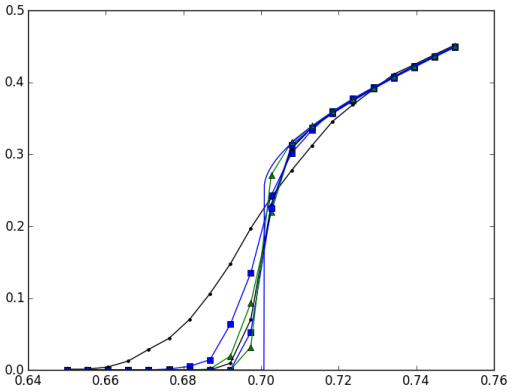

Figure 2.2 Convergence of robustness vs attack strength for completely Interdependent i.i.d. networks.

In the above figure the solid blue curve without markers represents the theoretical estimate. The sizes of the network used to generate the above curves are: 5000, 10000, 20000, 30000, 4000, 50000. As the network size increases the robustness vs attack strength curve approaches the theoretical estimate.

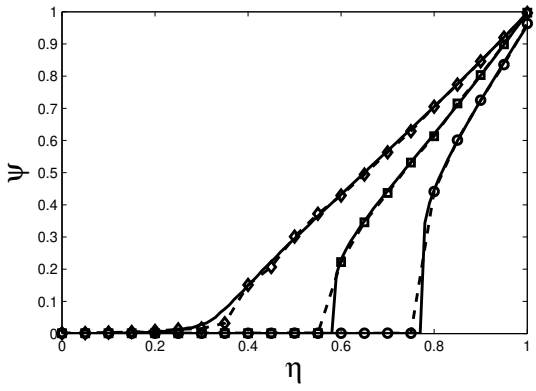

Figure 2.3 Simulation vs analytical results for interdependent networks under randomized attack model with layers generated by the ER model.

The three sets of plots represent the three cases of 1) 'o' markers: completely interdependent networks with identical layers ($\lambda = 4$), 2) '$\square$' markers: completely interdependent networks with non-identical layers ($\lambda_A = 4, \lambda_B = 6$), and 3) '$\diamond$' markers: partially interdependent networks with identical layers ($\lambda = 4$) and 50% interdependent nodes. The dotted line with markers give the simulation performance whereas the solid lines give the analytical performance.

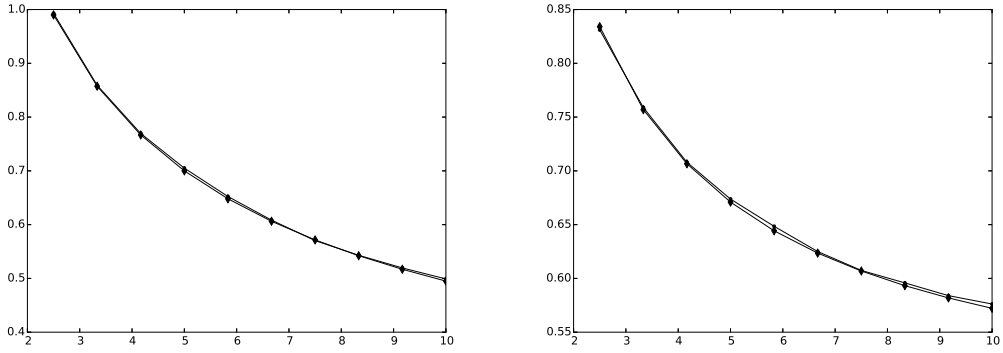

Figure 2.4 Comparison of simulation results to analytical approximations for critical node fraction (η_c) for completely interdependent generated by the ER model.

Here x-axis denotes the variation in the mean degree and the y-axis denotes the critical fraction of nodes (η_c). The solid line with markers represent the theoretical predictions whereas the solid line without the markers represent the simulation values. The left plot gives the result for the case of completely interdependent network with identically distributed degrees, where the mean degrees of both layers of the network is denoted by the x-axis; whereas the right plot gives the result for the case of completely interdependent networks with non-identically distributed layers, where the mean degree of layer A is 6 and the mean degree of layer B is represented by the x-axis.

component is our metric (ψ) to quantify the robustness of the network against failure of nodes.

For the validation of all other results presented here, we have generated synthetic networks based on the Erdos-Renyi and the Barabasi-Albert model [Alb02]. The sizes of both layers of the network has been taken as $N = 50,000$ unless otherwise mentioned.

- Our first result is to test the validity of the expressions of robustness derived for the case of Erdos-Renyi (ER) networks. Fig. 2.2 clearly shows that the theoretical predictions are in agreement with the simulation result. Furthermore, it can be observed that as the size of the simulated network increases, the simulation results tend to become closer to the theoretical predictions. This is an expected result as the theoretical predictions are valid for networks of infinite size and thus as we increase size of our simulated network we expect to get results closer to the theoretical predictions. The point of intersection of the robustness vs attack strength curves gives us the critical size of the mutually connected component. The corresponding η is nothing but the critical node fraction η_c which is the minimum fraction of nodes which should survive the initial attack so as to result in a non-zero network component in the steady state.

- It can be easily verified from Fig. 2.3 that the analytical expressions very closely fit the simulation results for all the different scenarios of network construction when the constituent layers of the network are generated by the ER model.

- In Fig. 2.4, we show a comparative result of the theoretically predicted critical fraction with that obtained by simulation. It can be clearly observed that the theoretical and the simulated

results are in agreement with each other. It can be noted at this point, that each point in these curves represents the intersection point of the robustness vs strength of attack curves for for corresponding scenarios.

- Fig. 2.5 gives the comparative results for the network performance approximations in case of interdependent networks where the layers are generated as Scale-Free graphs. We have used the Barabasi-Albert model [Alb02] for the generation of the networks. As discussed in Section 3.4 the analytical results are derived as a lower bound to the actual performance. This phenomena is clearly observed in all the plots. It was also discussed that our bounds are tight as long as the fractional size of the surviving component is greater than 0.5; our analysis was tight for $p > 0.5$. However for the case of partially interdependent networks ($\diamond$ and $\triangle$ markers), we can see that as the fraction of autonomous nodes increases the tightness of the bounds diminish. This loosening of the bound is a predictable result since as the fraction of autonomous nodes increases the system becomes more robust and thus operates in region of small fractional sizes of surviving components.

- For the targeted attack approximations we can refer to Fig. 2.6. This gives the comparative results for two different cases of completely interdependent networks with identically distributed layers having mean degrees of $\lambda = 5, 8$. The figure shows that our approximations lower bound the simulation results for regions with high η: the fraction of nodes surviving the attack. However, the approximations become loose for near-critical regions of η.

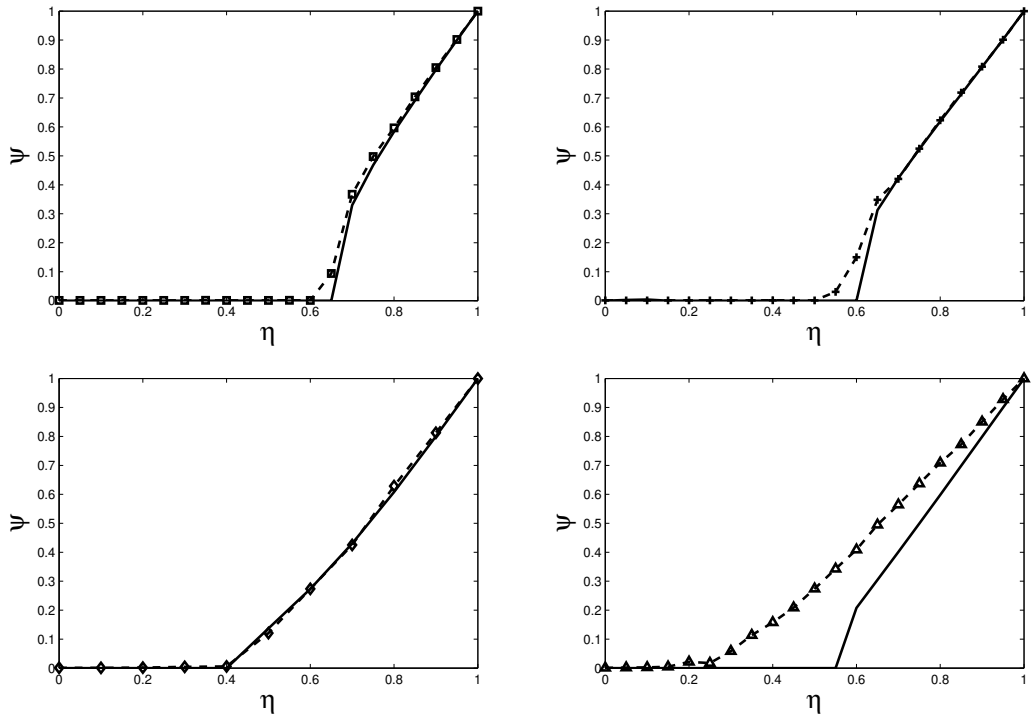

Figure 2.5 Comparison of simulation results to analytical approximations for random attack on interdependent Scale Free (SF) networks generated by the Barabasi-Albert model.

The dotted curve with markers gives the simulation results whereas the solid curve gives the analytical approximations. The different scenarios plotted here are: 1) '□' markers for completely interdependent networks with identically distributed layers with exponent $m = 4$, 2) '+' markers for completely interdependent networks with exponents $m_A = 3, m_B = 5$ for the two layers respectively, 3) '⋄' markers for partially interdependent networks with identically distributed layers of exponent $m = 3$ with 10% autonomous nodes, and 4)'△' markers for partially interdependent network as the previous case but with 50% autonomous nodes.

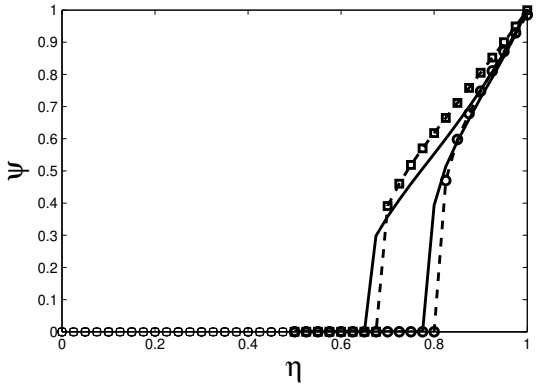

Figure 2.6 Comparison of simulation results to analytical approximations for targeted attack

We consider completely interdependent ER networks with mean degrees of $\lambda = 8$('□'$markers$) and $\lambda = 5$('o' markers) respectively. The dotted curve with markers gives the simulation results whereas the solid curve gives the analytical approximations.

CHAPTER

3

OPTIMAL INTERLINK DESIGN

In the previous chapter, we develop the mathematical framework for estimating the robustness of interdependent networks. An important aspect of interdependent networks which was ignored in the previous chapter is the structure of the interlinks connecting the different network layers. The network layers were assumed to be randomly interlinked in order to estimate the robustness. In this chapter we study the impact of interlink structures on the robustness of interdependent networks. Our ultimate aim is to optimize the structure of interlinks so as to maximize network robustness.

3.1 State of the Art

Most existing works are devoted towards a better understanding of cascading failure in interdependent networks. One widely adopted model in this field is the randomized attack on the one-to-one system with complete bidirectional interdependence, where every node in a layer is coupled to one node in the other layer and nodes are attacked randomly without any knowledge of the network topology [Bul10]. Recently, this basic model has been extended to consider targeted attacks, where nodes are attacked on the basis of their intra-layer degree [Hua11]; partial interdependence, where some nodes are autonomous meaning they can survive without being coupled to the other layer [Ran11]; and multiple interdependence, where a node may have multiple supporting nodes in the other layer [Yağ12; Sha10]. These works have focused on the modeling and analysis towards a better understanding of existing phenomena in interdependent networks. One exception is [Yağ12], which explores the optimal allocation of interlinks, maximizing the network robustness against random attacks, in the *absence* of intra-layer topology information. However, to the best of our knowledge, utilization of the topological properties of the constituent layers to design the structure of interlinks

is largely missing from the current literature. A few recent works such as [Min14a] have shown that particular interlink designs, like positive correlation of degrees of interdependent nodes, perform best under certain circumstances. However these works have supported their results mainly through simulations. In [Ran11] the authors have used the Kirchoff's index (a metric reflecting structural centrality) to show that partially interdependent networks are more robust when nodes of lowest centrality from two layers are coupled. Similar results have been indicated in [Sch13] as well.

The main focus of our dissertation [1] is to theoretically obtain the optimal interdependence structure between network layers so as to maximize the robustness against failure of nodes. In essence, we are interested in obtaining design principles on the basis of which interdependence between network layers are to be constructed such that the resulting network is most resilient to node failures. Our dissertation advances the current art in the following aspects. Firstly, we explicitly exploit the topological information; in particular, the intra-layer node degrees, to design more robust interdependent networks. Secondly, our mathematical model directly addresses the target metric - the fractional size of the surviving component of the interdependent network, rather than indirect metrics such as structural centrality. Finally, we provide rigorous mathematical proofs for all our results. To the best of our knowledge, this is one of the first works that utilizes topological information of constituent layers of interdependent networks to obtain the optimal interdependence structure. We believe that the design principles put forward in this dissertation would enable the design of more robust interdependent networks under various settings.

The remainder of this chapter is organized as follows. Section 3.2 presents the basic system model and the derivation of the system equations, which will be analyzed for different scenarios in the remainder of the chapter. Section 3.3 summarizes the main contributions of this dissertation. Section 3.4 and Section 3.5 contain the analysis for networks with complete and partial interdependence, respectively, under a randomized attack model. Targeted attack on interdependent networks is considered in Section 3.6. Finally, we present the simulation results supporting the theoretical analysis in Section 3.7, and conclude and indicate possible future works in Section 4.9.

3.2 System Model

We consider an interdependent system consisting of two layers A and B, as shown in Fig. 3.1. In this section, we will derive the system equations modeling the cascading failure for a simplistic network model of complete one-to-one interdependence, where each node in layer A is coupled to one node in layer B and vice versa. In later sections, we will generalize the network model from different perspectives, such as the type of interdependence (complete or partial), the structure of interdependence (one-to-one or one-to-many) and the nature of attack (random and targeted). We assume that the two network layers have small average degrees $\lambda_A, \lambda_B \ll N$, where N is the number of nodes in each layer. The average degree constraint is necessary to ensure the locally tree-like property of the network layers, which is required for the formulation of the system equations. This

[1] A subset of the work presented here was published in IEEE Globecom 2015 [**gc15**].

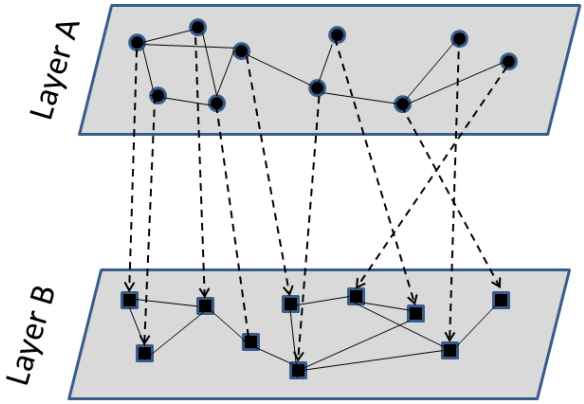

Figure 3.1 Interdependent system model with one-to-one structure. Solid lines give intra-layer topology and dotted arrows showing inter-layer topology.

constraint is also consistent with the observation from a wide range of cyber-physical networks [**netsci**]. We consider a general probabilistic model of the interdependence structure, where the probability of inter-coupling a node a in layer A to a node b in layer B is given by $P[k_a^{\{A\}}, k_b^{\{B\}}]$, where $k_a^{\{A\}}$ and $k_b^{\{B\}}$ are the intra-layer degrees of a and b, respectively. These couplings define the interlinks between the network layers, i.e. if nodes $a \in A$ and $b \in B$ are coupled, failure of a will cause b to fail and vice versa. Here we have abused the notation A and B to represent the names of the two network layers and also the set of nodes in the respective layers. At each stage of the iterative cascading failure, a node will survive if [Bul10; Val13]: i) it has one supporting node, and ii) it belongs to the largest connected component in its layer. The cascade stops when a double-layer mutually connected component (MCC) is obtained, where every node belongs to the largest connected component in its own layer and has a surviving supporting node. Thus any failure of nodes initiates a recursive cascade of failures among the two layers, which ultimately gives rise to a mutually connected network component in the steady state. The fractional size of the MCC with respect to (w.r.t.) the network layers, i.e. the ratio of the number of layer A (or layer B) nodes belonging to the MCC to the total number of nodes in layer A (or layer B), is taken to be the metric for robustness as is common in literature [Bul10; Hua11; Val13]. The aim of this dissertation is to optimally design the interdependence structure to jointly maximize this robustness metric for both layers of the interdependent network.

For ease of discussion, let us index the nodes in both layers in the decreasing order of their intra-layer degrees, i.e. the ith node in each layer has the ith highest intra-layer degree. The probability that the ith highest intra-layer degree node in layer A is coupled to the jth highest intra-later degree node in layer B is $P[k_i^{\{A\}}, k_j^{\{B\}}]$, where $k_i^{\{l\}}$ is the intra-layer degree of the ith node in layer l. Thus the interdependence structure can be represented by the $N \times N$ matrix, $\mathbf{P} = [P[k_i^{\{A\}}, k_j^{\{B\}}]]$ where

$(i, j) \in [1, N]$. The one-to-one interdependence structure, where every node is coupled to one node in the other layer, imposes the following restriction on **P**:

$$\sum_{i=1}^{N} P[k_i^{\{A\}}, k_j^{\{B\}}] = 1 \ \forall \ j \in [1, N], \qquad \sum_{j=1}^{N} P[k_i^{\{A\}}, k_j^{\{B\}}] = 1 \ \forall \ i \in [1, N], \tag{3.1}$$

where i and j denote the index of nodes in layers A and B, respectively. In other words, matrix **P** is doubly stochastic.

Our aim is to design the optimal interdependence structure ($\mathbf{P}^{\star}$) which maximizes the robustness of the network against node failures. In later sections of this dissertation, we will relax the constraints on **P** to generalize to networks with one-to-many interdependence, where a node in a given layer can support multiple nodes in the other layer, i.e. row sums of **P** can exceed 1, and partial interdependence, where only a fraction of nodes from both layers are interdependent; while the rest are autonomous which do not require any supporting node to survive. As is common in research on complex networks [Bul10; Hua11; Val13], we characterize nodes on the basis of their intra-layer degrees. Although the qualitative features of the results proved in this dissertation are valid for other centrality measures as shown in Section 3.7, all theoretical results presented here are derived under the assumption that only degree based information is available to us.

Next, we will focus on the derivation of the system equations relating the steady state size of the MCC (metric for robustness) to the network topology. Similar system equations have been presented in works such as [Val13] for explaining other phenomenon on interdependent networks. We want to study the steady state effect of the removal of $(1-\eta)$ fraction of nodes from the network and thereby design **P** so as to maximize the steady state size of the MCC. We have considered both cases of double-layer attack, where nodes are attacked in both layers, and single-layer attack, where only one layer is attacked. Throughout this dissertation, we will be analyzing the case of double-layer attack unless mentioned otherwise. Initially, we assume that the attacker (or mother nature) fails nodes randomly, i.e. all nodes of the network have the same probability of failure. Thereafter in Section 3.6, we also consider the case of targeted attack, where the attacker fails nodes on the basis of their intra-layer degrees.

Let the node percolation probability for the two layers be represented by ψ_A and ψ_B, denoting the probability of a randomly chosen node (from layer A or B) to belong to the MCC in the steady state. ψ_A and ψ_B can also be thought of as the fraction of nodes from each layer which survive the cascading failure. Thus ψ_A and ψ_B are nothing but the metrics of robustness that we intend to maximize in this dissertation. For the derivation of the system equations, we need to further define the edge percolation probabilities (p_A and p_B) to denote the probability that a randomly selected edge from layer A or B, on traversal in an arbitrary direction, connects to a node in the MCC. For the first set of system equations, we will express robustness (ψ) as a function of attack strength (η), intra-layer topology (degree sequence of nodes), interdependence structure (**P**) and

edge percolation probability (p_A and p_B). The system equations for ψ_A and ψ_B can be written as:

$$\psi_A = \frac{\mathbf{a}_1^T \mathbf{P} \boldsymbol{b}_1}{N} = \psi_B, \tag{3.2}$$

where $\mathbf{a}_1$ and $\mathbf{b}_1$ are the column vectors of a_{1i}'s and b_{1i}'s, with $a_{1i} \triangleq \eta[1-(1-p_A)^{k_i^{\{A\}}}]$ and $b_{1i} \triangleq \eta[1-(1-p_B)^{k_i^{\{B\}}}]$. Note that ψ_A and ψ_B are equal in this case because of the particular construction of $\boldsymbol{P}$ as a doubly stochastic matrix due to the one-to-one nature of the interdependence. This equality will not be valid in later sections, where we generalize the network structure to one-to-many interdependence. Our aim is to optimally design $\boldsymbol{P}$ such that ψ_A and ψ_B are maximized. Note that ψ ($\psi_A = \psi_B = \psi$) is also dependent on p_A and p_B, which are themselves intertwined with the network model. Thus for the purpose of obtaining the robustness (ψ) for a particular network topology (degree sequence and $\boldsymbol{P}$) and attack strength (η), we need to define another set of equations describing p_A and p_B.

$$p_A = \frac{\boldsymbol{a}_2^T \boldsymbol{P} \boldsymbol{b}_1}{N}, \qquad p_B = \frac{\boldsymbol{a}_1^T \boldsymbol{P} \boldsymbol{b}_2}{N}, \tag{3.3}$$

where $\boldsymbol{a}_2$ and $\boldsymbol{b}_2$ are column vectors of a_{2i}'s and b_{2i}'s, where $a_{2i} \triangleq \eta k_i^{\{A\}}[1-(1-p_A)^{k_i^{\{A\}}-1}]/\lambda_A$ and $b_{1i} \triangleq \eta k_i^{\{B\}}[1-(1-p_B)^{k_i^{\{B\}}-1}]/\lambda_B$. Thus for a particular network topology, ψ is obtained by solving the self-consistent equations (3.3) and substituting the solution into (3.2). We are interested in finding the optimal $\boldsymbol{P}^\star \in \mathbb{P}$ that maximizes the robustness ψ, where $\mathbb{P}$ is the set of all doubly stochastic matrices. Furthermore, (3.3) defines a set of self-consistent equations since the elements of the vectors $\boldsymbol{a}_i$ and $\boldsymbol{b}_i$, where $i = (1,2)$, are themselves dependent on p_A and p_B. The method of solving such self-consistent equations is explained in Section 3.4.

3.3 Summary of Results

The main contributions of this dissertation are summarized as follows:

- For the one-to-one structure with complete interdependence, we show that the interlinking of nodes by their intra-layer degrees in the monotonic order (ith highest degree nodes in layer A coupled to ith highest degree node in layer B, $\forall\ i \in [1,N]$) leads to maximal network robustness against a randomized attack model, i.e. $\boldsymbol{P}^\star = \boldsymbol{I}$, where $\boldsymbol{I}$ denotes the $N \times N$ identity matrix. This result holds true for both single-layer and double-layer randomized attacks. To the best of our knowledge, this is one of the first general results in this field that has been theoretically verified, although similar experimental results have been shown in [Min14a] and some other relevant works. Furthermore, the anti-monotonic matching (ith highest degree node coupled to ith lowest degree node) leads to the minimal network robustness.

- For one-to-many structure, we impose the restriction of regular interlink allocation (all nodes in a layer have the same number of inter-layer links) and obtain the optimal interdependence

structure which is valid for both single-layer and double-layer randomized attacks. This optimal structure can be mathematically represented as: $\boldsymbol{P}^{\star} = [\boldsymbol{I}|\cdots|\boldsymbol{I}]_{M\times N}$, where $M = cN$ is the size of the larger layer, c is an integer denoting the ratio of the sizes of the two layers, and $\boldsymbol{I}$ is repeated c times in $\boldsymbol{P}^{\star}$.

- For one-to-one structure with partial interdependence ψ_A and ψ_B cannot be simultaneously maximized, and thus we focus on the problem of obtaining a pareto-optimal interdependence structure w.r.t. the two network layers. We show that for both single-layer and double-layer randomized attacks, decoupling highest degree nodes from both layers, i.e. allocating nodes of highest intra-layer degrees to the set of autonomous nodes, is pareto-optimal. This result conforms to the finding in [Ran11] which explored the problem from the network geometry perspective.

- For the case of preferential targeted attack on lower degree nodes, all results described above hold true. For preferential targeted attack on higher degree nodes, we have shown that the monotonic arrangement of nodes is the optimal strategy for a perfect targeted double-layer attack, where nodes are attacked in the descending order of their intra-layer degrees. For a perfect single-layer attack, we have shown that the optimal interdependence structure is dependent on the strength of attack and thus universally optimal structures cannot be obtained by the tools used herein.

- We have presented the simulation results corroborating these theoretical findings. We have also tested the applicability of our results when the inter-links are designed on the basis of other centrality measures like betweenness and closeness. The simulation results show that even for these cases the monotonic arrangement is better than anti-monotonic and random arrangements. This gives some indication as to whether relationships between interdependence structure and robustness, which have been theoretically obtained in this work assuming knowledge of degree-based topological information, hold true for other measures of centrality.

3.4 Analysis: Complete Interdependence

3.4.1 One-to-one structure

In this section, we analyze the system equations for completely interdependent networks with one-to-one interdependence. It can be observed that the relationship between network robustness (ψ) and interdependence structure ($\boldsymbol{P}$) is complicated due to the fact that ψ depends on the values of p_A and p_B by (3.2) which themselves are dependent on $\boldsymbol{P}$ by (3.3). Furthermore, (3.3) is defined as self-consistent equations whose solution is not straightforward. It is known from [Bra07; Cal00] that such self-consistent equations typically have no closed form solutions and they are solved

iteratively as follows:

$$p_{A_{n+1}} = f_A(p_{A_n}, p_{B_n}), \qquad p_{B_{n+1}} = f_B(p_{A_n}, p_{B_n}), \tag{3.4}$$

where p_{l_n} denotes the value of p_l in the nth iteration. Starting from $p_{A_0} = p_{B_0} = 1$, the final solution is obtained when the iterations converge, i.e. $p_A = \lim_{n\to\infty} p_{A_n}$, $p_B = \lim_{n\to\infty} p_{B_n}$. It is also known from [Bra07] that such iterations always converge to fixed points between 0 and 1.

Lemma 3.4.1 *If there exists an interdependence matrix $\boldsymbol{P}^\star \in P$, where P is the set of doubly stochastic matrices, such that $\boldsymbol{P}^\star$ individually maximizes all of the following:*

- *$p_{A_{n+1}}$ for fixed p_{A_n} and p_{B_n}, $\forall\ n$, i.e. $\boldsymbol{P}^\star = _{\boldsymbol{P}\in P} \frac{\boldsymbol{a}_2^T \boldsymbol{P} \boldsymbol{b}_1}{N}$*
- *$p_{B_{n+1}}$ for fixed p_{A_n} and p_{B_n}, $\forall\ n$, i.e. $\boldsymbol{P}^\star = _{\boldsymbol{P}\in P} \frac{\boldsymbol{a}_1^T \boldsymbol{P} \boldsymbol{b}_2}{N}$*
- *ψ for fixed p_A and p_B, i.e. $\boldsymbol{P}^\star = _{\boldsymbol{P}\in \mathbb{P}} \frac{\boldsymbol{a}_1^T \boldsymbol{P} \boldsymbol{b}_1}{N}$,*

such a $\boldsymbol{P}^\star$ maximizes the network robustness ψ.

We will prove the above Lemma in two steps. Firstly, we will show that simultaneous satisfaction of the first two conditions implies maximization of both p_A and p_B. Thereafter, we will couple the third condition with the (verifiable) fact that ψ is increasing w.r.t. p_A and p_B.

Firstly, denote $\delta_n^A \triangleq p_{A_n} - p_{A_{n+1}}$ and $\delta_n^B \triangleq p_{B_n} - p_{B_{n+1}}$ as the difference between the nth and $(n+1)$th iterations. Note that $\boldsymbol{P}^\star$, satisfying the conditions listed in the Lemma, minimizes δ_{A_n} and δ_{B_n} in each iteration step (for all n) and $p_{A_0} = p_{B_0} = 1$. Thus we can write:

$$\boldsymbol{P}^\star = _{\boldsymbol{P}\in P} (\sum_n \delta_n^A) = _{\boldsymbol{P}\in \mathbb{P}} (1 - \sum_n \delta_n^A) = _{\boldsymbol{P}\in \mathbb{P}}\ p_A, \tag{3.5}$$

where the last step follows from the fact that $p_{A_0} = 1$ and the changes in p_A for each iteration n is denoted by δ_n^A. Similar argument holds for p_B. Thus we can observe that $\boldsymbol{P}^\star$ maximizes both p_A and p_B. Secondly, it can be easily verified that ψ is increasing w.r.t. p_A and p_B. Furthermore, $\boldsymbol{P}^\star$ maximizes ψ for any fixed p_A and p_B. Combining these, it can be concluded that $\boldsymbol{P}^\star$ maximizes ψ.

Remark: The above discussion indicates that the maximization of robustness of a network can be achieved theoretically if we can find an interdependence structure $\boldsymbol{P}^\star$ satisfying the (strong) conditions in Lemma 3.4.1. For networks where such an optimal ordering cannot be found, the tools described in this dissertation are insufficient for obtaining the optimal interdependence structures. However, it will be shown below that for several cases, including the complete one-to-one interdependence, such an optimal $\boldsymbol{P}^\star$ can be found.

To prove the main result in this section, we need the following technical result:

Lemma 3.4.2 *For any two sequences of real numbers, $\{x_1, x_2, \cdots, x_n\}$ and $\{y_1, y_2, \cdots, y_n\}$ which are monotonic in the same sense and any permutation ρ of $\{1, 2, \cdots, n\}$*

$$x_n y_1 + \cdots + x_1 y_n \le x_{\rho_1} y_1 + \cdots + x_{\rho_n} y_n \le x_1 y_1 + \cdots + x_n y_n, \tag{3.6}$$

where ρ_i is the ith element of ρ.

This is referred to in literature as the Rearrangement Inequality. A proof can be found in [Har52].

Theorem 3.4.3 *For the one-to-one structure with complete interdependence, the optimal interdependence structure, for both single-layer and double-layer randomized attack, is the matching of nodes by their intra-layer degrees in the monotonic order. Furthermore, the anti-monotonic arrangement of nodes is the worst possible interdependence structure.*

Note that the system equations given by (3.2) and (3.3) were derived for the double-layer attack. Thus we focus on this case initially. Lemma 3.4.1 indicates that if we can find a $\boldsymbol{P}^\star$ which satisfies all the maximization criteria presented therein, such a $\boldsymbol{P}^\star$ would also maximize the network robustness measured by ψ. Here we would prove that for a general mixed quadratic form $\boldsymbol{a}^T\boldsymbol{P}\boldsymbol{b}$, where $\boldsymbol{a}$ and $\boldsymbol{b}$ are decreasingly sorted column vectors and $\boldsymbol{P}$ is a doubly stochastic matrix:

$$\boldsymbol{I} = _{\boldsymbol{P}\in\mathbb{P}}\, \boldsymbol{a}^T\boldsymbol{P}\boldsymbol{b}. \tag{3.7}$$

It can also be observed that proving the above equation is equivalent to proving each of the criteria described in Lemma 3.4.1 since both $\boldsymbol{a}_i$'s and $\boldsymbol{b}_i$'s, where $i=(1,2)$, are decreasingly sorted column vectors. Although the value of p_A and p_B influences the magnitude of the terms in the column vectors $\boldsymbol{a}_i$'s and $\boldsymbol{b}_i$'s, the decreasing nature of the vectors is always guaranteed. Denoting a permutation matrix by $\boldsymbol{P}_j$, i.e. doubly stochastic matrices of 0's and 1's, and α_j as the corresponding scalar weights, according to Birkhoff's Theorem [**birkhoff**]: $\boldsymbol{P}=\sum_{j=1}^{N!}\alpha_j\boldsymbol{P}_j$, where α_j's are non-negative, $\sum_j\alpha_j=1$, and $N!$ is the number of possible permutation matrices. Thus we can write:

$$\boldsymbol{P}^\star = _{\boldsymbol{P}\in\mathbb{P}}\, \boldsymbol{a}^T\boldsymbol{P}\boldsymbol{b} = _{\boldsymbol{P}\in\mathbb{P}}\, \boldsymbol{a}^T\left(\sum_{j=1}^{N!}\alpha_j\boldsymbol{P}_j\right)\boldsymbol{b} = _{\boldsymbol{P}\in\mathbb{P}}\, \sum_{j=1}^{N!}\alpha_j\boldsymbol{a}^T\boldsymbol{P}_j\boldsymbol{b}. \tag{3.8}$$

Let ρ_j denote the ordering corresponding to the permutation matrix P_j, and a_i and b_i denote the ith elements of $\boldsymbol{a}$ and $\boldsymbol{b}$, respectively. It can be verified that the terms $\boldsymbol{a}^T\boldsymbol{P}_j\boldsymbol{b}$ are nothing but the various possible sequence pairings as considered in the Rearrangement Inequality in Lemma 5.4.4, i.e. $\boldsymbol{a}^T\boldsymbol{P}_j\boldsymbol{b}=\sum_{i=1}^{N}a_{\rho_j(i)}b_i$, where $\rho_j(i)$ is the ith element of the ordering ρ_j. Thus we can write:

$$\sum_{j=1}^{N!}\alpha_j\boldsymbol{a}^T\boldsymbol{P}_j\boldsymbol{b} = \sum_{j=1}^{N!}\alpha_j\left(\sum_{i=1}^{N}a_i b_{\rho_j(i)}\right). \tag{3.9}$$

Since $\sum_j\alpha_j=1$, invoking Lemma 5.4.4 we can write the following inequality:

$$\boldsymbol{a}^T\boldsymbol{I}^\dagger\boldsymbol{b} \le \sum_{j=1}^{N!}\alpha_j\boldsymbol{a}^T\boldsymbol{P}_j\boldsymbol{b} \le \boldsymbol{a}^T\boldsymbol{I}\boldsymbol{b}, \tag{3.10}$$

where $\boldsymbol{I}^\dagger$ is the ordering corresponding to the anti-monotonic arrangement, i.e. ith highest degree node in layer A coupled to ith lowest degree node in layer B, and $\boldsymbol{I}$ is the $N\times N$ identity matrix

corresponding to the monotonic arrangement. This proves that $\boldsymbol{P}^\star = \boldsymbol{I}$ maximizes and $\boldsymbol{P}^\star = \boldsymbol{I}^\dagger$ minimizes the mixed scalar terms $\boldsymbol{a}^T \boldsymbol{P}^\star \boldsymbol{b}$ measuring the network robustness.

For the case of single-layer attack, let us assume without loss of generality that layer A is subject to the initial attack. This implies that the probability of a node in layer B to survive the initial attack is 1. Thus the system equations can be written in the same form as:

$$\psi_A = \frac{\boldsymbol{a}_1^T \boldsymbol{P} \boldsymbol{b}'_1}{N} = \psi_B, \quad p_A = \frac{\boldsymbol{a}_2^T \boldsymbol{P} \boldsymbol{b}'_1}{N}, \quad p_B = \frac{\boldsymbol{a}_1^T \boldsymbol{P} \boldsymbol{b}'_2}{N}, \tag{3.11}$$

where $\boldsymbol{a}_1$ and $\boldsymbol{a}_2$ are defined in Eqn.s (3.2) and (3.3), while $\boldsymbol{b}'_1 = [b'_{11} \cdots b'_{1N}]^T$ with $b'_{1i} \triangleq (1-(1-p_B)^{k_i^{\{B\}}})$ and $\boldsymbol{b}'_2 = [b'_{21} \cdots b'_{2N}]^T$ with $b'_{2i} \triangleq k_i^{\{B\}}[1-(1-p_B)^{k_i^{\{B\}}-1}]/\lambda_B$. It can be verified that both $\boldsymbol{a}_i$'s and $\boldsymbol{b}'_i$'s $(i = (1,2))$ are still decreasingly sorted column vectors and thus the arguments presented above for the double-layer attack case hold true for this case as well. Thus the monotonic and anti-monotonic ordering of interdependent nodes are still the best and worst structures, respectively.

Next we will state and prove another result which will be used in further analysis for obtaining the optimal interdependence structures for other system models.

Lemma 3.4.4 *Let* $\boldsymbol{a} \triangleq \begin{bmatrix} a_1 & a_2 & \cdots & a_N \end{bmatrix}^T$ *and* $\boldsymbol{b} \triangleq \begin{bmatrix} b_1 & b_2 & \cdots & b_N \end{bmatrix}^T$ *be decreasingly sorted column vectors and* $\boldsymbol{\Phi} = [\phi_{ij}]$ *is a matrix with the following properties:*

- $0 \leq |\phi_{ij}| \leq 1$
- *Row-sums and column-sums of* $\boldsymbol{\Phi}$ *are 0*
- *Diagonal elements of* $\boldsymbol{\Phi}$ *are non-negative, i.e.* $\phi_{ij} \geq 0$ *if* $i = j$
- *Off-diagonal elements of* $\boldsymbol{\Phi}$ *are non-positive, i.e.* $\phi_{ij} \leq 0$ *if* $i \neq j$.

The mixed quadratic forms are always positive, i.e. $\boldsymbol{a}^T \boldsymbol{\Phi} \boldsymbol{b} \geq 0$.

Let us assume that for some $\boldsymbol{\Phi}$ satisfying the properties mentioned above, $\boldsymbol{a}^T \boldsymbol{\Phi} \boldsymbol{b} < 0$. Adding $\boldsymbol{a}^T \boldsymbol{I} \boldsymbol{b}$ to the negative of this gives us: $\boldsymbol{a}^T (\boldsymbol{I} - \boldsymbol{\Phi}) \boldsymbol{b} > \boldsymbol{a}^T \boldsymbol{I} \boldsymbol{b}$. Furthermore, since row and column sums of $\boldsymbol{\Phi}$ is 0, $(\boldsymbol{I} - \boldsymbol{\Phi})$ is a doubly stochastic matrix. However, we proved in Theorem 3.4.3 that $\boldsymbol{I} = \max_{\boldsymbol{P} \in P} \boldsymbol{a}^T \boldsymbol{P} \boldsymbol{b}$, which is in contradiction with the above inequality. This shows that there cannot exist any $\boldsymbol{\Phi}$ with the properties defined above where $\boldsymbol{a}^T \boldsymbol{\Phi} \boldsymbol{b} < 0$. Thus the lemma follows.

3.4.2 One-to-Many Structure

In this section we extend our study to one-to-many interdependence, where the two layers of the network have different sizes, $|A| = N$ and $|B| = M = cN$, with $|l|$ denoting the number of nodes in layer l, and c is an integral constant. Due to the difference in the size of the two network layers, our previous assumption that every node is coupled to one node in the other layer will not hold. Thus the interdependence matrix $\boldsymbol{P} = [p_{ij}]$ is neither a square matrix nor is it doubly stochastic. However utilizing the completely interdependent network structure, we can obtain certain conditions which

$\boldsymbol{P}$ needs to satisfy. As we are dealing with the complete one-to-many interdependence, every node in layer B (the larger layer) should be coupled to one node in layer A. Thus the column sums of $\boldsymbol{P}$ is still 1, i.e. $\sum_j p_{ij} = 1$. For simplicity of analysis, we impose the additional constraint that the row-sums of $\boldsymbol{P}$ are all equal to c, the ratio of the sizes of the two network layers. This assumption imposes the regularity in the structure of the interdependence as it implies that all nodes $a \in A$ are coupled to the same number of nodes ($= c$) in layer B. As done previously, defining $a_{1i} \triangleq \eta(1-(1-p_A)^{k_i^{\{A\}}})$, $b_{1i} \triangleq \eta(1-(1-p_B)^{k_i^{\{B\}}})$, $a_{2i} \triangleq \eta k_i^{\{A\}}[1-(1-p_A)^{k_i^{\{A\}}-1}]/\lambda_A$, and $b_{2i} \triangleq \eta k_i^{\{B\}}[1-(1-p_B)^{k_i^{\{B\}}-1}]/\lambda_B$, the system equations can be written as:

$$\psi_A = \frac{\boldsymbol{a}_1^T \boldsymbol{P} \boldsymbol{b}_1}{N}, \qquad \psi_B = \frac{\boldsymbol{b}_1^T \boldsymbol{P}^T \boldsymbol{a}_1}{M}, \tag{3.12}$$

$$p_A = \frac{\boldsymbol{a}_2^T \boldsymbol{P} \boldsymbol{b}_1}{N}, \qquad p_B = \frac{\boldsymbol{b}_2^T \boldsymbol{P}^T \boldsymbol{a}_1}{M}. \tag{3.13}$$

Thus the system equations essentially are of the same form as that in the case of one-to-one interdependence with the only difference that $\boldsymbol{P}$ is an $N \times M$ matrix whose row-sums are c.

Theorem 3.4.5 *For an interdependent network with one-to-many interdependence and a probabilistic interdependence structure $\boldsymbol{P}$ characterized by equal row-sums (= an arbitrary constant c) and equal column-sums (= 1), the optimal interdependence, for both single-layer and double-layer randomized attacks, is given by: $\boldsymbol{P}^\star = [\boldsymbol{I}|\boldsymbol{I}|\cdots|\boldsymbol{I}]$, where $\boldsymbol{I}$ is the identity matrix of size $N \times N$ and $\boldsymbol{P}^\star$ is of size $N \times M$, where $M = cN$.*

As done in the case of one-to-one interdependence, we will start with the double-layer randomized attack and extend the arguments to the single-layer case. We will prove this theorem by contradiction. Let us assume there exists a $\boldsymbol{P}^\dagger \neq \boldsymbol{P}^\star$, s.t. $\boldsymbol{a}^T \boldsymbol{P}^\dagger \boldsymbol{b} \geq \boldsymbol{a}^T \boldsymbol{P} \boldsymbol{b}\ \forall\ \boldsymbol{P} \in P_{N\times M}$, where $\boldsymbol{a}$ and $\boldsymbol{b}$ are decreasingly sorted column vectors, and $P_{N\times M}$ is the set of all matrices of non-negative elements whose row-sums are c and column-sums are 1. Thus $\boldsymbol{P}^\dagger$ is the optimal interdependence structure. Since $\boldsymbol{P}^\dagger \neq \boldsymbol{P}^\star$, we have that at least one of the $N \times N$ sub-matrices of $\boldsymbol{P}^\dagger$ is not $\boldsymbol{I}_{N\times N}$. Let this $N \times N$ sub-matrix be denoted by $\boldsymbol{R}$ and let us represent $\boldsymbol{P}^\dagger$ as: $\boldsymbol{P} = [\boldsymbol{P}_1|\boldsymbol{P}_2|\cdots|\boldsymbol{R}|\cdots|\boldsymbol{P}_c]$, where $\boldsymbol{P}_i$'s are all $N \times N$ sub-matrices. Let us consider a transformation in $\boldsymbol{R}$ involving a movement towards the diagonal elements, i.e. we want to transform $\boldsymbol{R}$ into $\tilde{\boldsymbol{R}}$ such that the diagonal elements in $\tilde{\boldsymbol{R}}$ are greater than or equal to the diagonal elements of $\boldsymbol{R}$. This can be mathematically represented as:

$$\tilde{\boldsymbol{R}}_{ij} = \begin{cases} \boldsymbol{R}_{ij} + X_i & \text{if } i = j \\ \boldsymbol{R}_{ij} - \phi_{ij} & \text{if } i \neq j \end{cases} \tag{3.14}$$

where X_i's are the non-negative increments ($0 \leq X_i \leq 1$) of the diagonal elements and ϕ_{ij}'s are the non-negative decrements ($0 \leq \phi_{ij} \leq 1$) of the off-diagonal elements following the relationship:

$$X_i = \sum_{\substack{j=1 \\ j\neq i}}^{N} \phi_{ij} = \sum_{\substack{j=1 \\ j\neq i}}^{N} \phi_{ji}. \tag{3.15}$$

Thus the robustness for this transformed interdependence structure is given by:

$$\tilde{\psi} = \boldsymbol{a}^T \tilde{\boldsymbol{P}} \boldsymbol{b} = \boldsymbol{a}^T [\boldsymbol{P}_1 | \boldsymbol{P}_2 | \cdots | \tilde{\boldsymbol{R}} | \cdots | \boldsymbol{P}_c] \boldsymbol{b} \tag{3.16}$$

$$= \boldsymbol{a}^T [\boldsymbol{P}_1 | \boldsymbol{P}_2 | \cdots | \boldsymbol{R} | \cdots | \boldsymbol{P}_c] \boldsymbol{b} + \boldsymbol{a}^T [\boldsymbol{0} | \boldsymbol{0} | \cdots | (\tilde{\boldsymbol{R}} - \boldsymbol{R}) | \cdots | \boldsymbol{0}] \boldsymbol{b} \tag{3.17}$$

$$= \boldsymbol{a}^T \boldsymbol{P} \boldsymbol{b} + \boldsymbol{a}^T \begin{bmatrix} [c\,c\,c\,c] X_1 & -\phi_{12} & \dots & -\phi_{1N} \\ -\phi_{21} & X_2 & \dots & -\phi_{2N} \\ \vdots & \vdots & \vdots & \vdots \\ -\phi_{N1} & -\phi_{N2} & \dots & X_N \end{bmatrix} \boldsymbol{b}^\dagger = \psi + \boldsymbol{a}^T \boldsymbol{X} \boldsymbol{b}^\dagger, \tag{3.18}$$

where $\boldsymbol{b}^\dagger$ is the $N \times 1$ component of $\boldsymbol{b}$ corresponding to the sub-matrix $(\tilde{\boldsymbol{R}} - \boldsymbol{R})$, ψ is the network robustness for the interdependence structure $\boldsymbol{P}$, and $\boldsymbol{X} = \tilde{\boldsymbol{R}} - \boldsymbol{R}$. It can be observed that $\boldsymbol{X}$ satisfies the conditions of Lemma 3.4.4 and thus $\boldsymbol{a}^T \boldsymbol{X} \boldsymbol{b}^\dagger \geq 0$, since $\boldsymbol{a}$ and $\boldsymbol{b}^\dagger$ are decreasingly sorted column vectors. Thus we have $\tilde{\psi} \geq \psi$. This indicates that $\boldsymbol{P}^\dagger$ is not the optimal interdependence structure as $\boldsymbol{a}^T \tilde{\boldsymbol{P}} \boldsymbol{b} \geq \boldsymbol{a}^T \boldsymbol{P}^\dagger \boldsymbol{b}$.

The above discussion shows that as long as $\boldsymbol{P}^\dagger \neq \boldsymbol{P}^\star$, $\boldsymbol{P}^\dagger$ will always have an $N \times N$ sub-matrix which can be transformed to obtain a $\tilde{\boldsymbol{P}}$, which has a higher robustness than $\boldsymbol{P}^\dagger$. Thus we can conclude that:

$$\boldsymbol{P}^\star =_{\boldsymbol{P}} \boldsymbol{a}^T \boldsymbol{P} \boldsymbol{b} = [\boldsymbol{I} | \boldsymbol{I} | \cdots | \boldsymbol{I}], \tag{3.19}$$

where $\boldsymbol{I}$ is the identity matrix of size $N \times N$, which is repeated c times.

Similar to the case of completely interdependent networks with one-to-one interdependence structure, it can be verified that under a single-layer attack (assuming layer A is attacked without loss of generality) the system equations are in the same form as those for the case of the double-layer attack, with the only difference being in the elements of the column vectors $\boldsymbol{b}_1$ and $\boldsymbol{b}_2$. It can be verified for this case that a change from a double-layer attack to a single-layer attack does not alter the nature of the system equation w.r.t. the interdependence structure because it essentially only influences the scaling. Thus all results derived above hold true under the single-layer attack.

3.5 Analysis: Partial Interdependence

In this section, we will generalize our system model to analyze partially interdependent networks where the N nodes in each layer of the network can be divided into two sets: a) autonomous nodes, which do not require support from the other layer, and b) interdependent nodes, which require support from nodes of the other layer. The nature of interdependence between the two layers is still taken to be one-to-one as is shown in Fig. 3.2. Let us define $\boldsymbol{Q_A}$ and $\boldsymbol{Q_B}$ as the allocation strategy for the two layers, i.e. $\boldsymbol{Q_A}$ and $\boldsymbol{Q_B}$ are diagonal matrices whose diagonal elements are given by column vectors of the form $[q_1 q_2 \cdots q_N]^T$ with:

$$q_i = \begin{cases} 1 & \text{if } a_i \text{ or } b_i \text{ is autonomous} \\ 0 & \text{if } a_i \text{ or } b_i \text{ is interdependent,} \end{cases} \tag{3.20}$$

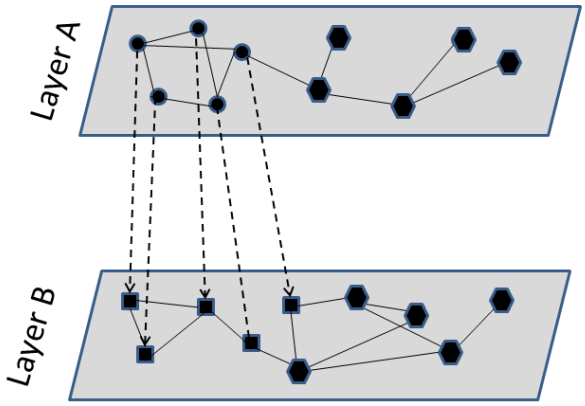

Figure 3.2 Interdependent system model: one-to-one structure with partial interdependence. Hexagonal nodes are autonomous, while the rest are interdependent.

where a_i and b_i are the nodes with the ith highest intra-layer degree in layers A and B, respectively. Thus the system equations for this case can be written as:

$$\psi_A = \frac{(\boldsymbol{Q_A a}_1)^T \mathbf{1}}{N} + \frac{(\bar{\boldsymbol{Q}}_{\boldsymbol{A}} \boldsymbol{a}_1)^T \boldsymbol{P} (\bar{\boldsymbol{Q}}_{\boldsymbol{B}} \boldsymbol{b}_1)}{N}, \qquad \psi_B = \frac{\mathbf{1}^T (\boldsymbol{Q_B b}_1)}{N} + \frac{(\bar{\boldsymbol{Q}}_{\boldsymbol{A}} \boldsymbol{a}_1)^T \boldsymbol{P} (\bar{\boldsymbol{Q}}_{\boldsymbol{B}} \boldsymbol{b}_1)}{N}, \tag{3.21}$$

$$p_A = \frac{(\boldsymbol{Q_A a}_2)^T \mathbf{1}}{N} + \frac{(\bar{\boldsymbol{Q}}_{\boldsymbol{A}} \boldsymbol{a}_2)^T \boldsymbol{P} (\bar{\boldsymbol{Q}}_{\boldsymbol{B}} \boldsymbol{b}_1)}{N}, \qquad p_B = \frac{\mathbf{1}^T (\boldsymbol{Q_B b}_2)}{N} + \frac{(\bar{\boldsymbol{Q}}_{\boldsymbol{A}} \boldsymbol{a}_1)^T \boldsymbol{P} (\bar{\boldsymbol{Q}}_{\boldsymbol{B}} \boldsymbol{b}_2)}{N}, \tag{3.22}$$

where $\mathbf{1}$ is the column vector of all ones of length N (size of network layers), and $\boldsymbol{a}_i$'s and $\boldsymbol{b}_i$'s ($i = 1, 2$) are column vectors defined previously in Section 3.2. $\bar{\boldsymbol{Q}}_{\boldsymbol{l}}$ is the complementary allocation strategy denoting the interdependent nodes in layer l, which can be obtained by interchanging 0's and 1's in the diagonal of $\boldsymbol{Q_l}$. Note that the two components in the system equations correspond to the contribution of autonomous and interdependent nodes towards network robustness.

The problem of obtaining the optimal interdependence structure in this case is considerably more complicated than the complete interdependence case because we have to consider the joint optimization of the allocation of nodes ($\boldsymbol{Q_A}$ and $\boldsymbol{Q_B}$) and the interdependence structure ($\boldsymbol{P}$). In this case, as will be evidenced below, it is usually not feasible to optimize the MCC for both layers (ψ_A and ψ_B) simultaneously. Instead, we will endeavor to achieve a pareto-optimal robustness which cannot be strictly dominated by any other interdependence structure.

Theorem 3.5.1 *Given any $\boldsymbol{Q_A}$ and $\boldsymbol{Q_B}$, the optimal interdependence structure is $\boldsymbol{P}^\star = \boldsymbol{I}$.*

It can be observed from the system equations (3.21)-(3.22), that the interdependence structure $\boldsymbol{P}$ only influences the contribution of the interdependent nodes in the network. Focusing on the case of maximization of ψ_A, we can write:

$$\boldsymbol{P}^\star = {}_{\boldsymbol{P}\in\mathbb{P}}\, \psi_A = {}_{\boldsymbol{P}\in\mathbb{P}}\, \frac{(\bar{\boldsymbol{Q}}_{\boldsymbol{A}} \boldsymbol{a}_1)^T \boldsymbol{P} (\bar{\boldsymbol{Q}}_{\boldsymbol{B}} \boldsymbol{b}_1)}{N}. \tag{3.23}$$

It can be concluded from the above equation that any element $p_{ij} \in \boldsymbol{P}$ would contribute to ψ only if both $a_i \in A$ and $b_j \in B$ are allocated to the interdependent set of nodes. Let $\tilde{\boldsymbol{a}}_{\mathbf{1}}$ and $\tilde{\boldsymbol{b}}_{\mathbf{1}}$ denote the non-zero components of the column vectors $\bar{\boldsymbol{Q}}_{\boldsymbol{A}}\boldsymbol{a}_1$ and $\bar{\boldsymbol{Q}}_{\boldsymbol{B}}\boldsymbol{b}_1$. Similarly, we define $\tilde{\boldsymbol{P}}$ to be the reshaped interdependence matrix obtained by removing rows and columns from $\boldsymbol{P}$ corresponding to zero elements in $\bar{\boldsymbol{Q}}_{\boldsymbol{A}}\boldsymbol{a}_1$ and $\bar{\boldsymbol{Q}}_{\boldsymbol{B}}\boldsymbol{b}_1$. Thus we can write: Due to our indexing of nodes in the decreasing order of their intra-layer degrees, it can be concluded that the elements of the column vectors $\tilde{\boldsymbol{a}}_{\mathbf{1}}$ and $\tilde{\boldsymbol{b}}_{\mathbf{1}}$ are still decreasingly sorted. Thus by using the technique used for proving Theorem 3.4.3, we can show that $\boldsymbol{I} = _{\boldsymbol{P}\in P}\, \tilde{\boldsymbol{a}}_{\mathbf{1}}\tilde{\boldsymbol{P}}\tilde{\boldsymbol{b}}_{\mathbf{1}}$. Furthermore, it can be verified that the above analysis can be applied to all cases $(\psi_A, \psi_B, p_A, p_B)$ given by (3.21) and (3.22) and thus $\boldsymbol{P}^\star = \boldsymbol{I}$ maximizes the robustness of partially interdependent networks for any given allocation strategy.

Theorem 3.5.1 essentially allows us to decouple the joint maximization problem which was discussed previously. This is due to the fact that since the optimal ordering of nodes in Y is independent of the allocation strategy, we can look at these two optimization problems individually. Thus the problem of identifying the optimal interdependence structure reduces to the problem of identifying the optimal allocation strategy $\boldsymbol{Q}^\star_{\boldsymbol{A}}$ and $\boldsymbol{Q}^\star_{\boldsymbol{B}}$, as $\boldsymbol{P}^\star = \boldsymbol{I}$ for any $\boldsymbol{Q}_{\boldsymbol{A}}$ and $\boldsymbol{Q}_{\boldsymbol{B}}$. Since the optimal interdependence structure ($\boldsymbol{P}^\star = \boldsymbol{I}$) maximizes the network robustness for any allocation strategy $\boldsymbol{Q}_{\boldsymbol{A}}$ and $\boldsymbol{Q}_{\boldsymbol{B}}$, we can write the system equations as:

$$\psi_A = \frac{1}{N}\Big(\sum_{i=1}^{N} q_i^{\{A\}} a_{1i} + \sum_{i=1}^{N} \bar{q}_i^{\{A\}} a_{1i} \bar{q}_i^{\{B\}} b_{1i}\Big), \quad \psi_B = \frac{1}{N}\Big(\sum_{i=1}^{N} q_i^{\{B\}} b_{1i} + \sum_{i=1}^{N} \bar{q}_i^{\{A\}} a_{1i} \bar{q}_i^{\{B\}} b_{1i}\Big), \tag{3.24}$$

$$p_A = \frac{1}{N}\Big(\sum_{i=1}^{N} q_i^{\{A\}} a_{2i} + \sum_{i=1}^{N} \bar{q}_i^{\{A\}} a_{2i} \bar{q}_i^{\{B\}} b_{1i}\Big), \quad p_B = \frac{1}{N}\Big(\sum_{i=1}^{N} q_i^{\{B\}} b_{2i} + \sum_{i=1}^{N} \bar{q}_i^{\{A\}} a_{1i} \bar{q}_i^{\{B\}} b_{2i}\Big), \tag{3.25}$$

where $a_{1/2i}$'s and $b_{1/2i}$'s are the elements of the column vectors $\boldsymbol{a}_{1/2}$ and $\boldsymbol{b}_{1/2}$ defined earlier in Section 3.2, while $q_i^{\{l\}}$ and $\bar{q}_i^{\{l\}}$ denotes the ith diagonal element of the allocation matrices $\boldsymbol{Q}_{\boldsymbol{l}}$ and $\bar{\boldsymbol{Q}}_{\boldsymbol{l}}$, respectively. Focusing on the objective function for p_A in (3.25) and noticing that the first term is independent of $\boldsymbol{Q}_{\boldsymbol{B}}$, we observe that the allocation strategy maximizing the first component of p_A would be to allocate the highest degree nodes $a \in A$ to X as $a_{2i} > a_{2i} \cdot b_{1i}$ due to the fact that $b_{1i} \leq 1$. For maximization of the interdependent (second) component, the highest degree nodes $b \in B$ should be allocated to Y. On the contrary, individual maximization of p_B in (3.25) leads to the opposite allocation strategy: putting the highest degree nodes $a \in A$ to Y and the highest degree nodes $b \in B$ to X. This argument also holds for the case of ψ_A and ψ_B given by (3.24). It can be clearly observed here that there exists a conflict of interest between the maximization strategies for layers A and B, which is why we cannot obtain a joint maximization, in contrast to the previously analyzed cases. Instead we have looked at the problem of obtaining a pareto-optimal allocation strategy w.r.t. the two layers, where we are interested in obtaining an allocation strategy $\boldsymbol{Q}^\star_{\boldsymbol{A}}$ and $\boldsymbol{Q}^\star_{\boldsymbol{B}}$ such that no other strategy can lead to an increase in the robustness of both layers. We have used the Nash Bargaining framework to solve this problem.

3.5.1 Description of Nash Bargaining Problem

We provide a brief description of the Nash Bargaining Problem here. Let $\boldsymbol{P} = \{1, 2, \cdots, P\}$ be the set of players involved in the bargaining game. Let $\boldsymbol{S}$ be a closed convex subset of $\mathbb{R}^P$ representing the set of all possible pay-offs which can be received by the different players participating in the bargaining game. Let $\boldsymbol{d} = \{d_1, d_2, \cdots, d_P\}$ denote the set of dis-agreement pay-offs for the P players, representing the pay-offs that the various players will receive if they do not reach a mutual agreement through the bargaining game. The pair $(\boldsymbol{S}, \boldsymbol{d})$ is called a P-person bargaining problem. Multiple kinds of co-operative game solutions to the bargaining problem exist in literature [Owe]. One of the most popular ones among them is the Nash Bargaining Solution (NBS) as it provides a unique and fair pareto-optimal solution to the bargaining problem. Next, we will formally define the Nash-Bargaining Solution.

Lemma 3.5.2 *$\boldsymbol{s}^\star = \phi(\boldsymbol{S}, \boldsymbol{d})$ is said to be a NBS for the bargaining problem $(\boldsymbol{S}, \boldsymbol{d})$, if it satisfies the following axioms:*

1. *Feasibility: $\boldsymbol{s}^\star \in \boldsymbol{S}$.*
2. *Individual Rationality: $s_i^\star \geq d_i \ \forall \ i$, where $s_i^\star$ is the pay-off received by the i th player.*
3. *Pareto Optimality: There does not exist any $\boldsymbol{s} \in S$ such that $\boldsymbol{s} \succ \boldsymbol{s}^\star$, i.e. no other solution can strictly dominate the NBS thus leading to a better pay-off for all players. Therefore the solution $\boldsymbol{s}^\star$ should be such that $s_i^\star$ cannot be increased without decreasing $s_j^\star$ for some $j \neq i$, i.e. there is no alternative allocation which can result in a higher pay-off for all players.*
4. *Independence of Irrelevant Alternatives: Let the solution to the bargaining problem $(\boldsymbol{S}, \boldsymbol{d})$ be denoted by $\phi(\boldsymbol{S}, \boldsymbol{d})$. If $\boldsymbol{s}^\star = \phi(\boldsymbol{S}, \boldsymbol{d})$ and $\boldsymbol{s}^\star \in \boldsymbol{S}' \subset \boldsymbol{S}$, then $\boldsymbol{s}^\star = \phi(\boldsymbol{S}', \boldsymbol{d})$.*
5. *Independence of Linear Transformation: For any linear scale transformation τ, $\tau(\phi(\boldsymbol{S}, \boldsymbol{d})) = \phi(\tau(\boldsymbol{S}), \tau(\boldsymbol{d}))$.*
6. *Symmetry: If the players of the game are indistinguishable, $s_i^\star = s_j^\star \ \forall \ i, j \in \boldsymbol{P}$.*

Furthermore, the solution point satisfying the above axioms is unique and can be obtained by solving the following maximization problem:

$$\boldsymbol{s}^\star = \phi(\boldsymbol{S}, \boldsymbol{d}) = \underset{\boldsymbol{s} \in \boldsymbol{S}, s_i \geq d_i \ \forall \ i}{} \prod_{i=1}^{P} (s_i - d_i). \tag{3.26}$$

It is shown in Lemma 3.5.2 that any solution point which satisfies the six axioms is the Nash Bargaining Solution. We will use this idea to obtain the pareto-optimal node allocation for networks with partial interdependence.

Theorem 3.5.3 *For the one-to-one structure with partial interdependence, where the allocation strategies $\boldsymbol{Q_A}$ and $\boldsymbol{Q_B}$ have an arbitrary fixed number of 1's (= q) in the diagonals, the allocation*

strategy leading to a pareto-optimal robustness of the two network layers against both the single-layer and double-layer randomized attacks is: $\boldsymbol{Q}^{\star}_{\boldsymbol{A}} = \boldsymbol{Q}^{\star}_{\boldsymbol{B}} = diag([1,1,\cdots,1,0,0,\cdots,0])$*, where the number of non-zero diagonal elements in* $\boldsymbol{Q}^{\star}_{\boldsymbol{A}}$ *and* $\boldsymbol{Q}^{\star}_{\boldsymbol{B}}$ *is* q*.*

Starting with the double-layer attack case, we formulate the optimal allocation problem as a bargaining problem:

- The two players involved in the bargaining game are layers A and B.
- The set of possible agreements or the set of possible allocation strategies is of the form:

$$\boldsymbol{F} = \begin{pmatrix} q_1^{\{A\}} & q_2^{\{A\}} & \cdots & q_N^{\{A\}} \\ q_1^{\{B\}} & q_2^{\{B\}} & \cdots & q_N^{\{B\}} \end{pmatrix}$$

  where N is the number of nodes in each layer of the network, and the elements of the matrix can be written as:

$$q_i^{\{l\}} = \begin{cases} 1, \text{ if } i\text{th node in layer } l \text{ is autonomous,} \\ 0, \text{ if } i\text{th node in layer } l \text{ is interdependent.} \end{cases}$$

  As both layers have q autonomous nodes, the set of possible agreements is the set of all $\boldsymbol{F}$'s such that the two row-sums of F are both q.

- The utility functions for the two players is given by (3.25) and denoted by u_1 and u_2, respectively, which maps an allocation profile corresponding to $\boldsymbol{F}$ to the utility for each player:

$$u_1(\boldsymbol{F}) = \frac{1}{N}\Big(\sum_{i\in X_1} a_{2i} + \sum_{i\in Y_1, j\in Y_2} a_{2i}\, b_{1j}\Big), \tag{3.27}$$

$$u_2(\boldsymbol{F}) = \frac{1}{N}\Big(\sum_{i\in X_2} b_{2i} + \sum_{i\in Y_2, j\in Y_1} a_{1j}\, b_{2i}\Big), \tag{3.28}$$

  where X_1, X_2 denote the set of autonomous nodes in layers A and B, respectively; whereas Y_1 and Y_2 denote the set of interdependent nodes in the two layer. Note that the second summation is over all interdependence links in the network.

- Let us define the disagreement pay-off $\boldsymbol{d} = [d_1, d_2]$, where d_1 and d_2 are the pay-offs received by the two players if an agreement is not reached. Both d_1 and d_2 are taken to be the case where nodes are chosen to be autonomous or interdependent randomly, i.e. if the two players fail to arrive at an agreement after the bargaining process then a random allocation strategy would be adopted.
- The set of possible pay-offs is denoted by $\boldsymbol{U}$, which can be defined as:

$$\boldsymbol{U} = \{(v_1, v_2) | u_1(x) = v_1, u_2(x) = v_2 \text{ for some } x \in F\}. \tag{3.29}$$

Note here that the utility functions for both players (u_1, u_2) described by (3.27)-(3.28) are bounded above and below $(u_i(x) \in [0,1] \; \forall \; i)$ and thus have non-empty and closed support with a convex hull, which is necessary for the existence of a Nash Bargaining Solution.

- The Bargaining Problem is thus represented as $(\boldsymbol{U}, \boldsymbol{d})$ over the space of possible agreements $\boldsymbol{F}$.

It is known that a solution to such Bargaining Problems has to satisfy the six axioms described in Lemma 3.5.2 in Appendix 3.5.1. Let us take a particular allocation strategy for the two layers, where the nodes of highest degrees in both layers of the network are autonomous. We want to show that this allocation strategy satisfies all the axioms of Nash Bargaining Solutions (N.B.S.). As we have indexed the nodes in the network in the decreasing order of their intra-layer degrees, we can describe the allocation strategy defined above in terms of $\boldsymbol{F}$ as :

$$\boldsymbol{F}^\star = \begin{pmatrix} 1 & 1 & \cdots & 1 & 0 & 0 & \cdots & 0 \\ 1 & 1 & \cdots & 1 & 0 & 0 & \cdots & 0 \end{pmatrix}$$

where the number of 1's in each row of the allocation strategy is q. Let us now examine each of the six axioms for this particular solution.

- Feasibility: It can be clearly seen that the solution $(u_1(\boldsymbol{F}^\star), u_2(\boldsymbol{F}^\star)) \in \boldsymbol{U}$ and thus is feasible.

- Individual Rationality: At the dis-agreement point, nodes are allocated randomly. It can be easily examined that $u_i(\boldsymbol{F}^\star) \geq u_i(\boldsymbol{d})$ for both players $i = 1, 2$.

- Pareto Efficiency: A closer examination of the utility functions u_1 and u_2 defined by (3.27) and (3.28) reveals that it is always better to allocate a node to the autonomous set (X_1 and X_2) as $a_{2i} > a_{2i} b_{1i}$ and $b_{2i} > a_{1i} b_{2i}$. However since our particular solution allocates all highest degree nodes to X_1 and X_2, the only way of increasing the utility of a player (say player A) is by modifying the structure of interdependence, or in particular allocating nodes of higher degrees from layer B to Y_2. However, this will lead to a sub-optimal condition for player B by the same logic as before that $b_{2i} > b_{2i} a_{1i}$, i.e. from player B's perspective highest degree nodes of layer B should be allocated to X_2. Thus no other solution can strictly dominate $(u_1(\boldsymbol{F}^\star), u_2(\boldsymbol{F}^\star))$.

- Independence of Irrelevant Alternatives: Let us represent the solution to the Nash Bargaining problem $(\boldsymbol{U}, \boldsymbol{d})$ by $\phi(\boldsymbol{U}, \boldsymbol{d})$, i.e. $\phi(\boldsymbol{U}, \boldsymbol{d}) = (u_1(\boldsymbol{F}^\star), u_2(\boldsymbol{F}^\star))$. It can be trivially observed that $\phi(\boldsymbol{U}', \boldsymbol{d}) = (u_1(\boldsymbol{F}^\star), u_2(\boldsymbol{F}^\star))$ if $\boldsymbol{U'} \subset \boldsymbol{U}$ and $(u_1(\boldsymbol{F}^\star), u_2(\boldsymbol{F}^\star)) \in \boldsymbol{U}'$, i.e. if the new pay-off space $(\boldsymbol{U'})$ is a subset of $\boldsymbol{U}$ and contains $\phi(\boldsymbol{U}, \boldsymbol{d})$, $\phi(\boldsymbol{U'}, \boldsymbol{d}) = \phi(\boldsymbol{U}, \boldsymbol{d})$.

- Independence of Linear Transformation: It can be verified from (3.27) and (3.28) that for any player i

$$_{x \in \boldsymbol{F}} u_i(x) =_{x \in \boldsymbol{F}} \Big(\alpha \, u_i(x) + \beta \Big), \tag{3.30}$$

where (α, β) represents a linear transformation τ. As τ is independent of the allocation strategy, we can observe that the axiom holds true in this case.

- Symmetry: The symmetry condition occurs in this bargaining problem when $\lambda_A = \lambda_B$, i.e. two layers are identically distributed. Under this condition, the two players cannot be differentiated from one another. As the allocation strategy $\boldsymbol{F}^\star$ does not differentiate between the two layers, we can see that $u_1(\boldsymbol{F}^\star) = u_2(\boldsymbol{F}^\star)$ if $\lambda_A = \lambda_B$.

As the NBS is unique and the particular solution chosen by us satisfies all the six axioms, we can conclude that the particular solution is the NBS. To complete the proof, we need to verify that the particular solution leads to pareto-optimal robustness of ψ_A and ψ_B given by (3.24). Modeling (3.24) as the utility functions for the two players, we can obtain this result in a very similar way by showing that the same particular solution $\boldsymbol{F}^\star$ satisfies all axioms of NBS for this case and thus the theorem follows.

Under a single-layer attack (assuming layer A is attacked without loss of generality), the system equations can be written in the exact same form as (3.21)-(3.22) with the difference that the factor η is dropped from the elements of the column vectors $\boldsymbol{b}_1$ and $\boldsymbol{b}_2$. The main difference in terms of analysis is that the system equations loose their symmetry even for the case when $\lambda_A = \lambda_B$. However, since we intend to achieve a pareto-optimal solution to the robustness of the two layers, we can proceed as in the previous section to show that the five axioms (there is no symmetry in this case) are satisfied by the particular solution as given in Theorem 3.5.3. Thus the same result holds for the single-layer attack as well.

Remark: It is interesting to note here that this particular solution can be derived by obtaining the NBS under the symmetry condition of $\lambda_A = \lambda_B$, where the two layers of the network are identically distributed and thus the two players of the Nash Bargaining Problem cannot be differentiated from each other. It can be observed from (3.27)-(3.28) that under the symmetry condition, $u_1 = u_2 \; \forall \; x \in F$ and also $d_1 = d_2$, where d_1 and d_2 are the dis-agreement pay-offs for the two players. Thus we can write the NBS as:

$$\phi(\boldsymbol{U}, \boldsymbol{d}) = \max_{\boldsymbol{u} \in \boldsymbol{U}, u_i \geq d_i \forall i} (u_1 - d_1)(u_2 - d_2) = \max_{\boldsymbol{u} \in \boldsymbol{U}, u_i \geq d_i \forall i} (u_1 - d_1)^2, \tag{3.31}$$

which is a maximization problem in one variable that can easily be solved to obtain $\boldsymbol{F}^\star$.

3.6 Analysis: Targeted Attack Model

In this section, we will examine the robustness of interdependent networks under a targeted attack model, where the probability of a node to be attacked is dependent on its intra-layer degree.

3.6.1 Double-Layer Targeted Attack model

We focus on the same model introduced in Section 3.2: complete one-to-one interdependence. Let us define $w_i^{\{l\}}$ as the probability of the ith node in layer l to survive the initial attack. For a randomized

attack structure: $w_i = \eta,\ \forall\ i$. Using a generalized attack model (w), the system equations modeling the cascading failure can be written as:

$$\psi_A = \frac{(\boldsymbol{W}\boldsymbol{a}_1)^T \boldsymbol{P}(\boldsymbol{W}\boldsymbol{b}_1)}{N} = \psi_B, \tag{3.32}$$

$$p_A = \frac{(\boldsymbol{W}\boldsymbol{a}_2)^T \boldsymbol{P}(\boldsymbol{W}\boldsymbol{b}_1)}{N}, \qquad p_B = \frac{(\boldsymbol{W}\boldsymbol{a}_1)^T \boldsymbol{P}(\boldsymbol{W}\boldsymbol{b}_2)}{N}, \tag{3.33}$$

where $\boldsymbol{W} = diag([w_1\, w_2 \cdots w_N])$. All results presented in this chapter are dependent on the decreasingly sorted nature of the column vectors $\boldsymbol{a}_i$'s and $\boldsymbol{b}_i$'s, where $i = (1,2)$. It can be observed from the system equations presented above that the components of the two layers in the system equations are the product of the attack matrix $\boldsymbol{W}$ and the respective $\boldsymbol{a}_i$'s and $\boldsymbol{b}_i$'s. Thus if the monotonicity of these products remain unaltered then all results obtained for the case of randomized attack will be valid for the targeted attack case as well. It can be verified that if w_i is also a decreasing function of i all previous results would be valid. A decreasing w_i implies nodes of lower degree have a lower probability of surviving the initial attack since the indexing of the nodes (i) has been done on the basis of decreasing intra-layer degrees. Thus this scenario represents the case of targeted attack on lower degree nodes. As the monotonicity of the products is unaltered, all results proved for the case of randomized attack in Section 3.4and 3.5 hold true for this case.

However the opposite targeted attack model, which preferentially selects nodes of higher degree, is a more practical and interesting setting. This is because an attack on nodes of higher connectivity (hubs) would cause a much more devastating effect on the network than a preferential attack on lower degree nodes or a randomized attack. As a first step towards characterization of optimal interdependence structures for this type of targeted attack, we will analyze the case of perfect targeted attack where the nodes of the network are attacked in the strict descending order of their intra-layer degrees. The perfect targeted attack model can be mathematically represented as:

$$w_i = \begin{cases} 0 & \text{for } i \in \{1,2,\cdots,N'\} \\ 1 & \text{for } i \in \{N'+1, N'+2, \cdots, N\} \end{cases} \tag{3.34}$$

where $N' = (1-\eta)N$. Note that nodes in both layers of the network have been indexed in the descending order of their intra-layer degrees and thus (3.34) represents the case of targeted removal of the $(1-\eta)N$ nodes with the highest intra-layer degrees.

Theorem 3.6.1 *For a double-layer perfect targeted attack on interdependent networks with complete one-to-one interdependence, the optimal interdependence structure is the monotonic arrangement of nodes, i.e.* $\boldsymbol{P}^\star = \boldsymbol{I}$.

It can be observed here that for the above structure of $\boldsymbol{W}$, all the product terms ($\boldsymbol{W}\boldsymbol{a}_i$'s and $\boldsymbol{W}\boldsymbol{b}_i$'s) are still decreasingly sorted column vectors if the zero components are removed in a way similar to that in the proof of Theorem 3.5.1. Thus it can be shown that the optimal structure of $\boldsymbol{P}^\star$ maximizing network robustness is $\boldsymbol{P}^\star = \boldsymbol{I}$.

3.6.2 Single-Layer Targeted Attack model

In this section, we will focus on the case where only one of the network layers (say layer B without loss of generality) is subjected to the initial attack. Under this condition, the system equations modeling the cascading failure can be written as:

$$\psi_A = \frac{\boldsymbol{a}_1^T \boldsymbol{P}(\boldsymbol{W}\boldsymbol{b}_1)}{N} = \psi_B, \tag{3.35}$$

$$p_A = \frac{\boldsymbol{a}_2^T \boldsymbol{P}(\boldsymbol{W}\boldsymbol{b}_1)}{N}, \qquad p_B = \frac{\boldsymbol{a}_1^T \boldsymbol{P}(\boldsymbol{W}\boldsymbol{b}_2)}{N}. \tag{3.36}$$

As we are considering a perfect targeted attack in this case, $w_i^{\{b\}}$ is 0 for the first $(1-\eta)N$ indices and 1 elsewhere. We focus on the case of ψ given by (3.35) and the same arguments can be applied to the case of p_A and p_B in (3.36). Let us define the non-zero component of the column vector $\boldsymbol{W}\boldsymbol{b}_1$ as $\tilde{\boldsymbol{b}}$. Let $\boldsymbol{P}^\star$ be the interdependence structure maximizing ψ. Thus we can write: where $N_1 = (1-\eta)N$ and $N_2 = \eta N$, and $\boldsymbol{P}$ has been decomposed into two components $\boldsymbol{P}^{\{1\}}$ and $\boldsymbol{P}^{\{2\}}$ of sizes $N \times N_1$ and $N \times N_2$, respectively. It can be shown in a way similar to that in Theorem 3.4.5 that an increment in the diagonal elements of $\boldsymbol{P}^{\{2\}}$ always leads to an increment in ψ. Thus given N_1 and N_2, i.e. for a particular strength of attack (η), we can design the optimal interdependence. Thus we can see here that the optimal interdependence structure is dependent on the attack strength (η). This dilutes the significance of this result as compared to others obtained in this work because a network designer has to know about the strength of attack beforehand, which is not a practical assumption. It should be remembered at this stage that for all other cases, we could obtain optimal strategies which would maximize the robustness of the network for all attack strengths.

Since an optimal interdependence structure which maximizes network robustness for any strength of attack could not be obtained for this case, we test two particular interdependence structures, namely, monotonic and anti-monotonic arrangement of nodes, which were the best and worst case interdependence structures for networks with one-to-one interdependence under random node failure. The results have been presented in Section 3.7. The reason of choosing these particular structures is that they are popular in literature ([Min14a]) and have emerged as optimal or worst structures in the previous part of our analysis.

3.7 Simulation Results

For the testing of the theoretical results derived in this dissertation, we have constructed a Python based test bench, using the NetworkX library, to emulate cascading failure in interdependent networks, obtaining the largest connected component in each layer for the successive stages of the cascading failure. The algorithm stops when a mutually connected bi-layer component is obtained in the steady state. The individual layers are scale-free networks generated by the Barabási-Albert (BA) model [Alb02] with N=1000. Similar results have been observed for other network sizes as well, and $N = 1000$ is chosen as an example without any preference. We present the fractional size ψ of

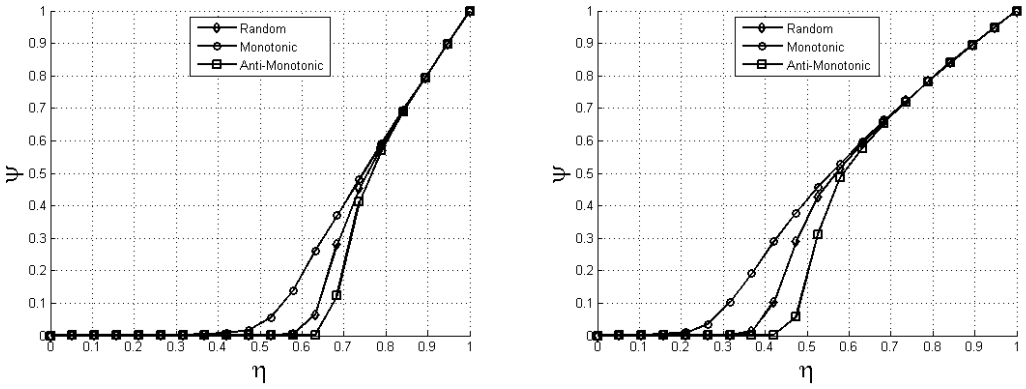

Figure 3.3 Completely interdependent networks with one-to-one interdependence. The individual layers have been generated by the Barabasi-Albert model with $m = 3$. '$\diamond$', '$\square$', and 'o' markers represent the random, monotonic, and anti-monotonic arrangement of interdependent nodes, respectively, on the basis of their intra-layer degrees. The left and right figures correspond to the cases of double-layer and single-layer randomized attacks, respectively.

the surviving component of layer A versus the attack strength η (note that the smaller the η, the more severe the attack). The curves are average results out of 20 instances of network generation each with 10 instances of initial attack on the nodes (thus a total of 200 runs). Next we present a brief description of the simulation results.

- Fig. 3.3 presents the simulation results for the comparison of three different interdependence structures, namely, monotonic, random, and anti-monotonic, for the case of randomized attack on networks with complete one-to-one interdependence. It can be observed that the simulation results corroborate with the theoretical findings presented in Theorem 3.4.3 that monotonic ordering of interdependent nodes on the basis of their intra-layer degrees is the optimal structure and anti-monotonic is the worst structure.

- For the case of randomized attack on networks with one-to-many interdependence structure, we consider $c = 3$ as the ratio of the size of the two interdependent layers in Fig. 3.4. As discussed in Section 3.4.2, we focus on the case of regular allocation of interlinks, and observe that the simulation results support Theorem 3.4.5. Particularly, the optimal interdependence structure $\boldsymbol{P} = [\boldsymbol{I}|\boldsymbol{I}|\cdots|\boldsymbol{I}]_{N\times M}$ outperforms the random and anti-monotonic arrangement $\boldsymbol{P} = [\boldsymbol{I}^{\dagger}|\boldsymbol{I}^{\dagger}|\cdots|\boldsymbol{I}^{\dagger}]_{N\times M}$, where $\boldsymbol{I}$ and $\boldsymbol{I}^{\dagger}$ correspond to the monotonic and anti-monotonic arrangements, respectively.

- The simulation results for the case of partially interdependent networks are presented in Fig. 3.5. As discussed in Section 3.5, the joint maximization of node allocation and node arrangement can be separated into individual maximization problems. Thus in this case, we have considered the node arrangement to be monotonic in nature (which has been shown to be optimal in Theorem 3.5.1) and simulated three allocation strategies, namely, high-high, low-low and random, which correspond to the cases of decoupling nodes of highest, lowest

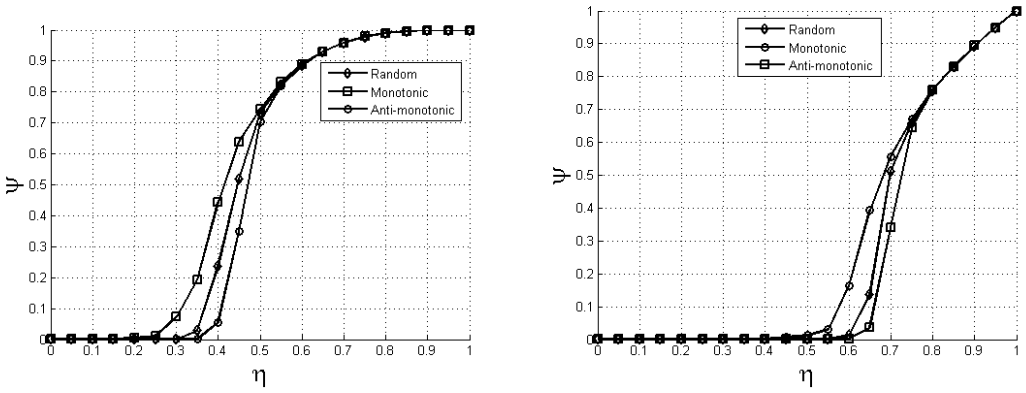

Figure 3.4 Completely interdependent networks with one-to-many interdependence under randomized attack. The individual layers have been generated by the Barabasi-Albert model with $m = 3$, and the allocation of interlinks is regular. '$\diamond$', '$\square$', and 'o' markers represent the random, monotonic, and anti-monotonic arrangement of interdependent nodes on the basis of their intra-layer degrees, respectively. The left and right figures correspond to the cases of double-layer and single-layer attacks, respectively.

and random intra-layer degree, respectively. The results, as can be seen from Fig. 3.5, adhere to those presented in Theorem 3.5.3 that decoupling nodes of high intra-layer degree is the optimal strategy.

- In Fig. 3.6, we present the case of targeted attack on completely interdependent networks with one-to-one interdependence. Similar to the previous cases, we focus on the three interdependence arrangements, and show that the monotonic arrangement of nodes outperforms the others for the case of double-layer (left in Fig. 3.6) perfect targeted attack on the network. The case of single-layer attack (right in Fig. 3.6) has also been presented, where we can observe that the anti-monotonic arrangement is better for this case.

- In Fig. 3.7, we have considered ordering strategies based on other measures of centrality, namely, betweenness and closeness. All theoretical results in this dissertation have been obtained by utilizing the knowledge of degree centrality of the nodes of the network. This is a popular approach in research on complex networks, since analysis of other measures of centrality is very complicated and obtaining system equations relating these measures to network robustness is a very daunting task. In Fig. 3.7, we test our proposed interdependence structure (monotonic arrangement of nodes) on other centrality measures to observe whether these results apply for such cases. To simulate a practical scenario, instead of using random graph generation models, we used the Gnutella peer-to-peer network dataset available from [**real**] to mimic network layers encountered in the real world. It can be observed that even in this case the monotonic arrangement of nodes is the best among the three simulated cases. These results indicate that the theoretical results derived here have a wider applicability since the suggested design guidelines are valid for other forms of centrality as well.

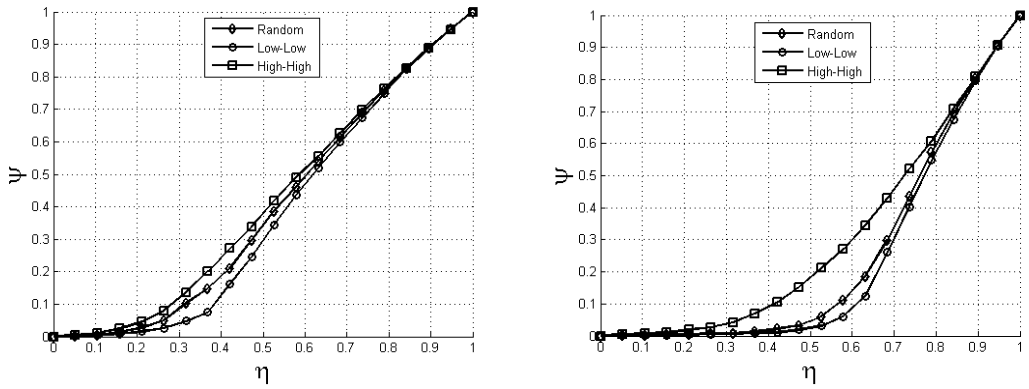

Figure 3.5 Partially interdependent networks with one-to-one interdependence. The individual layers have been generated by the Barabasi-Albert model with $m = 3$ and 75% of nodes in the network are autonomous. '$\diamond$', '$\square$', and 'o' markers represent the cases of random, low-low, and high-high, respectively, which are strategies of decoupling of nodes. The left and right figures correspond to the cases of double-layer and single-layer randomized attacks, respectively.

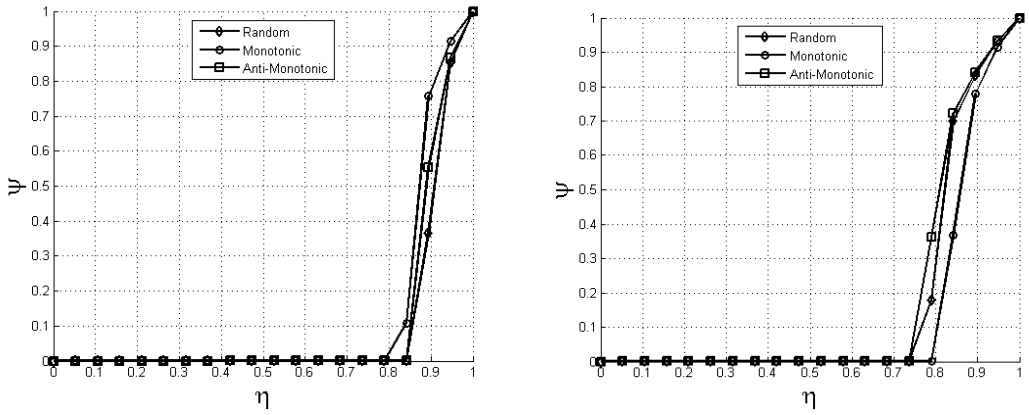

Figure 3.6 Completely interdependent networks with one-to-one interdependence under perfect targeted attack. The individual layers have been generated by the Barabasi-Albert model with $m = 3$. '$\diamond$', '$\square$', and 'o' markers represent the random, monotonic, and anti-monotonic arrangement of interdependent nodes, respectively, on the basis of their intra-layer degrees. The left and right figures correspond to the cases of double-layer and single-layer attacks, respectively.

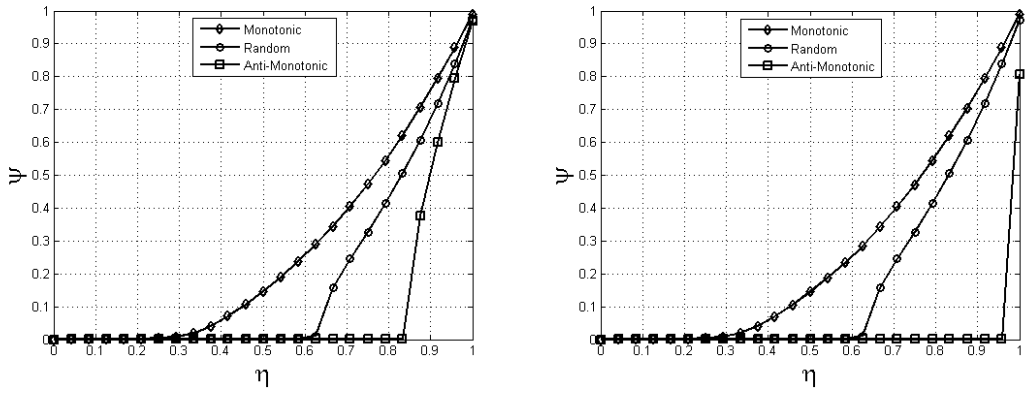

Figure 3.7 Completely interdependent networks with one-to-one interdependence under perfect targeted attack. The individual layers have been generated by the Barabasi-Albert model with $m = 3$. '$\diamond$', '$\square$', and 'o' markers represent the random, monotonic, and anti-monotonic arrangement of interdependent nodes, respectively, on the basis of their intra-layer betweenness (left) and closeness (right).

3.8 Conclusion and Future Work

In this dissertation we have exploited the intra-layer node degree information to obtain some quantitative results towards optimal interlink designs for maximizing robustness of interdependent networks. As discussed in Section 3.2, exploitation of intra-layer degrees can yield the optimal interdependence structures only if the strong conditions in Lemma 3.4.1 are satisfied. We have shown in this dissertation that these conditions are in fact satisfied by a wide variety of network and attack models. However as we further generalize our network to emulate those encountered in the practical world, we need to look at other analytical techniques like utilization of the adjacency matrix of the coupled network, exploiting other types of topological information like betweenness, closeness etc., which is a part of our on-going research work. Although the results presented here represent an initial step in this burgeoning field, we believe that such rigorously derived results regarding the effect of interdependence structure on network robustness enable the scientific community to gain a better understanding of interdependent networks and obtain principles to design better networks.

CHAPTER

4

INTERLINKS WITH COST

The inherent assumption in previous chapters was that all interlinks are equally feasible and there was no concept of different interlinks requiring different costs for construction. However as we begin to apply our theoretical knowledge of interlink optimization to real world engineering problems, various constraints emerge which were not considered in previous chapters; cost being our primary focus here.

4.1 Background

Research interest in interdependent networks is largely attributed to the seminal paper by Buldyrev et. al. [Bul10], where the authors mathematically characterize a failure spreading process in interdependent networks. Later works [Hua13b; Ran11] extend the study focusing on developing a better understanding of the cascading failure on more generalized system models. These works study the steady state properties of interdependent networks using generating function based approaches. However, the shortcoming of this approach is that the mathematical analysis is only valid for random graphs which have a locally tree-like structure, which implies that the graph structure does not have any loops in the local neighborhood of the nodes or in other words is 'tree-like' when observed from the perspective of individual nodes. Recent works have shown that the topology of networks encountered in the real worlds can differ drastically from random graphs. Apart from connected component based cascading failure, other multi-layer network processes like load distribution [Zha17; Lv17] and connectivity [Zha18] have also been studied but again under the domain of locally tree-like random graphs. Thus this avenue of research endeavors to accurately characterize the dynamics of different processes but considers relatively simple network models which might vary

significantly from real world networks.

On the other end of the spectrum, a few recent works ignore the actual process occurring on interdependent networks and use classical metrics to characterize the robustness of multilayer networks. But instead of focusing on the degree distribution of the nodes, these works consider the exact topology of the network layers. Thus these works are agnostic to the intricacies of the failure spreading process but can study networks with arbitrary topology. Popular metrics used in these works are algebraic connectivity [Zhe17; Sha16], number of spanning trees [Men16; Zav11], and effective resistance [Sha16]. In the context of single layer networks, there is extensive literature justifying the use of these metrics for studying robustness [Jam07], information spreading and control [Zav11] among others. It is important to note here that for the case of multi-layer networks, the role of these metrics is relatively unexplored. Furthermore, these works impose a simplification of the multilayer structure of the network by considering the supra-adjacency matrix which is described in detail in Section 4.4. The supra-adjacency matrix essentially flattens the multi-layer network to a single layer, where different layers of the interdependent networks can be thought of different communities in a single layer network. Although this might serve as a good starting point, it suffers from a fundamental shortcoming– there is no distinction between inter- and intra-layer links. This occurs due to the fact that studying the supra-adjacency matrix of the multilayer network dissolves the difference between different kinds of links and cannot model cases where the inter- and intra-layer links perform different functions. It is important to state here that even with flattened network models and metrics based on single layer networks, optimal interlink structures maximizing these metrics could not be obtained and the state of the art in this area comprises mainly heuristic algorithms involving matrix update approximations [Cha16]. Thus we can see that on one hand a degree distribution based analysis of networks has the advantage that various multilayer network processes can be analyzed mathematically but these results are obtained for locally tree-like graphs and might not be applicable for networks with arbitrary topology. On the other hand, works which essentially 'flatten' the multilayer network can be applied to networks with arbitrary topology with the shortcoming that particular failure spreading processes are not considered and the robustness is measured by applying metrics developed for single layer networks which might not be related to robustness with respect to (w.r.t.) the specific processes.

4.2 Our Approach

The work presented here falls midway between these two avenues of research. We consider interdependent networks where the constituent layers have an arbitrary topology. We propose new metrics of robustness corresponding to specific failure spreading processes. These metrics are an approximate characterization of the dynamics of these processes. This is in contrast to works like [Bul10; Lv17; Zha18] which model the cascading failure process exactly albeit on locally tree-like networks. It should be clarified here that an exact characterization of any process on an arbitrary network topology is a complicated problem and an active area of research [Rad16]. The advantage

of using an approximate characterization is that the metrics of robustness are tractable allowing us to solve the interlink optimization problem using a convex optimization framework. Furthermore, this tractability enables us to consider a general model for the cost of construction of interlinks. The interlink construction cost is an important factor which has been largely ignored in works focusing on multilayer network design. The underlying assumption in most works [Bru12; Cha17] is that all interlinks are feasible. It is easy to see that this assumption might not be valid for many applications where there are practical constraints, like geographical distance, aversion to interlinking, etc., governing the construction of interlinks. Although works like [Gho06] consider specific cost structures, our model in this dissertation is a generalization and results presented in the above paper can be obtained as special cases of our results. Furthermore, the metrics of robustness proposed here consider distinct functions for the inter- and intra-layer links. Due to the distinct modeling of the inter- and intra- layer links, we essentially analyze the multi-layer network as is instead of 'flattening' it as is done in works like [Sha16; Men16]. Thus our work can be thought of to be orthogonal to both approaches discussed previously, since we are not constrained to locally tree-like graphs and our metrics of robustness are not agnostic to the failure spreading process. The trade-off lies in the fact that the proposed metrics of robustness are an approximate characterization of the failure spreading processes. In essence, the fundamental problem which we tackle in this dissertation is to construct an interlink structure maximizing the robustness of multilayer networks under a total budget constraint, where the cost structures of the interlinks and the intra-layer topology is known to the network designer.

The remainder of this chapter is organized as follows. Section 4.3 highlights the main contributions of our dissertation. Section 4.4 establishes the system model and problem formulation for a general metric. Section 4.5 presents the calculation of the optimal resource allocation for a simple metric of robustness. We propose and analyze the process dependent metrics in Section 4.6. Finally, we present the simulation results in Section 4.8 and conclude and indicate future avenues of research in Section 4.9.

4.3 Contributions

The contributions of this dissertation can be summarized as follows:

- We consider the problem of designing interlinks under budget constraints for multi-layer networks to maximize its robustness against different failure spreading processes. To the best of our knowledge, this is one of the first works where a cost constraint modeling is employed for interlink optimization.

- We propose heuristic metrics for three failure spreading processes popular in the context of interdependent networks, namely, connected component based cascading failure [Bul10], load distribution in interdependent networks [Bru12], connectivity in demand-supply networks [Zha18]. These metrics are an approximate characterization of the failure spreading processes

although their effectiveness in capturing the dynamics of the processes have been supported by simulation results.

- The design of interlinks is modeled as a convex optimization problem with the proposed metrics of robustness as the objective functions. Under certain constraints, we have been able to obtain closed form solutions for the optimal resource allocation for constructing interlinks achieving maximum network robustness. Furthermore, the optimal resource allocation can be obtained in a distributed fashion by local computations without the guidance of any central controller.

4.4 System Model

We consider an interdependent network comprising two network layers A and B of size m and n, respectively. The fundamental problem which we study in this dissertation is that given a total budget, how should this budget be optimally distributed among mn possible interlinks such that the robustness of the resulting interdependent network is maximized. We use l to index the interlinks. Let the amount of resource allocated to construct the lth interlink be denoted by x_l. Thus the vector $\mathbf{x} \in \mathbb{R}^{mn\times 1}$ is the resource allocation strategy indicating the resource allocated to each interlink. We are interested in obtaining the optimal $\mathbf{x}^\star$ which maximizes the robustness of the network. We will discuss about the different metrics of network robustness later in Section 4.5 and 4.6.

We use a general framework to model the weights of the interlinks (w_l) as a function of the resource allocated to them:

$$w_l = r(x_l, \alpha_l), \tag{4.1}$$

where $r : \mathbb{R}^+ \to \mathbb{R}^+$ is the function mapping the allocated resource (x_l) to the interlink weight (w_l) and α denotes a feasibility parameter. We will refer to the functions $r(x_l, \alpha_l)$ as the return on investment (R.O.I.) since they model the weight (return) obtained from the lth link after an investment of x_l. This is a generalization of cost models considered in works like [Gho06], where the interlink construction cost is a parameter which is known a priori. This kind of modeling is in fact a discrete version of our model, since the domain of the R.O.I.'s are $\{0, c_l\}$ for this case as compared to $\mathbb{R}^+$ for our case. The α parameter models the feasibility of interlinks wherein infeasible interlinks, for example, an interlink between two nodes which are geographically separated by a large distance, have a low α value implying that such interlinks require a much larger investment to obtain similar weights (w_l) as compared to feasible interlinks. The work presented here is applicable for any R.O.I. function subject to the constraint that they are concave w.r.t. x_l in order to pose the interlink construction as a convex optimization problem. It is interesting to note that a concave modeling of return on investments is quite intuitive since the marginal (incremental) gain from an investment is expected to decrease with increase in investment. This is also related to the law of diminishing returns in economics. In this dissertation, we have modeled the R.O.I.'s by two family of graphs to serve as examples, the details of which are presented later.

Let us denote a general metric of robustness by $f_0(\mathbf{w}, G_A, G_B)$, where $\mathbf{w}$ is the weight of the interlinks given by the R.O.I. functions ($w_l = r(x_l, \alpha_l)$) and (G_A, G_B) are the topologies of the layers comprising the interdependent network. Note that the metric f_0 takes the interlink weights and the intra-layer topology (G_A, G_B) as separate inputs. This modeling differentiates our work from [Sha16; Men16] which consider a flattened network and even works like [Bul10; Yag12] which consider the degree distribution of nodes and focus on locally tree-like random graphs. The problem which we are trying to solve here can be mathematically written as:

$$\begin{aligned} \underset{\mathbf{x}}{\text{minimize}} \quad & f_0(\mathbf{w}, G_A, G_B) \\ \text{subject to} \quad & \mathbf{1}^T\mathbf{x} = b, \\ & \mathbf{x} \succeq 0, \end{aligned} \tag{4.2}$$

where b is the total budget available for the construction of interlinks. The first constraint in (5.21) specifies the total budget, i.e. the sum of resources allocated to construct all interlinks ($\sum_l x_l = \mathbf{1}^T\mathbf{x} = b$). The second constraint restricts the allocated resource to be non-negative. For simplicity of notation, we shorten the representation of the objective function to $f_0(\mathbf{w})$, where G_A and G_B can be thought of as implicit inputs. Note that we have written (5.21) as a minimization problem to adhere to the popular framework of convex optimization. As our problem deals with the maximization of the network robustness, we will use a negative sign while defining the metrics of robustness. It can be clearly observed from (5.21) that the equality constraint is affine and the inequality constraint is linear (convex). Thus (5.21) is a convex optimization problem [Boy04] subject to the condition that the objective function $f_0(\mathbf{w})$ is convex. It can be shown that if the R.O.I.'s are concave, then the objective functions considered in this work would be convex. The details are presented in Appendix 4.10.1.

Let us write the Lagrangian of (5.21):

$$L(\lambda, \nu) = \inf_x \left[f_0(\mathbf{w}) + \sum_{l=1}^{mn} \lambda_l(-x_l) + \nu(\mathbf{1}^T\mathbf{x} - b) \right], \tag{4.3}$$

where $\lambda = [\lambda_1 \cdots \lambda_{mn}]^T$ denotes the multipliers for the inequality constraints and ν is the multiplier for the equality constraint. Applying the KKT conditions on the optimization problem (5.21) enables us to eliminate the λ multipliers and yield the equation:

$$\nu^\star = -\frac{\partial f_0(\mathbf{w})}{\partial x_l}\bigg|_{x_l = x_l^\star}, \text{ if } x_l^\star \neq 0, \tag{4.4}$$

where $\nu^\star$ and $x_l^\star$ are the optimal values of the multiplier ν and the resource allocation x_l, respectively. The relevant mathematical details have been presented in Appendix 4.10.2. (4.4) is the fundamental equation which will be used to obtain the optimal interlink structure maximizing the metric of choice. Note that $\nu^\star$ is just a scalar quantity since there is only one equality constraint in our optimization problem (5.21). Thus the KKT conditions allow us to reduce the problem of computing the optimal

resource allocation $\mathbf{x}^\star \in \mathbb{R}^{mn\times 1}$ to computing the scalar $\nu^\star \in \mathbb{R}$, which can be achieved easily by binary search or other descent algorithms. We remind that reader that we have not characterized the metric of robustness yet and (4.4) was obtained by considering a general metric $f_0(\mathbf{w}, G_A, G_B)$. In the next section, we propose a simple metric and using (4.4) derive the optimal resource allocation strategy maximizing the metric. Thereafter, in Section 4.6 we propose metrics of robustness corresponding to specific failure spreading processes and optimize the resource allocation for these specific cases.

4.5 Studying a Simple Metric

One of the simplest metric for single layer networks is average degree. Here we propose a variation of average degree for the case of interdependent networks, where the intra-layer and inter-layer links play different roles. Let us present the mathematical details first and we will define the intuition behind the equations later. Let the interlink resource allocation be $\mathbf{x} = \{x_1, \cdots, x_{mn}\}$, where x_l is the resource allocated to the lth interlink leading to an interlink weight of $w_l = r(x_l, \alpha_l)$. The metric of robustness can be written as:

$$f_0(\mathbf{w}) = -\sum_{l=1}^{mn} r(x_l, \alpha_l) D_l(l_A, l_B), \tag{4.5}$$

where $D_l(l_A, l_B)$ denotes some topological property of the end-points $l_A \in A$ and $l_B \in B$ of the interlink l. Note that the negative sign is due to the fact that we have defined our optimization problem (5.21) as a minimization problem. Thus the negative sign ensures that we are maximizing the metric of robustness. In order to simplify the representations, we will use D_l to denote $D_l(l_A, l_B)$ henceforth. Note that D_l can denote any topological property of the end-points of interlink l. For instance, we can define D_l as the sum of the intra-layer degrees of the two endpoints of the interlink l, i.e. $D_l(l_A, l_B) \triangleq d_{l_A} + d_{l_B}$, where d_{l_A} and d_{l_B} denote the intra-layer degree of the nodes. Another instance of D_l might be the betweenness product of the two endpoints of l, i.e. $D_l(l_A, l_B) \triangleq b_{l_A} \cdot b_{l_B}$, where b_i denotes the intra-layer betweenness of node i. In this section, we use the first definition of D_l related to degree sum and name the metric effective degree. Thus the effective degree metric is a weighted average over the sum of the intra-layer degrees of the interdependent neighbors. It should be noted that although the proposed metric is simple, due to the general definition of D_l as any topological property of the endpoints of l, this metric can be tweaked to achieve interesting results. We show later how redefining D_l can help us to design metrics of robustness for different failure spreading processes. In particular, we will be using this idea while focusing on the connected component based cascading failure process[Bul10].

Let us now develop an intuitive understanding of the proposed metric. Consider the case of the multi-modal transportation network in cities, where we want to optimally design interlinks between different modes of transportation, like network of subway and bus stations, to alleviate congestion. Given isolated network layers of subway and busway and a fixed budget, how to optimally construct interlinks (walking paths) between subway and bus stops so as to minimize traffic congestion. The traffic at node i of a network can be loosely represented by its intra-layer degree. The weight of the

interlinks represents its quality, which might indicate the number of walking lanes. Thus average effective degree ($\triangleq \sum_l w_l(d_{l_a}+d_{l_B})$) can be thought of as the amount of traffic utilizing the interlinks, since it is a product of the quality of interlinks and the total traffic at the two endpoints. Maximizing the effective degree metric is thus similar to minimizing the congestion in the interdependent transportation network. Note that this metric models the intra- and inter- layer links distinctly. The intra-layer links control the amount of traffic arriving in the subway and bus stops whereas the interlinks control the amount of traffic offloaded between the two networks.

For this metric, we model the R.O.I.'s by shifted sigmoid functions given by $r(x_l,\alpha_l) = 2(1+e^{-\alpha_l x_l})^{-1}-1$. It is easy to see that this modeling satisfies the requirements of the R.O.I.'s wherein they are concave w.r.t. x_l and a higher value of the feasibility parameter α_l leads to a higher interlink weight for a fixed resource allocation. Solving the KKT conditions, the details of which are presented in Appendix 4.10.3, we get the following expression for the optimal resource allocation:

$$x_l^\star = \frac{1}{\alpha_l}\log\left(\frac{\sqrt{\frac{\alpha_l D_l}{2}}+\sqrt{\frac{\alpha_l D_l}{2}-\nu^\star}}{\sqrt{\frac{\alpha_l D_l}{2}}-\sqrt{\frac{\alpha_l D_l}{2}-\nu^\star}}\right), \tag{4.6}$$

where $x_l^\star$ is the optimal resource, α_l is the feasibility parameter for the lth link, $\nu^\star$ is the optimal value of the equality constraint multiplier ν and D_l denotes a topological property of the end-points of the interlinks defined in this case as the sum of the intra-layer degrees of the two endpoints l_A and l_B of interlink l. Next we develop an intuitive understanding of (4.6). It can be observed from (4.6) that $x_l^\star$, the optimal resource allocated to the lth interlink, has a real value when the value of $\alpha_l D_l/2$ exceeds $\nu^\star$, since the argument to the square root should be non-negative. If the value of $\nu^\star$ is small (close to 0), it implies that the term $\alpha_l D_l/2-\nu^\star$ is positive for most interlinks thereby indicating a strong interconnection between the interdependent layers as $x_l^\star$ is non-zero for most interlinks l. A larger value of $\nu^\star$ implies that $\alpha_l D_l/2-\nu^\star$ is positive only for a few interlinks thereby indicating sparse interconnection. The value of the optimal dual variable $\nu^\star$ thus controls the strength of interlinking among the two network layers. Note that the optimal resource allocation has to additionally satisfy the total budget constraint given by $\sum_l x_l^\star = b$. Substituting the expression for $x_l^\star$ given by (4.6) in the budget constraint results in:

$$\sum_{l=1}^{mn}\frac{1}{\alpha_l}\log\left(\frac{\sqrt{\frac{\alpha_l D_l}{2}}+\sqrt{\frac{\alpha_l D_l}{2}-\nu^\star}}{\sqrt{\frac{\alpha_l D_l}{2}}-\sqrt{\frac{\alpha_l D_l}{2}-\nu^\star}}\right) = b, \tag{4.7}$$

which is an equation with a single scalar variable $\nu^\star$ which can be easily solved by binary search or other descent methods. Thus for obtaining the optimal resource allocation $x_l^\star$, we firstly need to optimize the value of the dual variable $\nu^\star$ by applying descent methods to (4.7). The optimal $\nu^\star$ can then be plugged into (4.6) to obtain $x_l^\star$, the optimal resource allocation. These steps are summarized in Algorithm 1. In this way, the optimal resource allocation maximizing the effective degree metric can be computed. In the next section, we focus on metrics of robustness corresponding to specific failure spreading models.

Algorithm 1 Algorithm for the Effective Degree Metric

procedure OPT_ALLOC_SEP($\boldsymbol{\alpha}, G_A, G_B, b, \Delta_{th}$)
  $\boldsymbol{F} \leftarrow \frac{\alpha_l D_l}{2}$, $\forall\ l$ (where $D_l \triangleq d_{l_A} + d_{l_B}$)
  $limit_u \leftarrow \max \boldsymbol{F}$, $limit_l \leftarrow 0$
  $\Delta \leftarrow \inf$
  while $\Delta > \Delta_{th}$ **do**
    $\nu \leftarrow \frac{limit_l + limit_u}{2}$
    $x_l \leftarrow \max\left(0, \frac{1}{\alpha_l} \log\left[\frac{\sqrt{\frac{\alpha_l D_l}{2}} + \sqrt{\frac{\alpha_l D_l}{2} - \nu}}{\sqrt{\frac{\alpha_l D_l}{2}} - \sqrt{\frac{\alpha_l D_l}{2} - \nu}}\right]\right)$, $\forall\ l$
    $b_{curr} \leftarrow \sum_l x_l$
    if $b_{curr} > b$ **then**
      $limit_u \leftarrow \nu$
    else
      $limit_l \leftarrow \nu$
    $\Delta \leftarrow |b_{curr} - b|$
  return x_l, $\forall\ l$

4.6 Process Dependent Metrics

Although the effective degree metric differentiates between the inter- and intra-layer links, it does not consider any specific failure spreading process. It is purely a topological property of the interdependent network. The state of art in multilayer network research reveals that there are many distinct processes modeling the spread of failure of nodes in interdependent networks. In this dissertation, we focus on three distinct processes, namely, connected component based cascading failure [Bul10; Cha17], multilayer load distribution [Lv17], and connectivity in demand-supply networks [Zha18]. All of these are exciting fields of research and it is interesting to note that these models, which can be thought of as failure (or influence or load) spreading models, differ significantly from each other. For example the function of an interlink in connected component based cascading failure is to relay failures, i.e. if nodes $a \in A$ and $b \in B$ (where A and B are the two layers of the interdependent network) are connected by an interlink, failure of a leads to failure of b and vice versa. On the other hand, interlinks in the interdependent load distribution process do not relay failures rather offload a fraction of load from the failed node to its neighbors. Thus in such processes failure of a node a does not imply that its inter-layer neighbor b fails as well but rather means that a fraction of load being carried by a is offloaded to b which may or may not lead to the failure of b due to this offloaded load. Thus we can argue that metrics developed for a specific failure spreading process might not be applicable to other processes. In other words, metrics of robustness should be *process dependent*. In this section, we propose metrics of robustness corresponding to these distinct processes. It should be clarified at this point that the proposed metrics are approximate characterizations of the processes. An exact characterization of any failure spreading process in multilayer networks is an active area of research in itself. However developing a mathematical framework of tracking the dynamics of these processes is a challenging task even after imposing constraints like locally tree-like nature on

the networks. Although there exist some theoretical results related to interlink optimization for the connected component based cascading failure process [Ran11; Cha17] under a random node failure model in locally tree-like graphs, most processes become intractable especially when arbitrary network topologies are considered. In this dissertation, we propose approximate metrics for the failure spreading processes which are tractable. This allows us to solve the interlink optimization in a budget constrained setting with a generalized cost structure as defined in Section 4.4. It is important to note that the proposed metrics have also been analytically shown to be positively correlated to the network robustness for the three processes. Thus the proposed metrics are essentially a trade-off between mathematical tractability and exact characterization of the failure spreading processes.

4.6.1 Cascading Failure in Interdependent Networks

The seminal paper in the area of interdependent networks was the work by Buldyrev et al. in [Bul10], where they considered a connected component based cascading failure model and analyzed the steady state properties an interdependent network under random initial failure of nodes. These results are obtained under the constraint of locally tree-like graphs with a given degree distribution. Furthermore, the generating function based approach is not applicable for specialized node failure models like betweenness based attacks which have attracted research interest in recent works [Cun15; Rue16] as a very disruptive failure model compared to popular models like random node failure and degree targeted failure. Thus although this cascading failure process is relatively well studied, the generating function based approach has its shortcomings.

We propose a heuristic metric of robustness for this process and focus on the problem of optimal interlink design under a betweenness-based attack. The reason for choosing this specific attack model is that classical analysis techniques cannot be applied for this case. This is because generating functions capture the degree distribution of nodes in a network but cannot capture other topological properties like betweenness or closeness. Similar to previous cases, an exact characterization of the steady state surviving size of the network is computationally expensive if not intractable. Although works like [Rad16] study the problem of estimating network robustness in single layer networks without the locally tree-like network constraint, such studies have not yet been extended to multilayer networks. To study this problem, we propose a simple variation of the effective degree metric. The basic idea behind the metric is the observation that anti-monotonic ordering outperforms monotonic ordering for the case of degree targeted attacks [Cha17; Min14b]. Although this observation was made under a node failure model based on intra-layer degrees, we conjecture that similar results hold for betweenness based attacks as well. Thus we propose: the optimal interlinking strategy for maximizing robustness of interdependent networks against targeted betweenness based attack is the anti-monotonic ordering, where the nodes in layer A with the highest betweenness are preferentially coupled to low betweenness nodes of layer B. The intuition behind this metric is that since the attacker chooses nodes of high betweenness, coupling these to nodes of low betweenness (less important nodes) checks the spread of failures.

Recall that the effective degree metric can be written as:

$$f_0(\mathbf{w}) = -\sum_l w_l D_l(l_A, l_B), \tag{4.8}$$

where the summation is over all possible interlinks l, and D_l denotes some topological property of the endpoints of the lth interlink. To capture the dynamics of the process, we model D_l as a distance metric between the two endpoints $l_A \in A$ and $l_B \in B$ of the lth interlink. Since we want to preferentially construct interlinks between nodes of high and low betweenness, we want to model D_l in such a way that D_l has a low value when the betweenness of l_A and l_B are similar to each other and has a high value when there is a large difference in the betweenness values. As we are maximizing our metric of robustness which is a weighted sum of the D_l values, such a definition of D_l will ensure that we give preference to anti-monotonically ordered interlinks. Note that $D_l(l_A, l_B)$ can be defined in many ways as long as its value increases with the betweenness difference. Examples of D_l might be:

- $D_l(l_A, l_B) = |b_{l_A} - b_{l_B}|$ (absolute distance)
- $D_l(l_A, l_B) = e^{(-\frac{1}{|b_{l_A} - b_{l_B}|})}$ (exponential distance)

The actual choice of D_l is dependent on the process and more involved expressions might help in capturing the dynamics of the failure spreading process more accurately. Note that the proposed algorithms for computing the optimal resource allocations hold for any arbitrary definition of D_l, although the performance of the algorithms is dependent of how well the proposed metrics capture the dynamics of the failure spreading processes. However we show that even the simple definitions shown above can achieve an improvement in performance compared to state of the art algorithms. In this work, we consider the absolute distance for modeling D_l. We perform simulation studies on how well our proposed metric captures the dynamics of the network which are presented in Fig. 4.1. The plots in Fig. 4.1 were obtained by considering a given intra-network topology and initial set of failed nodes and computing the network robustness and metric values for various interdependent networks by varying the interlinking structure. Let us clarify this notion of varying interlinking structure. Ideally we are interested in observing the relationship between the value of the proposed metrics and the robustness for all possible interlinking structures. However it was observed that varying the interlinking structure uniformly at random does not lead to different kinds of interlinking structures due to the huge space of possible interlinks. Note that even for the simplistic case of one-to-one interlinking with unweighted interlinks, where every node $a \in A$ is interlinked to only one node $b \in B$, the total number of possible interlinking structures is $n!$, where $|A| = |B| = n$. In our dissertation, we do not put any restrictions on the interlinking structure and also consider interlinks with $w_l \in \mathbb{R}^+$. Due to this reason the number of possible interlinking structures for our case is infinitely large and a uniformly random sampling is unable to explore these structures. Thus in order to observe the metric value and robustness for a variety of interlinks we perform a preferential sampling. Our conjecture is based on the intra-layer betweenness of the nodes for the current

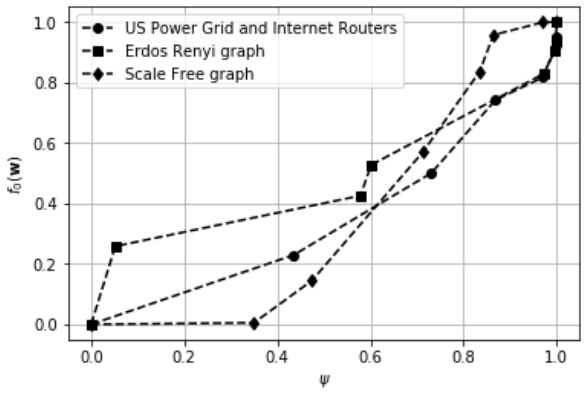

Figure 4.1 Plot of metric versus network robustness values for the connectivity based cascading failure process under node degree based targeted model.

failure spreading process. In order to observe the whole spectrum of the interlinks, we generate various interlinking strategies with varying preference allocated to monotonic and anti-monotonic coupling of the nodes. The points in the figure correspond to interdependent networks with these different interlinking strategies and the x and y coordinates of the points denote the average network robustness (ψ) and metric value ($f_0(\mathbf{w})$), respectively, for 500 instances of these strategies. It can be observed from Fig. 4.1 that $f_0(\mathbf{w})$ and ψ are related monotonically. Furthermore, the monotonic trend can be observed for different classes of networks, both synthetic and real. This indicates that the proposed metric sufficiently characterizes the robustness of the interdependent network and we can conclude that network robustness increases with the metric value in the mean sense. This enables us to use the proposed metrics to characterize the robustness of the interdependent network corresponding to this specific failure spreading process. The simplicity and mathematical tractability of the proposed metrics allows us to not only solve the interlink optimization problem but also incorporate the cost of construction of interlinks into the interlink design problem and obtain closed form solutions for the resource allocation maximizing network robustness.

Since the proposed metric is structurally identical to the effective degree metric it is easy to see that the optimal resource allocation for this case can be obtained by solving (4.6)-(4.7), where D_l is the distance metric defined above as $D_l(l_A, l_B) \triangleq |b_{l_A} - b_{l_B}|$. This establishes the generality of the effective degree metric as by modifying the definition of the D_l term, we can apply it to a specific failure spreading process. It is important to state here that for the other failure spreading processes, to be discussed next, we can apply a similar method of altering the definition of D_l to capture the dynamics of particular failure spreading spreading processes. Note that the optimization based framework can be applied to any failure spreading process as long as we can smartly design metrics of robustness which can (approximately) characterize the process. However we diverge from the effective degree based modeling, which is essentially a weighted average, for the other two processes and focus on a information theoretic modeling based on logarithms.

4.6.2 Load Distribution in Interdependent Networks

After connected component based cascading failure, load distribution in interdependent networks is one of the most popular models due to its applicability in many research domains like smart grids for power distribution [Par13], modeling traffic in multilayer transportation networks [Min14a], and also modeling flow of asset and liabilities in financial networks [Hua13a]. Although the system model used in these works have slight differences, the underlying principle is similar– all nodes have an initial load and capacity. When a node fails, its load is redistributed among its neighbors and if any node has a current load, defined as the sum of initial and offloaded load, that exceeds its capacity then it is assumed to fail. The failure spreading process continues until no more failures occur and the network reaches steady state. An exact characterization of the steady state dynamics for this process is a challenging task and works like [Lv17; Zha17; Bru12] study this problem by imposing constraints on the network model like random graphs [Lv17] or by considering simplifications of the failure spreading process [Zha17]. Furthermore these works do not focus on the optimization of the interlink design since they assume the network layers to be interlinked randomly.

Instead of the effective degree modeling (4.5), we use a logarithmic modeling to design the metrics for this process. Note that if we wanted to proceed with an effective degree based modeling, we could have altered the definition of D_l in (4.5) to capture the dynamics of this process. Under the logarithmic modeling, the metric is defined as:

$$f_0(\mathbf{x}) = -\sum_{l=1}^{mn} \log(D_l + r(x_l, \alpha_l)). \tag{4.9}$$

This kind of modeling can be seen in Information Theory where it is desirable to allocate power optimally to different communication channels with varying levels of interference with the aim of maximizing the network throughput. The D_l term in (4.9) corresponds to this variable interference and the $r(x_l, \alpha_l)$ term corresponds to the allocated power. In our problem, we are interested in obtaining the optimal resource allocation ($\mathbf{x} = [x_1, \cdots x_{mn}]^T$) to the different interlinks with the objective of maximizing the network robustness. D_l should be defined in such a way that it captures dynamics of the load distribution process (approximately) and is also tractable enough to solve the convex optimization problem. For interlinks l which are beneficial in maximizing network robustness, the value of D_l should be low indicating a noise-free wireless channel to which more power (resource) should be allocated. On the contrary, interlinks that harm the network robustness should have high D_l values indicating a noisy channels to which we should allocate less power.

In order to define D_l, let us develop a better understanding of this failure spreading process. Let us define the *free space* of a node i as $s_i \triangleq c_i - l_i$, where c_i and l_i denote the capacity and load of the ith node. Since a node fails only when the amount of load it handles exceeds its capacity, the difference between the load and capacity indicates the additional 'space' of each node to handle load offloaded from neighbors. Free space is also loosely indicative of the likelihood of failure of a node, i.e. if a node has low free space it is more likely to fail and vice versa. In most works in the literature [Lv17], the capacity of nodes is modeled as a fixed linear function of the load, i.e.

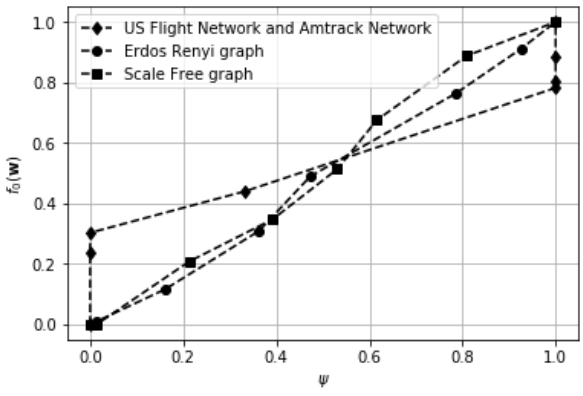

Figure 4.2 Plot of metric versus network robustness values for the load distribution process under random attack model.

$c_i \triangleq (1+\beta)l_i$. We model load and capacity by distinct albeit known parameters and thus our model relaxes the linear relationship. In fact, the optimal resource allocation for this process is applicable for any general load and capacity as long as the values are independent of the resource allocation $\mathbf{x}^\star$, i.e. the interlinks. We conjecture that interlinking nodes of low free space to nodes of high free space is a good strategy. This is intuitive since nodes of high free space can handle the load offloaded from nodes of low free space upon failure. Thus by coupling the nodes which are most likely to fail to the nodes which are best at handling failure, we check the spread of failures thereby maximizing the network robustness. Simulation studies presented later in this section corroborate this conjecture thus establishing that increasing the proposed metric leads to increase in network robustness.

Coming to the definition of D_l, recall that D_l corresponds to interference in a wireless channel. Here we are trying to capture the free space 'distance' (difference) between the two endpoints of the lth interlink:

- $D_l = |s_{l_A} - s_{l_B}|^{-1}$
- $D_l = 1 - e^{(-\frac{1}{|s_{l_A} - s_{l_B}|})}$

Note that for any valid definition, the value of D_l should be low when there exists high difference in the free space of the two endpoints and D_l should have a high value for endpoints which have similar free spaces. Note that this definition is essentially a myopic characterization of the load distribution process. We prefer interlinks between nodes that are likely to fail (low free-space) and nodes that can handle significant offloaded load (high free-space). Our interlink design algorithm thus optimizes the robustness of the network against a single step of the load distribution process. An exact characterization of the dynamics should also consider further steps in the spread of failures.

The next logical step is to ascertain how well our proposed metric, given by (4.9), captures the dynamics of the load distribution process. If we observe that the metric values and network robustness for different interlinking structures are monotonically related, we can conclude that

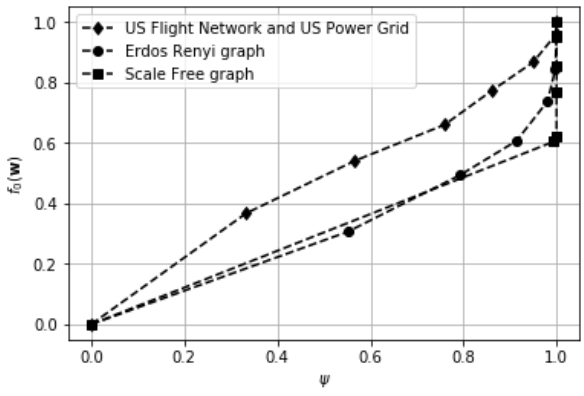

Figure 4.3 Plot of metric versus network robustness values for the connectivity process in demand-supply networks under a random attack model.

the proposed metric captures the dynamics of the load distribution process. This can be observed from Fig. 4.2 thus implying maximization of the metric is equivalent to maximization of network robustness. Note that the different interlinking strategies were based on the free-space of the nodes which in the earlier case of connected component based cascading failure were based on intra-layer betweenness. We use (4.4) to derive the optimal resource allocation maximizing our proposed metric:

$$x_l^\star = -\frac{1}{\alpha_l}\log\left(\frac{-D_l\,\nu^\star + \alpha_l + \sqrt{\alpha_l^2 + \nu^{\star 2} - 2D_l\,\nu^\star\alpha_l}}{(D_l-1)\,\nu^\star}\right), \tag{4.10}$$

where $\nu^\star$ is the optimal dual variable. The details of the analysis is presented in Appendix 4.10.4.

4.6.3 Connectivity in Demand-Supply Networks

Interdependent demand-supply networks have recently come to the attention of researchers [Zha18]. These networks comprise a demand layer and a supply layer, where supply nodes feed in to the demand nodes and maintain their functionality. In the original model in [Zha18], a demand node survives as long as it is connected to at least one surviving supply node. We consider a general setting with weighted interlinks where the amount of supply received by the ith demand node from the jth supply node is given by $w_{ij}s_j$, where s_j is a supply capacity parameter and w_{ij} is the weight of the ijth interlink. Every demand node is assumed to have a survival threshold indicating the minimum total supply required for its survival. Note that the value of this threshold for the model in [Zha18] is 1 as every demand node needs to be interlinked to at least one supply node. In [Zha18], the robustness of the network is measured by the minimum number of supply nodes which on removal fragments the demand network into disconnected components. The computation of this robustness has been shown to be an NP-hard problem. Since the computation of network robustness is critical to our framework, we modify the notion of robustness to be defined as the fractional size of the demand network which survives after the removal of a given fraction of supply nodes. This is in adherence to the notion of robustness defined in the seminal paper [Bul10]. Note that the same

metric of robustness is used in all three failure spreading processes in this dissertation.

We model the initial failure of supply nodes both randomly and preferentially based on the supply node capacities. The survival thresholds are modeled preferentially based on the node intra-layer degree. It is intuitive that demand nodes which play an important role in maintaining the connectivity of the demand network should be strongly interlinked to the supply network as we want to ensure the survivability of these important demand nodes. One possible candidate of measuring this 'importance' maybe intra-layer betweenness, which measures how often do shortest path between different nodes in the network pass through a particular node. Thus based on this candidate, an optimal resource allocation strategy should preferentially interlink demand nodes of high betweenness strongly to the supply network, whereas demand nodes of low betweenness can be ignored and interlinked weakly. The objective function for this process is also based on the logarithmic modeling:

$$f_0(\mathbf{x}) = -\sum_{i=1}^{m} \log\left[\frac{1}{b_i} + \sum_{j=1}^{n} s_j\, r(x_{ij}, \alpha_{ij})\right], \tag{4.11}$$

where $r(x_{ij}, \alpha_{ij})$ gives the weight of the interlink between nodes $i \in A$ and $j \in B$ to which x_{ij} resource is allocated, b_i is the betweenness of the ith demand node, and s_j is the supply capacity of j. It is important to note that there exists a fundamental difference between this metric and the load distribution metric. Although both are based on a logarithmic modeling, the interlinks for these processes perform different functions. In the load distribution process, interlinks offload load to their neighbors. This offloading process on the interlinks occurs independently, i.e. interlinks do not influence the functionality of each other. However for the case of demand-supply networks, all interlinks feeding into a demand node maintains the supply. The demand node cares about the total supply it receives and thus the interlinks cooperate in maintaining the supply to the demand nodes. Thus it is easy to see that the interlink functions are not independent in this case. Due to this reason the proposed metric is not separable w.r.t. the interlinks indexed by l but is separable w.r.t. the demand nodes indexed by i, since the interlinks feeding into a particular demand node are independent of the interlinks feeding into another node. Although the proposed metric is only a heuristic approximation, simulation studies reveal that the metric is monotonically related to network robustness and thus is a fair choice. The results for this case are presented in Fig. 4.3.

For the R.O.I. functions, we use a logarithmic modeling instead of the shifted sigmoid modeling. The purpose of this is to show that the optimization framework in this dissertation can be applied for different kinds of cost modeling as long as the objective function remains convex. The logarithmic model for R.O.I. can be written as:

$$r(x_{ij}, \alpha_{ij}) = \log(\alpha_{ij} x_{ij} + 1), \tag{4.12}$$

where α_{ij} is interlink quality parameter and x_{ij} is the resource allocated. The optimal resource

allocation to the interlink between the ith demand node and the jth supply node can be written as:

$$x^{\star}_{ij} = \max\left(0, \frac{1}{\nu^{\star}(1/b_i + w_i)} - \frac{1}{\alpha_{ij}}\right), \tag{4.13}$$

where $\nu^{\star}$ is the optimal dual variable, b_i denotes the intra-layer betweenness of the ith demand node, α_{ij} denotes the quality of the ij interlink, and $w_i \triangleq \sum_{j=1}^{n} s_j r(x_{ij}, \alpha_{ij})$. The details of the derivation is presented in Appendix 4.10.5. Note that the objective function for this process is not separable in the interlinks l but is separable w.r.t. the demand nodes indexed by I. Due to this reason, the algorithm for obtaining the optimal resource allocation requires an extra step to compute the total supply feeding into the demand nodes given by w_i. The details are presented in Algorithm 2 which essentially follows similar steps with the difference that an extra binary search block (EVAL_-BUDGET) required at each node a which computes the total interlink weight feeding into a for a given ν. In Algorithm 1, this operation is essentially performed by (4.6).

Algorithm 2 Algorithm for Connectivity in Demand Supply Networks

procedure OPT_ALLOC_NSEP($\boldsymbol{\alpha}, G_A, G_B, b, \Delta_{th}$)
  $limit_u \leftarrow \max(size(G_A), size(G_B))$, $limit_l \leftarrow 0$
  $\Delta \leftarrow \inf$
  while $\Delta > \Delta_{th}$ **do**
    $\nu \leftarrow \frac{limit_l + limit_u}{2}$
    $b_{curr} \leftarrow \sum_i EVAL\_BUDGET(a_i, \nu)$
    if $b_{curr} > b$ **then**
      $limit_u \leftarrow \nu$
    else
      $limit_l \leftarrow \nu$
    $\Delta \leftarrow |b_{curr} - b|$
  $x_l \leftarrow EVAL\_RESOURCE(\nu)$
  return $x_l, \forall\ l$

4.7 Distributed Implementation

An important aspect of our dissertation is that the interlink design algorithm can be implemented in a distributed way, where every node in the network only needs local information to compute the optimal resource allocation to the interlinks. Distributed implementation of network design algorithms has become more of a necessity than a feature in recent years as many practical applications involve networks of large size on the order of 10^6 nodes or higher. For such networks, a centralized algorithm is impractical since computing optimal resource allocation for all interlinks at a centralized controller is both infeasible and computationally expensive. Separability and local computation are two main features of our proposed metrics that enable us to obtain the optimal

resource allocation for maximizing network robustness distributively.

In the interest of space, we restrict the discussion to effective degree proposed in Section 4.5. Similar algorithms can be designed for the other failure spreading processes utilizing the separability of the metrics w.r.t. the interlinks for the first two processes and w.r.t the demand nodes for the third processes. Recall that the effective degree metric is given by the expression:

$$f_0(x) = \frac{1}{N}\sum_{l=1}^{m} r(x_l, \alpha_l)(d_{l_A} + d_{l_B}), \tag{4.14}$$

where d_i denotes the degree (or any other topological property of the ith node in the network). Algorithm 1 is a centralized solution where it is assumed that there exists a central controller having knowledge of the entire network topology. The distributed algorithm focuses on solving the optimal allocation problem distributively through local exchange of information among neighbors. The two main building blocks for the algorithm are broadcast and distributed consensus, both of which have extensive literature studying them. Broadcasting is used to inform every node the current value of the dual variable ν whereas distributed consensus is essentially used to compute the sum of the resource allocated for each node (b_a) to estimate the current budget. As done for the case of centralized algorithms, we iteratively converge to the optimal $\nu^\star$ subject to the total budget constraint b. Algorithm 3 summarizes the steps. Note that Algorithm 3 has been defined from the perspective of nodes $a \in A$. Here the nodes $a \in A$ are taken to be the distributed computation unit which store the intra- and inter-layer neighborhood information and compute the optimal resource to be allocated to the interlinks connecting a to layer B.

Algorithm 3 Distributed Algorithm for Effective Degree

procedure OPT_ALLOC_DIST($\boldsymbol{\alpha}_a, N(a), b, \Delta_{th}$)
  $limit_u \leftarrow \max(size(G_A), size(G_B))$, $limit_l \leftarrow 0$
  $\Delta \leftarrow \inf$
  while $\Delta > \Delta_{th}$ **do**
    $\nu = \frac{limit_l + limit_u}{2}$
    $x_{aj} = \max\left(0, \frac{1}{\alpha_l}\log\left[\frac{\sqrt{\frac{\alpha_{aj}D_{aj}}{2}} + \sqrt{\frac{\alpha_{aj}D_{aj}}{2} - \nu}}{\sqrt{\frac{\alpha_{aj}D_{aj}}{2}} - \sqrt{\frac{\alpha_{aj}D_{aj}}{2} - \nu}}\right]\right) \forall\ j \in N(a)$
    $b_a = \sum_{j \in N(a)} x_{aj}$
    Compute $\sum_a b_a$ using Distributed Consensus
    if $b_{curr} = \sum_a b_a > b$ **then**
      $limit_u \leftarrow \nu$
    else
      $limit_l \leftarrow \nu$
    $\Delta \leftarrow |b_{curr} - b|$
  return $x_{aj}, \forall\ j \in \tilde{N}(a)$

The inputs to the algorithm are $N(a)$: the inter-layer neighborhood of a; α_a: α's corresponding to the interlinks between a and $N(a)$; b: the total available budget for constructing interlinks; and Δ_{th}: the error threshold for obtaining ν. Although the algorithm can theoretically work for any size of the neighborhood $N(a)$, a large neighborhood implies that a lot of data has to be stored at each node which is not feasible in a distributed setting. Note that among all possible interlinks from $a \in A$ to nodes of layer B only a few interlinks will be feasible for most practical applications. This is easy to see as most multilayer network applications have sparse interlinking due to various constraints. For smart grid or transportation networks, geographical constraint might be a determining factor, where it is impractical to interlink a power station and a communication router or a subway and bus station which have a large geographical distance between them. In this case, the feasible inter-layer neighborhood of a particular node $a \in A$ can be defined as the set of nodes $b \in B$ which are geographically close to a. Note that the size of the feasible neighborhood $N(a)$ will usually be much smaller compared to the size of the entire network.

4.8 Simulation Results

In this section, we present simulation results in three domains. Our goal here is to study the performance of the convex optimization framework in computing the optimal resource allocation for interlink construction for all three failure spreading processes considered in this dissertation. Firstly, we simulate the failure spreading processes to compare the network robustness for various interlinking strategies. Secondly, we study the performance gain under a varying total available budget. As discussed previously, the generating function based approach of analysis has the weakness that the network topology is constrained to be locally tree-like. Many recent works indicate that network topologies encountered in practice can be dramatically different. Due to this reason, we consider real world networks for generating the simulation results. These real world networks have been chosen to serve as examples of practical network design problems utilizing the convex optimization based approach proposed in this dissertation.

4.8.1 Implementation of Processes

We compare the effects of various interlink construction algorithms from the state of the art with our convex optimization framework. The main roadblock in the way of such comparisons is that as we consider a general model with weighted inter-links and include the effects of interlink construction cost, similar models do not exist in the state of the art to the best of our knowledge. Most works in literature studying the impact of interlink structure on network robustness consider unweighted links and are agnostic to the interlink construction cost. In order to provide a fair comparison of our algorithm with the state of the art, we modify the state of the art metrics to incorporate the interlink construction cost by considering a linear combination of the heuristics with the interlink quality parameter α_l. This modification is intuitive as in a cost constrained setting, interlinking two nodes $a \in A$ and $b \in B$ is not a good strategy if the corresponding α_{ab} has a low value. Thus interlinks

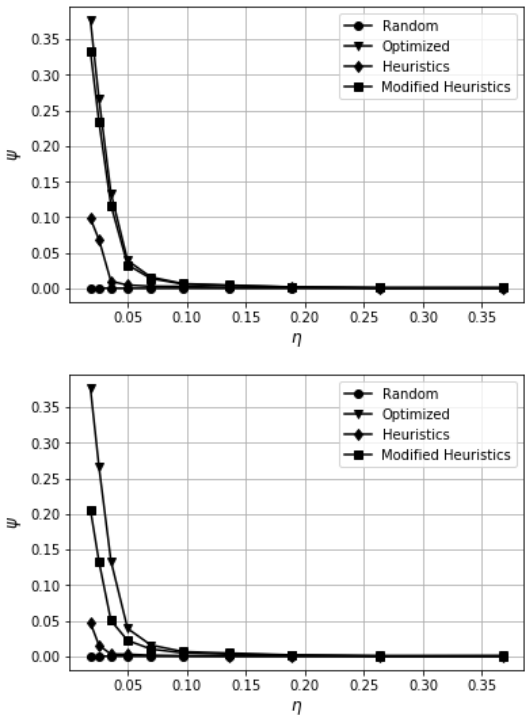

Figure 4.4 Connected component based cascading failure under stringent (top) and sufficient (bottom) budget constraints.

which are recommended by the heuristics but a very low R.O.I.'s are ignored. In the following set of results, we have shown the network robustness under four interlink construction strategies: i) convex optimization based approach proposed in this dissertation, ii) random resource allocation, iii) state of the art heuristic strategies, and iv) modified state of the art heuristics considering interlink construction cost. An interesting point to note here is that under certain budget constraints, random resource allocation can outperform the state of the art heuristics. This is counterintuitive due to the fact that a random distribution of resources is agnostic to both network topology and interlink construction cost. The reason behind this observation is that heuristic interlinking strategies do not consider cost and thus the heuristic recommended interlinks might end up being very expensive owing to low α_l values. This establishes the importance of cost in real world interlink optimization problems. In order to observe the robustness performance for the various cases, we study the variation of network robustness (ψ) at various strength of attacks (η). η is defined as the fraction of nodes removed from the network initially and ψ is defined as the fraction of nodes which survive in the steady state of the failure spreading process.

4.8.1.1 Connected component based cascading failure

We generalize the popular cascading failure process introduced in the seminal paper [Bul10]. We consider weighted interlinks wherein the weights correspond to the probability of propagation

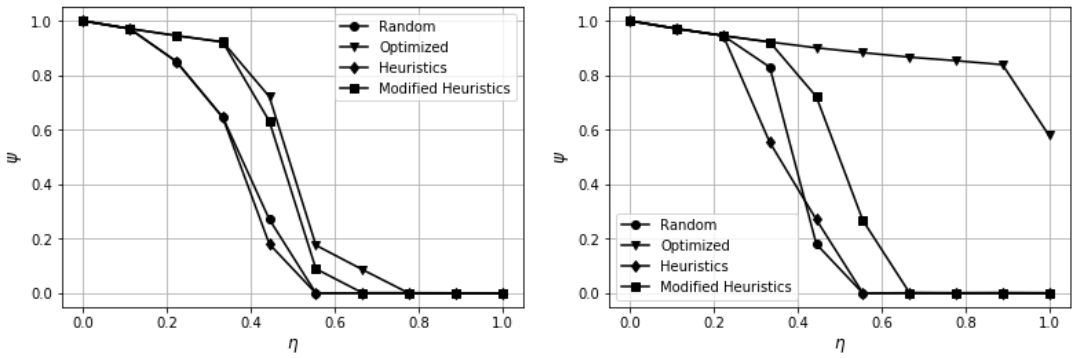

Figure 4.5 Load distribution in interdependent networks under stringent (top) and sufficient (bottom) budget constraints.

of failure. In the classical model, it is assumed that failure of a node strictly implies the failure of its inter-layer neighbor. In our model, interlink weights are indicative of the probability of failure propagation. We consider a preferential betweenness based attack which has been identified as a very disruptive node failure scheme. Degree based anti-monotonic interlinking where the highest degree node in layer A is coupled to the lowest degree node in layer B have been shown to be good strategies for degree based preferential attacks. We conjecture and establish through simulation tests that betweenness based anti-monotonic interlinking is a good strategy and hence use that as our state of the art due to lack of a better candidate. We use a linear combination of this heuristic and interlink quality (α_l) for the modified heuristic.

Smart power distribution grids involving interdependent network layers of power stations and communication routers are one of the prime examples of connected component based cascading failure [Bul10]. The power stations support the communication nodes and the communication nodes enable the power stations to 'talk' to each other. Furthermore, the constituent layers must be connected ensuring that information can spread among all surviving components. In our simulations, we consider the Western States Power Grid of the United States [Wat98] and an Autonomous System AS-733 topology [Les07] which is representative of the network of routers comprising the Internet. The simulation results for this case is presented in Fig. 4.4. It can be observed from Fig. 4.4 that the considered interdependent network is extremely vulnerable to node failures as even an η as low as 0.05 leads to the failure of more than 95% of the network in the steady state. This further establishes the importance of studying multi-layer networks which under certain scenarios can be dramatically more susceptible to node failures compared to single layer networks due to the cascade of failures.

4.8.1.2 Load Distribution

We extend the single layer load distribution model presented in [Lv17] to multiple layers based on ideas from [Zha17] where the authors impose certain assumption on the failure spreading process to make it amenable for analysis. Similar models have been used in works like [Pen15; Hon15]. We

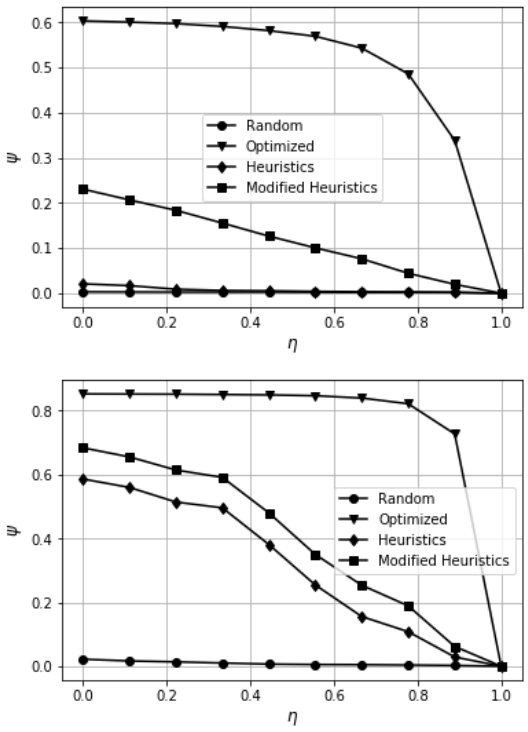

Figure 4.6 Connectivity in demand-supply networks under stringent (top) and sufficient (bottom) budget constraints.

model the load to be proportional to the intra-layer degrees of nodes. When a node fails, its load is redistributed among its inter-layer and intra-layer neighbors. The fraction of load offloaded to the inter-layer neighbors is proportional to the weight of the inter-links. The remaining load is offloaded to the intra-layer neighbors based on the capacity ratio. Degree based monotonic interlinking has been identified to be a good strategy in some simulation based works [Che15; Tan13] and we use it as the state of the art heuristic.

A multi-modal transportation network is a practical instance for this failure spreading process where traffic (load) of failed nodes can be offloaded to their intra- and inter- layer neighbors. We consider the US Airport network [Ops11] and a network of Amtrak Railway routes downloaded from the Bureau of Transportation Statistics under United States Department of Transportation. Thus the problem we are looking at is optimizing the interlinks, which may be shuttle bus services, between airports and railway stations so as to maximize the robustness of the interdependent transportation network against failure of nodes. The simulation results are presented in Fig. 4.5 from which we observe that the performance gain is marginal for stringent budget requirements. However under sufficient budgets, using the optimization framework to design the interlinks lead to significant improvement in ψ.

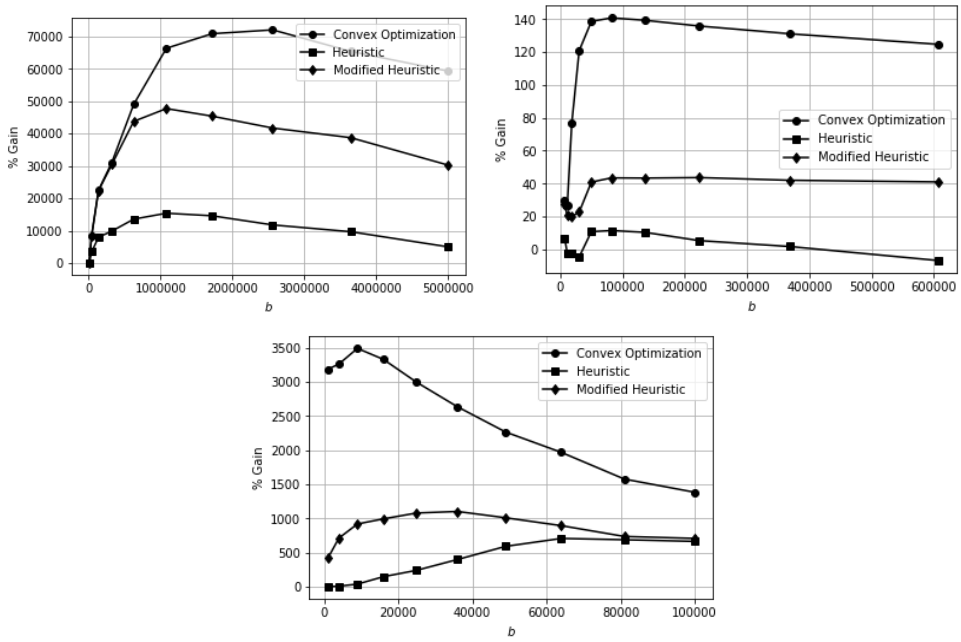

Figure 4.7 Variation of performance gain w.r.t. random resource allocation for different interlink construction strategies. The three figures correspond to processes: i) connected component based cascading failure (top), ii) load distribution (middle), and iii) connectivity in demand supply networks (bottom).

4.8.1.3 Connectivity in Demand-Supply networks

For this process, we consider a generalization of the model considered in [Zha18]. In particular, we consider weighted interlinks and the survival of a demand node is subject to the condition that the total supply feeding into a demand node, given by the weighted sum of the interlinks, exceeds a threshold known a priori. We consider a degree based modeling of the threshold, where demand nodes of high degree have a higher supply requirement. A demand node survives if the incoming supply exceeds the threshold and it belongs to the largest connected component in the demand network. Path-based interlink assignment, where the demand nodes constituting the node disjoint paths between two randomly chosen demand nodes are interlinked to distinct supply nodes, has been identified as a good heuristic algorithm in [Zha18] and we use it as the state of the art.

These supply demand interdependencies are common in many practical instances of multilayer networks. In this dissertation, we consider the case of a network of the busiest commercial airports in the United States as the demand network [Col07] and the US Power Grid dataset as the supply network. Thus we consider the problem of optimally interlinking airports to power distribution stations to maximize the robustness of the demand network. The simulation results are presented in Fig. 4.6. We observe here that a stringent budget leads to a higher performance gain as compared to higher budgets.

4.8.2 Performance gain variation with total available budget

In this section, we are interested in studying the performance of the proposed interlinking strategy under different budget constraints b. The performance gain is computed w.r.t. the random resource allocation strategy and is defined as the relative difference in ψ averaged over η. The results presented in Fig. 4.7 have certain interesting implications. For the connected component based cascading failure, the performance gain obtained by employing the optimization framework is not significant for low b. The reason behind this is that under low availability of budget the number of interlinks constructed between the two network layers is small leading to a partially interdependent network [Ran11; Cha17] comprising interdependent and autonomous nodes that are interlinked and not interlinked, respectively, to nodes of other layers. The dynamics of partially interdependent networks differs from completely interdependent ones due to the fact that autonomous nodes can survive without interlinks. Furthermore, simulation results also indicate that the proposed metric and simulated robustness, as studied in Fig. 4.1, are not monotonically related when the number of interlinks between the two networks is small. This essentially means that the proposed metric is unable to characterize the failure spreading process when the number of interlinks between the two networks is very low. This implication reveals the limitation of the optimization framework proposed in this dissertation. Performance gain is significant only when the designed metrics are monotonically related to robustness. This is intuitive as well since a monotonic relationship ensures that maximization of ψ, which is very complicated if not intractable for most realistic problems, can be achieved by maximization of the proposed metrics which are mathematically tractable.

4.9 Conclusion and Future Work

In this dissertation we model the construction of interlinks between the interdependent layers of a network as a convex optimization problem. Departing from traditional approaches of simplistic network models and flattened multilayer models, we propose new approximate metrics of robustness for different failure spreading processes in multilayer networks with arbitrary topology. These proposed metrics have been analytically shown to capture the dynamics of the processes. Due to the mathematical tractability of the proposed metrics, we are able to solve the interlink design problem in closed form and also take into account the cost of construction of interlinks into the network design problem. Furthermore, the interlink optimization algorithms can be implemented in a distributed fashion. In essence, this work establishes a framework for dealing with interlink optimization problems with budget constraints which can be applied to various failure spreading processes. As long as we can design a separable metric which can be analytically shown to be monotonically related to network robustness, the proposed framework is applicable.

With regard to further research in this area, a prime focus is to extend the framework to non-separable metrics like algebraic connectivity, effective resistance etc. We are also exploring more involved metrics of robustness which are fine-tuned to capture the properties of the failure spreading processes. This line of research is important as the performance gain when considering sophisticated

metrics will reveal whether accurate characterization of the processes is necessary or whether approximate characterizations, like those presented in this dissertation, can achieve reasonably good performance.

4.10 Mathematical Details

4.10.1 Convexity of Optimization Problem

The general optimization problem can be written as:

$$\begin{aligned} \underset{\mathbf{x}}{\text{minimize}} \quad & f_0(\mathbf{x}, \mathbf{G_A}, \mathbf{G_B}) \\ \text{subject to} \quad & \mathbf{1}^T\mathbf{x} = b, \\ & \mathbf{x} \succeq 0, \end{aligned} \tag{4.15}$$

As discussed in Section 4.4, the above problem is a convex optimization problem if the objective function is convex. Let us now examine the metrics proposed in this work to examine the conditions for their convexity. In this section, we only state the mathematical equations describing the proposed metrics. The physical meanings and intuitions behinds these metrics are presented in the main body of the dissertation.

The first proposed metric is the generic effective degree metric which is later modified in relation to the connected component based cascading failure process. It can be written as:

$$f_0(\mathbf{x}) = -\sum_{l=1}^{mn} r(x_l, \alpha_l) D_l(l_A, l_B). \tag{4.16}$$

It is easy to see that the metric is a linear combination of the R.O.I. functions $r(x_l, \alpha_l)$. Thus $f_0(\mathbf{x})$ is convex when the R.O.I.'s are concave since linear combination of concave functions is also concave and the negative of a concave function is convex.

The second metric of robustness for the load distribution process is based on a logarithmic modeling. The metric can be written as:

$$f_0(\mathbf{x}) = -\sum_{l=1}^{mn} \log(D_l + r(x_l, \alpha_l)). \tag{4.17}$$

Since logarithm preserves concavity, we can see that concavity of the R.O.I.'s guarantee the convexity of $f_0(\mathbf{x})$. The metric corresponding to the connectivity in demand supply networks is similar to this with the difference that the argument to the logarithm is a linear combination of R.O.I.'s. Since both linear combination and logarithms preserve concavity, we can conclude that for all metrics proposed in this work concavity of R.O.I.'s guarantee that the interlink optimization problem is convex. This enables us to use the rich literature in the domain of convex optimization problems [Boy04] to solve our problem.

4.10.2 Analysis for general metric

The optimization problem for the general metric $f_0(\mathbf{x})$ can be written as:

$$\begin{aligned} \underset{\mathbf{x}}{\text{minimize}} \quad & f_0(\mathbf{x}) \\ \text{subject to} \quad & \mathbf{1}^T\mathbf{x} = b, \\ & \mathbf{x} \succeq 0, \end{aligned} \tag{4.18}$$

Let us write the Lagrangian of the above optimization problem:

$$L(\lambda, \nu) = \inf_{\mathbf{x}} \left[f_0(\mathbf{x}) + \sum_{l=1}^{m} \lambda_l(-x_l) + \nu(\mathbf{1}^T\mathbf{x} - b) \right], \tag{4.19}$$

where $\lambda = [\lambda_1 \cdots \lambda_m]^T$ denotes the multipliers for the inequality constraints and ν is the multiplier for the equality constraint. It is shown in Appendix 4.10.1 that (5.21) is a convex optimization problem if the return on investment functions (f_l's) are all concave in x_l. Under that assumption, we can invoke the KKT conditions to conclude that:
If $\exists\ (\mathbf{x}^\star, \lambda^\star, \nu^\star)$ such that:

1. $x_l^\star \geq 0\ \forall l$
2. $\mathbf{1}^T\mathbf{x} - b = 0$,
3. $\lambda_l^\star \geq 0\ \forall l$,
4. $\lambda_l^\star x_i^\star = 0\ \forall l$,
5. $\nabla f_0(\mathbf{x}^\star) + \sum_{l=1}^{mn} \lambda_l^\star(-\nabla x_l) + \nu^\star \nabla(\mathbf{1}^T\mathbf{x} - b) = 0$.

Now $\mathbf{x}^\star = [x_1^\star x_2^\star \cdots x_m^\star]^T$. Thus the last KKT condition can be written in terms of the individual variables (x_l) as:

$$\frac{\partial f_0(\mathbf{x})}{\partial x_l} - \lambda_l^\star + \nu^\star = 0, \ \ \forall l. \tag{4.20}$$

Substituting the value of $\lambda_l^\star$ from (4.20) into the 4th and 3rd condition gives:

$$x_l^\star \left(\nu^\star + \frac{\partial f_0(\mathbf{x})}{\partial x_l} \right) = 0 \ \ \forall l, \tag{4.21}$$

$$\nu^\star + \frac{\partial f_0(\mathbf{x})}{\partial x_l} \geq 0 \ \ \forall l. \tag{4.22}$$

These two equations have very interesting implications. (4.21) implies that whenever $x_l^\star \neq 0$:

$$\nu^\star = -\frac{\partial f_0(\mathbf{x})}{\partial x_l}. \tag{4.23}$$

Further note that since we have already eliminated $\lambda^\star$ (vector of λ_i's) knowing $\nu^\star$ directly gives us $\mathbf{x}^\star$, which is the resource allocation optimizing the network robustness measured by $f_0(\mathbf{x}^\star)$.

4.10.3 Analysis for Effective Degree

The optimization problem for this case can be written as:

$$\begin{aligned} \underset{\mathbf{x}}{\text{minimize}} \quad & f_0(\mathbf{x}) = -\sum_{l=1}^{m} r(x_l, \alpha_l)(d_{l_A} + d_{l_B}) \\ \text{subject to} \quad & \mathbf{1}^T \mathbf{x} = b, \\ & \mathbf{x} \succeq 0. \end{aligned} \tag{4.24}$$

In the following analysis, we model the R.O.I.'s as shifted sigmoid functions defined in Section 4.4. The shifted sigmoid functions can be written as:

$$r(x_l, \alpha_l) = \frac{2}{1 + e^{-\alpha_l x_l}} - 1. \tag{4.25}$$

Using the KKT equations (4.21),(4.22), we can write:

$$x_l^\star \Big(\nu^\star - r'(x_l^\star, \alpha_l)(d_{l_A} + d_{l_B}) \Big) = 0 \ \ \forall l. \tag{4.26}$$

Plugging in the shifted sigmoid modeling given by (4.25) into the above equation gives us:

$$x_l^\star \Big(\nu^\star - \frac{2e^{-\alpha_l x_l^\star} \alpha_l}{(1 + e^{-\alpha_l x_l^\star})^2} (d_{l_A} + d_{l_B}) \Big) = 0 \ \ \forall l. \tag{4.27}$$

The above equation implies that for all active interlinks where $x_l^\star \neq 0$, denoting $e^{-\alpha_l x_l^\star} \triangleq t$ and $(d_{l_A} + d_{l_B}) \triangleq D_l$, we get:

$$\nu^\star - \frac{2\alpha_l t D_l}{(1+t)^2} = 0. \tag{4.28}$$

The above equation represents the relationship between the optimal dual $\nu^\star$ and the optimal primal $x_l^\star$ which denotes the optimal resource allocation to the lth link. We use this relationship coupled with the fact that $\sum_l x_l^\star = b$ to derive the optimal dual variable $\nu^\star$ and then extract the optimal primal $x_l^\star$ using $\nu^\star$ and (4.28). Let us now try to solve the quadratic equation (4.28). It can be written as:

$$\nu^\star t^2 + 2t(\nu^\star - \alpha_l D_l) + \nu^\star = 0. \tag{4.29}$$

The solution for the above equation can be written as:

$$t = \frac{-(\nu^\star - \alpha_l D_l) \pm \sqrt{\alpha_l^2 D_l^2 - 2\alpha_l D_l \nu^\star}}{\nu^\star}. \tag{4.30}$$

Note that (4.30) is nothing but a one-to-one relationship between $x_l^\star$ and $\nu^\star$. In order to solve the system and obtain the optimal $\mathbf{x}^\star$, we would need to make use of $\sum_{l=1}^{m} x_l = b$ and substitute the x_l's using (4.30). After substitution the resulting expression will be an equation in single variable $\nu^\star$ (all α_l, D_l, b is known) which can readily solved.

Note that (4.30) will not have a real solution when $\nu^\star > \alpha_l D_l/2$. This is interesting because of the following reason. Let us index the possible interlinks in the network in the ascending order of $\alpha_l D_l/2$. Let us arrange these values in the number line and let us also plot $\nu^\star$ in the same line. $\nu^\star$ divides this line into two sections. In other words, of all possible interlinks some (or maybe all) of them will have the corresponding $\alpha_l D_l/2$ value greater than $\nu^\star$ and (4.30) will have a real solution only for those interlinks. Thus the final value of $\nu^\star$ would determine which of the interlinks will be allocated a non-zero resource.

Let us now simplify the expression in (4.30). Let us define $c_l \triangleq \alpha_l D_l/2$ and $p_l \triangleq c_l - \nu^\star$. Thus (4.30) can be written as:

$$t = \frac{(c_l + p_l) \pm 2\sqrt{c_l p_l}}{c_l - p_l} \tag{4.31}$$

$$= \frac{(\sqrt{c_l} \pm \sqrt{p_l})^2}{c_l - p_l} = \frac{\sqrt{c_l} \mp \sqrt{p_l}}{\sqrt{c_l} \pm \sqrt{p_l}} \tag{4.32}$$

Note that t was defined as $t = e^{-\alpha_l x_l^\star}$ is a real number between 0 and 1. Thus the only case which leads to a positive solution for x_l can be written as:

$$x_l^\star = \frac{1}{\alpha_l} \log\left(\frac{\sqrt{c_l} + \sqrt{p_l}}{\sqrt{c_l} - \sqrt{p_l}}\right) \ \forall \text{ active links } l, \tag{4.33}$$

$$= \frac{1}{\alpha_l} \log\left(\frac{\sqrt{\frac{\alpha_l D_l}{2}} + \sqrt{\frac{\alpha_l D_l}{2} - \nu^\star}}{\sqrt{\frac{\alpha_l D_l}{2}} - \sqrt{\frac{\alpha_l D_l}{2} - \nu^\star}}\right). \tag{4.34}$$

4.10.4 Analysis for load distribution

The optimization problem corresponding to the load distribution in interdependent networks can be written as:

$$\begin{aligned} \underset{\mathbf{x}}{\text{minimize}} \quad & f_0(\mathbf{x}) = -\sum_{l=1}^{mn} \log(D_l + f_l(x_l)) \\ \text{subject to} \quad & \mathbf{1}^T \mathbf{x} = b, \\ & \mathbf{x} \succeq 0, \end{aligned} \tag{4.35}$$

where $D_l \triangleq 1 - e^{(-\frac{1}{|s_{l_A} - s_{l_B}|})}$. Modeling the return on investments as sigmoid functions given by (4.25), we can write the following equations:

$$\nu^\star = -\frac{\partial}{\partial x_l}\left[-\log\left((s_{l_A} - s_{l_B})^2 + f_l(x_l)\right)\right] \tag{4.36}$$

$$= -\frac{\partial}{\partial x_l}\left[-\log\left(D_l + f_l(x_l)\right)\right] \tag{4.37}$$

$$= \frac{1}{D_l + \frac{2}{1+e^{-\alpha_l x_l}} - 1} \frac{\partial f_l(x_l)}{\partial x_l} \tag{4.38}$$

$$= \frac{1}{(D_l - 1 + \frac{2}{1+t})} \frac{2\alpha_l t}{(1+t)^2} \tag{4.39}$$

The above expression is quadratic in $t \triangleq e^{-\alpha_l x_l}$ and its solution can be written as:

$$x_l^\star = -\frac{1}{\alpha_l}\log\left(\frac{-D_l\nu^\star + \alpha_l + \sqrt{\alpha_l^2 + \nu^{\star 2} - 2D_l\nu^\star\alpha_l}}{(D_l-1)\nu^\star}\right). \tag{4.40}$$

4.10.5 Analysis for connectivity in demand-supply networks

The interlink optimization problem for the connectivity in Demand-Supply networks can be written as:

$$\begin{aligned} \underset{\mathbf{x}}{\text{minimize}} \quad & f_0(\mathbf{x}) = -\sum_{i=1}^{m}\log\left[\frac{1}{b_i} + \sum_{j=1}^{n} s_j f_{ij}(x_{ij})\right] \\ \text{subject to} \quad & \mathbf{1}^T\mathbf{x} = b, \\ & \mathbf{x} \succeq 0, \end{aligned} \tag{4.41}$$

where b_i is the intra-layer betweenness of the ith demand node, s_j is the supply capacity of the jth supply node, and $f_{ij}(x_{ij})$ is the weight of the interlink connecting the ith demand node and the jth supply node. Recall that the fundamental equation based on KKT which we obtained in the general analysis of the convex optimization problem is $\nu^\star = -\frac{\partial f_0(x)}{\partial x_{ij}}$. For the analysis of the problem, let us focus on all interlinks feeding into the ith demand node. We can write:

$$\nu^\star = -\frac{\partial}{\partial x_{ij}}\left[-\log\left(\frac{1}{b_i} + \sum_{j=1}^{n} f_{ij}(x_{ij})\right)\right] \tag{4.42}$$

$$= -\frac{\partial}{\partial x_{ij}}\left[-\log(D_i + w_i)\right] \tag{4.43}$$

$$= \frac{1}{D_i + w_i}\frac{\partial f_{ij}(x_{ij})}{\partial x_{ij}} \tag{4.44}$$

$$= \frac{1}{(D_i + w_i)(x_{ij} + \frac{1}{\alpha_{ij}})}, \tag{4.45}$$

where $D_i \triangleq 1/b_i$ and $w_i \triangleq \sum_j f_{ij}(x_{ij})$. It can be seen here that in contrast to the metric of robustness proposed earlier, the connectivity metric is not separable in all variables. We show that even for such non-separable metric the technique presented in this dissertation can be applied to determine the optimal resource allocation. It should be clarified that the non-separable nature of the metric results in a larger convergence time in the distributed algorithm as compared to the separable metrics. This is due to an additional computation of the term w_I before the computation of the individual x_{ij}'s. (4.45) can be rewritten as:

$$x_{ij} = \max\left(0, \frac{1}{\nu^\star(D_i + w_i)} - \frac{1}{\alpha_{ij}}\right). \tag{4.46}$$

CHAPTER

5

CONTROLLED INFECTION SPREADING

The study of epidemic spreading in complex network topologies has emerged as an area of broad and current interest in network science. One of the primary factors facilitating this is the ubiquity of contagion processes on networks as a framework for studying the propagation of various phenomena in multiple disciplines. The dynamics of traffic jams in transportation systems [Oro10], the spread of biological diseases through human contact networks [Vid11], rumor propagation through social networks [Liu11], the propagation of component failure in networked systems [Buz06], among many others, exemplify the wide and inter-disciplinary applicability of epidemic spreading models. Although the specific details of the propagation mechanisms in different application domains are not expected to remain exactly the same, stochastic agent-based models provide a popular and effective mathematical characterization of these processes.

5.1 Background

The main focus of research in this domain has been in the direction of evaluating the critical infection rate λ_c [Ber05; Gan05; Cas10], separating the abrupt outbreak of contagion in the super-critical regime, where an initial infection spreads throughout the network and affects a finite fraction of its constituents, with the healthy network state in the sub-critical regime, where any initial infection quickly converges to the all-healthy absorbing state of the network with no infected constituents. Later works [Gol12; Lee13] took a closer look into the epidemic dynamics near the critical infection rate and discovered the phenomenon of localized infections in networks, where long lasting localized epidemics can be sustained in the neighborhood of hubs of large degrees. The epidemic dynamics under this regime are referred to as “metastable” infection states. The

metastability refers to the fact that the infections can be maintained in apparent states of stability for a long time, albeit dying out eventually in the steady state. Moving away from a steady-state analysis of epidemic dynamics, studying the intermediate properties of metastable infections have come to the attention of researchers [Mou13; Liu18; Bov14]. The importance of studying the properties of metastable epidemics is further highlighted by the ongoing Covid-19 pandemic. Even if the death of the pandemic in the steady state is guaranteed, the intermediate properties of the epidemic dynamics, like, the infection size, time to steady state, etc., are also of enormous importance. In this disseration, we study the mean infection size for metastable infection states in multi-layer networks and explore the possibility of controlling this infection size by intelligent design of the inter-layer connections between the different network layers. Our main interest is in the region near the critical infection threshold, where localized long lasting infections can exist despite the absence of global infection patterns in the steady state.

The Susceptible–Infected–Susceptible (SIS) is one of the fundamental models for studying the propagation of epidemics in complex networks, where each agent (node) in the network can be in one of two infection states: susceptible or infected. Under this model, infected agents recover spontaneously at rate μ, which without loss of generality is set to unity. The infection propagation occurs via edges between infected and susceptible agents at a rate of λ. In this dissertation, we consider a generalization of this model, where the edges in different network layers have distinct infection propagation rates. Despite the simplicity of the SIS model, a general mathematical analysis on heterogeneous network topologies is still too complex [VM08] and very few exact results exist [Dur10; Cat13]. Due to the inherent complexity of models capable of tracking the epidemic dynamics exactly, most works in literature employ variants of mean-field approaches to study the dynamics approximately. In this dissertation, we employ the modified SIS dynamics valid over coarse-grained time scales introduced in [Bog13] as it can account for dynamical correlation in the infection states of distant nodes. The course-grained model characterizes the epidemic dynamics at a larger time-scale encompassing multiple infection and recovery events. This allows us to efficiently capture the correlation in infection states among nearby nodes. This coarse-grained model is particularly useful in studying the epidemic dynamics near the critical threshold and has been utilized in [Bog13; Fer16; Wei17] to uncover new results about epidemic threshold in complex networks. Utilizing this coarse-grained model, we are able to calibrate the conditions for the existence of long lasting epidemics in the local neighborhood of nodes of high intra-layer degrees referred to as hubs. We then utilize these conditions to realize infections in the multi-layer network of a desired size by manipulating the interlinking structure between the different network layers.

5.1.1 Related Works

It was a long standing belief in the network science community that the transition between the sub-critical and super-critical phases is specified by the epidemic threshold λ_c and epidemics with infection rate $\lambda < \lambda_c$ quickly converge to the absorbing healthy state, whereas epidemics with $\lambda > \lambda_c$ infect a finite fraction of the entire network. This viewpoint was challenged by works like [Gol12;

Lee13]. They showed that under certain conditions, the epidemic dynamics in complex networks just above the critical rate λ_c can be sustained in localized regions of the network for a long time. In other words, the epidemics neither die out quickly nor infect a finite fraction of the entire network, but are maintained in localized metastable infection states [Sch85].

We should clarify that the ideas of localization and metastability of the infections are rigorously defined only in the thermodynamic limit, when the network size approaches infinity. Furthermore, most theoretical results in related works in literature are obtained for scale-free (SF) networks, where the degree distribution $P[k]$, characterizing the probability that a node has k neighbors, exhibits a heavy-tailed distribution $P[k] \sim k^{-\gamma}$ with exponent γ. Investigation of the global epidemic dynamics in the thermodynamic limit for SF networks is undoubtedly important from a theoretical perspective. However, our main focus in this dissertation is to study epidemic dynamics from a network design standpoint, where we consider finite networks with arbitrary network topologies. We argue that such problem settings are important in many real world problems, where a global knowledge about the network topology or the degree distribution is not available. It is important to note that the concepts of localized infections and metastability of the infection states are not rigorously defined for finite networks. However, we reveal through this dissertation that the key ideas behind them can be applied to finite sized networks to realize controlled infection spreading in networks. Note that we are not interested in the super-critical phase, where epidemics in the network spread out globally, since it is contrary to our basic objective of achieving controlled infection spreading. Instead, we focus on the regime of low infection rates, where our goal is to skillfully design the interlinking structure between isolated network layers so as to achieve a localized metastable infection of a desired size in the network.

For multilayer networks, several works [Zhe18; SM12] have studied different epidemic models, focusing on the determination of the epidemic threshold. More recently, the localization phenomenon of SIS epidemics has also been studied on multiplex networks [Arr17]. However, to the best of our knowledge, manipulation of the network topology to control the propagation of epidemics in the network is largely missing from the current art.

5.1.2 Motivation

The motivation behind the current work stems from several mathematical papers investigating the critical infection rate λ_c for the SIS epidemic process on networks characterized by power law degree distributions. The seminal paper [Cha09] showed that $\lambda_c = 0$ for power law graphs. Later works extended some of these results to general graph structures [Mou16b; Mou16a; VH18]. Interestingly, this line of research can estimate the fraction of infected nodes in the metastable infection state under the setting that the infection propagation rate (λ) diminishes to 0. These works are developed under a stochastic framework, contrary to the agent based characterization of the epidemic dynamics popular in network science.

These results are not directly applicable to our problem, as we consider arbitrary network topologies and thus, the degree distribution is not guaranteed to be described by a power law.

Furthermore, our focus is on finite network sizes and finite λ. However, we show here that the fundamental principle behind these works can be leveraged in our setting–the large scale epidemic dynamics in networks can be approximated by studying the local epidemic dynamics around hubs and the interaction among different hubs. In the asymptotic setting, this approximation can be shown to be exact. However, for the finite setting considered here, this approximation amounts to characterizing the sufficient condition for the existence of the desired infection patterns in the network. If local epidemics in the neighborhood of hubs do not die out quickly, the global epidemics in these neighborhoods will also survive for a long time.

The main aspect of this dissertation is to develop network design principles and thus, instead of studying the epidemic dynamics around the nodes (hubs), we study epidemic dynamics in the neighborhood of the end-points of an inter-layer link. This microscopic region is referred to as the *interlink subgraph*, comprising of an interlink and the local neighborhood around its end-point in different network layers. The coarse-grained model for studying epidemics allows us to account for the local neighborhood without explicitly considering the neighborhood topology. It is easy to see that such a characterization is an approximation to the actual epidemic dynamics. However, in the regime of low infection rates near the infection threshold, this approximation is quite accurate. By appropriately maintaining the interaction between different hubs via the design of the interlinking structure, we can artificially create composite metastable infection states spanning multiple hubs. This is the fundamental idea of this work, wherein manipulation of the network structure allows us to *control* the infection size in the multi-layer network.

5.1.3 Our contribution

Due to the inherent complexity of studying epidemic models on complex multi-layer network topologies with arbitrary interlinking structures, our basic idea is to study the microscopic properties of the epidemic dynamics in the local neighborhood of nodes and characterize the macroscopic epidemic dynamics by the interaction between distinct microscopic regions–the interlink subgraphs. In spite of the approximate nature of such a characterization, we reveal through this dissertation that the properties of the epidemic dynamics uncovered through it can provide us the crucial building blocks, which can be leveraged to design the interlinking structure between different network layers to achieve controlled epidemic spreading in networks.

We start with the characterization of three main properties of the epidemic dynamics in the interlink subgraphs: i) quantify the definition of “hubs" in a multi-layer setting as a function of the infection propagation rate, where hubs are nothing but nodes with large neighborhoods which are capable of sustaining long lasting epidemics; ii) approximate the mean infection size in the intra-layer neighborhood of hubs; and iii) characterize the probability that infection from a hub propagates to an interlinked hub in a different network layer.

Utilizing these properties of the epidemics on the interlink subgraphs, we can approximate the average infection size in the multi-layer networks for any interlinking structure. The interlinking structure between the network layers is then designed with the objective of maximizing the estimated

infection size, while utilizing the minimum number of interlinks. Under certain conditions, we are able to rigorously obtain the theoretically optimal interlinking structure maximizing the infection size in the network. In the general case unfortunately, the optimization of the interlinking structure turns out to be a non-convex discrete optimization problem, which is too expensive to solve. For this case, we obtain approximate greedy strategies for the design of the interlinking structure which perform quite well in spite of being theoretically sub-optimal.

The various theoretical results obtained here are verified by extensive simulation experiments on both real world and synthetic networks. Due to the absence of relevant multi-layer interlinking strategies in literature, we compared our design of the interlinking structure with other variations and some heuristic designs to showcase the advantage of the proposed methods. Finally, we consider two case studies involving practical mutli-layer network design problems, wherein the ideas developed in this dissertation can be applied in real world problems.

5.2 System Model and Problem Statement

We represent a network layer by $G = (V, E)$, where V and $E \subseteq V \times V$ are the set of nodes and edges, respectively. Given two isolated network layers $G_a = (V_a, E_a)$ and $G_b = (V_b, E_b)$, where $|V_a| = m$ and $|V_b| = n$. Our aim is to design the interlinking structure $E_{ab} \in \{0,1\}^{m \times n}$ between G_a and G_b, with the objective of controlling the spread of epidemics on the multi-layer network $\mathscr{G} = (G_a, G_B, E_{ab}, E_{ba} = E_{ab}^T)$. We consider epidemics following the susceptible-infected-susceptible (SIS) dynamics, where the nodes in the network can only be in one of two infection states – susceptible (S) or infected (I). Infected nodes recover spontaneously at a rate of unity, so as to normalize the event of infection propagation with respect to the recovery event. Thus, the unit of time for our model is the average duration of the recovery event. Infections propagate from infected nodes to their susceptible neighbors via edges at fixed rates. The infection propagation rate via the intra-layer links is λ_a and λ_b, respectively, for the two network layers G_a and G_b. The propagation rate via the inter-layer links is represented as $\tilde{\lambda}$. In this dissertation, we assume that the infection spreading parameters $\boldsymbol{\lambda} = \{\lambda_a, \lambda_b, \tilde{\lambda}\}$ and the isolated network topologies $\{G_a, G_b\}$ are known, and our target is to design an interlinking structure E_{ab} between the isolated network layers which achieves controlled infection spreading in the multilayer network $\mathscr{G}$.

With the network architecture and the epidemic dynamics defined, let us focus on the specific problem statement. Our objective is to design the interlinking structure between the two isolated network layers so as to induce a metastable infection state in a desired region of the network, represented by the sub-graphs D_a and D_b. We assume that it is feasible to construct an interlink between any two nodes in the desired subgraphs: D_a and D_b. Our goal is to construct the interlinking structure in order to artificially create a metastable infection state in the desired subgraphs of the multi-layer network, i.e. $D_a \cup D_b$. To exercise further control on the epidemics, we consider a desired infection density $\Gamma = (\gamma_a, \gamma_b)$ for the subgraphs D_a and D_b, respectively, representing the desired fraction of nodes in the subgraphs that should remain infected on average, before the metastable

infection eventually dies out. Our problem statement can be mathematically stated as: Given two isolated network layers $\{G_a, G_b\}$ and SIS epidemic dynamics with normalized infection parameters $\boldsymbol{\lambda} = \{\lambda_a, \lambda_b, \tilde{\lambda}\}$, design an interlink structure to induce a metastable infection state of density $\Gamma = (\gamma_a, \gamma_b)$ in the desired subgraphs $D_a \subseteq G_a$ and $D_b \subseteq G_b$. It should not be difficult to see that the above problem statement is general in nature and it is unlikely that any Γ can be achieved for an arbitrary network topology and arbitrary infection propagation rate $\boldsymbol{\lambda}$. In fact, developing an understanding of the feasibility regions for which the Problem 5.2 can be solved is one of our key contributions. We present a brief discussion of the feasibility region here and these ideas will be progressively clarified throughout the remainder of the dissertation.

One of the central ideas in this dissertation is the concept of a *hub*, which can be defined as a node which can sustain a metastable infection state in its local neighborhood, i.e. the subgraph spanned by its intra- and inter-layer neighbors. We define two groups of hubs: core and supplementary. We do not discuss the specific details of these definitions here as they involve the theoretical concepts developed in the remainder of this dissertation. For an extended parameter range of $\boldsymbol{\lambda}$, it can be shown that these hubs infect a predictable fraction of their neighborhood. Utilizing this idea, we show that by carefully interlinking multiple hubs from both layers of the network, it is possible to realize controlled infection spreading. Thus, the feasibility region of Problem 5.2 is given by the maximum infection density achievable by the core and the supplementary group of hubs in the desired region of the network, D_a and D_b. This infection density threshold is represented as Γ^{cs}, indicating the constituent core and supplementary group of hubs. Note that the characterization of a hub is dependent on the infection propagation rates, i.e. the number of hubs in D_a and D_b can be varied by changing $\boldsymbol{\lambda}$. Although we discuss techniques to augment the metastable infection state comprising the core and supplementary hubs in D_a and D_b in later sections, the prime focus of this dissertation is in the regime where the desired infection density Γ is achievable by these hubs, i.e. $\Gamma \leq \Gamma^{\text{cs}}$.

Furthermore, we assume that the intra-layer infection rates, λ_a and λ_b, are not sufficiently high to induce global epidemics in the individual network layers, as we loose control over the resulting infection size in this regime. The exact characterization of the infection rate λ that leads to global epidemics in networks is a topic of current research, where modern methods, like, edge based compartmental models [Zhe18; She18], and pairwise approximation models [Mat14; Wu18], among many others generalize the results from classical works [PS01; VM08]. Here, we are not interested in global epidemic dynamics; we focus on infection rates λ_a and λ_b lower than the thresholds for global epidemic spreading. Thus, our main focus is on the low infection propagation rate regime, where an intelligent design of the interlinking structure can induce the desired metastable infection state in the network, thus achieving controlled infection spreading.

5.3 Analysis of Epidemic Dynamics

In this section, we will develop the mathematical model for tracking the epidemic dynamics. The infection state of a node at time t is specified by a Bernoulli random variable $X_i(t)$, where $X_i(t)=0$ for a healthy node and $X_i(t)=1$ for an infected node. We track the epidemic dynamics in the network $\mathcal{G}$ using the node infection probability $\rho_i(t)$, defined as the probability that node i is infected at time t, i.e. $\rho_i(t) \triangleq \Pr[X_i(t)=1]$. Let $\boldsymbol{\rho}_t \equiv [\rho_1^{(a)}(t)\cdots\rho_m^{(a)}(t)\rho_1^{(b)}(t)\cdots\rho_n^{(b)}(t)]^T$ be the vectorized infection probability of all nodes in $\mathcal{G}$. The epidemic dynamics on $\mathcal{G}$ is given by the time series $(\boldsymbol{\rho}_t)_{t\geq 0}$, where $\boldsymbol{\rho}_t \in \mathbb{R}^{m+n}$. The initial infection configuration is represented by $\boldsymbol{\rho}_0$ and the progression of the time series is governed by the SIS model of epidemic dynamics.

Despite the relative simplicity of the SIS infection spreading model, a general analytic treatment is not possible except for very special cases [VM08]. Most works analyze the epidemic dynamics approximately by using different mean-field approaches: classical examples are the heterogeneous mean field (HMF) model [PS01] and the N-intertwined mean field approximation (NIMFA) [VM08]. Here, we adopt the modified SIS dynamics valid over coarse-grained time scales, introduced in [Bog13], under which the system of differential equations governing the epidemic dynamics can be written as:

$$\begin{aligned}\frac{d\rho_i^{(a)}(t)}{dt} =& -\rho_i^{(a)}(t)\bar{\delta}_a(i) + \sum_{\substack{j\in V_A \\ j\neq i}} \bar{\lambda}_{aa}(i,j)\rho_j^{(a)}(t)(1-\rho_i^{(a)}(t)) \\ &+ \sum_{j\in V_B} \bar{\lambda}_{ab}(i,j)\rho_j^{(b)}(t)(1-\rho_i^{(a)}(t)), \qquad (5.1)\\ \frac{d\rho_i^{(b)}(t)}{dt} =& -\rho_i^{(b)}(t)\bar{\delta}_b(i) + \sum_{\substack{j\in V_B \\ j\neq i}} \bar{\lambda}_{bb}(i,j)\rho_j^{(b)}(t)(1-\rho_i^{(b)}(t)) \\ &+ \sum_{j\in V_A} \bar{\lambda}_{ba}(i,j)\rho_j^{(a)}(t)(1-\rho_i^{(b)}(t)), \qquad (5.2)\end{aligned}$$

where $\bar{\delta}_l(i)$ represents the coarse-grained recovery rate for node i in network layer l, and $\bar{\lambda}_{l_1 l_2}(i,j)$ denotes the coarse-grained infection propagation rate between nodes i in network layer l_1 and j in network layer l_2. The subscripts of these terms indicate the respective network layer(s) of the nodes. Note that the coarse-grained rates $\bar{\delta}$ and $\bar{\lambda}$ are the only difference of this model from standard models. Standard models define the recovery and the infection rates for individual nodes and edges without any consideration of the local topology around these nodes. The coarse-grained model is an improvement over this, where the local neighborhood of nodes is explicitly accounted for. This allows us to consider the dynamic correlation in the infection states of distant nodes without making the mathematical model very complex. The system of equations (5.1)-(5.2) are essentially a generalization of the model in [Bog13] to multiple network layers.

The coarse-grained recovery rate $\bar{\delta}(i)$ can be thought of as the effective recovery rate for infection at a node i, where we want to characterize the effective rate at which infection in the local neighbor-

hood of i dies out. It should not be difficult to see that as the neighborhood size of i increases, the infection in the local neighborhood of i will linger on for a long time leading to a lower effective recovery rate. The effective infection rate $\bar{\lambda}(i,j)$ between distinct nodes i and j should progressively decrease as the distance between the two nodes increases. These ideas are clarified in the following two lemmas, where we present the derivation of these two effective rates generalizing the arguments in relevant literature [Bog13; Fer16] to the case of multi-layer networks.

Lemma 5.3.1 *Under the SIS model of epidemic dynamics with parameters $\boldsymbol{\lambda} = \{\lambda_a, \lambda_b, \tilde{\lambda}\}$, the coarse-grained recovery rate $\bar{\delta}_l(i)$ for node i in layer l with k_i intra-layer neighbors and $\tilde{k}_i$ inter-layer neighbors is given by the expression:*

$$\bar{\delta}_l(i) = \left[\alpha \frac{1+X}{(1-X)^2} + \beta \frac{2}{(1-X)^2}\right]^{-1}, \tag{5.3}$$

where

$$\begin{aligned} X &= 1-(1-p_l^2)^{k_i}(1-\tilde{p}^2)^{\tilde{k}_i} \\ \alpha &= (1-p_l)^{k_i}(1-\tilde{p})^{\tilde{k}_i} \\ \beta &= (1-p_l^2)^{k_i}(1-\tilde{p}^2)^{\tilde{k}_i} - (1-p_l)^{k_i}(1-\tilde{p})^{\tilde{k}_i}. \end{aligned}$$

p_l (or $\tilde{p}$) in the above expressions can be written as $p_l \triangleq 1-e^(-\lambda_l)$ and $\tilde{p} \triangleq 1-e^(-\tilde{\lambda})$).

In this proof, we present the case $i \in V_a$. The same arguments can be applied to the case of $i \in V_b$. We extend the arguments in [Bog13; Fer16] to multi-layer networks, where i has k_i intra-layer edges with infection rate λ_a and $\tilde{k}_i$ inter-layer edges with infection rate $\tilde{\lambda}$. Even for this simple case, an exact analysis is very involved and can be done only for simplistic graph structures [Cat13]. Following the approach followed in the relevant works, the epidemic dynamics are discretized with respect to the recovery rate of the nodes, which is taken as unity. Thus, the average recovery time of a node is taken as the unit of time, and the probability that an infection propagation event occurs successfully in this time is given by [New18] $p_a \triangleq 1-e^(-\lambda_a)$ and $\tilde{p} \triangleq 1-e^(-\tilde{\lambda})$, for intra-layer links and inter-layer links, respectively.

The epidemic dynamics initiate with node i being infected, whereas all its neighbors are susceptible. The probability $P(n|k_i)$ that i has n infected intra-layer neighbors by the time it recovers is given by:

$$P(n|k_i) = \binom{k_i}{n} p_a^n (1-p_a)^{k_i-n}. \tag{5.4}$$

Furthermore, the probability that any one of these infected neighbors propagates the infection back to i is given by the expression:

$$\sum_{n=1}^{k_i} P(n|k_i)[1-(1-p_a)^n] = 1-(1-p_a^2)^{k_i}. \tag{5.5}$$

Similarly, the probability that i is re-infected by any of its inter-layer neighbors is given by $1-(1-\tilde{p}^2)^{\tilde{k}_i}$. Let X denote the probability that i is re-infected, once it recovers, through any of its neighbors. We can write:

$$X = 1-(1-p_a^2)^{k_i}(1-\tilde{p}^2)^{\tilde{k}_i}. \tag{5.6}$$

X denotes the probability that i goes through one round of re-infection, which, by our discretized approximation of the epidemic dynamics, takes 2 units of time. Note that for an infected central node i, three possible events are possible: i) i recovers before infecting any of its neighbors, which can be expressed as $(1-p_a)^{k_i}(1-\tilde{p})^{\tilde{k}_i}$, ii) i infects some of its neighbors before it recovers and the infected neighbors successfully re-infect i, which was previously calculated to be $1-(1-p_a^2)^{k_i}(1-\tilde{p}^2)^{\tilde{k}_i}$, and iii) i infects some of its neighbors before it recovers and the infected neighbors recover before re-infecting i, which can be computed from the above two probabilities to be $(1-p_a^2)^{k_i}(1-\tilde{p}^2)^{\tilde{k}_i}-(1-p_a)^{k_i}(1-\tilde{p})^{\tilde{k}_i}$. Now, there are two ways by which epidemics in and around i may die: Case a)–i goes through m rounds of re-infection and then fails to propagate its infection to any of its neighbors, and Case b)–i goes through m rounds of re-infection and then fails to get re-infected by any of its neighbors. Note that the infection duration in the two cases are $2m+1$ and $2m+2$, respectively. Using the expressions above, these two probabilities can be computed as:

$$P[\text{Case (a)}] = X^m(1-p_a)^{k_i}(1-\tilde{p})^{\tilde{k}_i}, \tag{5.7}$$

$$P[\text{Case (b)}] = X^m\left[(1-p_a^2)^{k_i}(1-\tilde{p}^2)^{\tilde{k}_i}-(1-p_a)^{k_i}(1-\tilde{p})^{\tilde{k}_i}\right]. \tag{5.8}$$

For simplicity, let us denote the above two probabilities by $X^m\alpha$ and $X^m\beta$, respectively. Thus, the expected lifetime $\mathbb{E}(T)$ of an infection starting from i can be written as:

$$\begin{aligned}\mathbb{E}(T) &= \sum_{m=0}^{\infty} X^m\alpha(2m+1)+\sum_{m=0}^{\infty} X^m\beta(2m+2)\\ &= \alpha\frac{1+X}{(1-X)^2}+\beta\frac{2}{(1-X)^2}.\end{aligned}$$

The effective recovery rate for an infection at i is given by the inverse of $\mathbb{E}(T)$.

Remark 1 *It is clear from the expression of the coarse-grained recovery rate $\bar{\delta}$ that it is difficult to develop a sense of the variation of $\bar{\delta}(i)$ with the infection propagation rate and the neighborhood size of i. In fact, even for the single layer networks, a succinct closed form expression does not exist. However at low infection rates $\lambda \ll 1$, the effective recovery rate can be shown to vary as $\bar{\delta}(i) \sim e^(-k_i\lambda_a^2-\tilde{k}_i\tilde{\lambda}^2)$.*

For single layer networks, the effective infection propagation rate $\bar{\lambda}(i,j)$ is computed [Bog13; Fer16] by considering the propagation of infection along the shortest path between i and j and under the assumption that the path comprises nodes of degree 2. In other words, the effective infection rate denotes the infection propagation rate along the shortest line graph between i and j. Thus, the computation of $\bar{\lambda}(i,j)$ lower bounds the actual propagation rate between the two nodes. This lower bound based characterization of the infection propagation is particularly useful in

studying the regime near the infection threshold, where the presence of metastable infection states in the lower bound based analysis guarantees the presence of such states in the exact dynamics. The fundamental purpose of the system equations (5.1)- (5.2) is to characterize the conditions under which metastable epidemic states can be sustained in the network and thus, the information revealed by the lower bound based analysis is useful. For multi-layer networks, we face the additional issue that the shortest path between i and j is not guaranteed to have the largest effective infection propagation rate, since different edges have distinct propagation rates λ_a, λ_b or $\tilde{\lambda}$. Although the effective rate along any path can lower bound the exact dynamics, we define $\bar{\lambda}(i,j)$ as follows to obtain a tighter bound:

$$\bar{\lambda}(i,j) = \max_{p \in \mathscr{P}} \bar{\lambda}_p(i,j), \tag{5.9}$$

where p denotes a particular path between two nodes i and j, $\mathscr{P}$ denotes the set of all such paths, and $\bar{\lambda}_p(i,j)$ is defined as the effective infection propagation rate along a particular path p. Note that i and j can belong to any layer of the multi-layer network.

Lemma 5.3.2 *Consider the SIS model of epidemic dynamics with parameters $\boldsymbol{\lambda} = \{\lambda_a, \lambda_b, \tilde{\lambda}\}$. Let a path p connecting two nodes i and j be of length $d_{ij} \equiv d_a + \tilde{d} + d_b$, where d_a and d_b represent the length of the section of the path in layers A and B, respectively, while $\tilde{d}$ represents the length of the section of the path comprising inter-layer links. The effective infection propagation rate between nodes i and j via path p is given by:*

$$\bar{\lambda}_p(i,j) = \lambda_a^{d_a} \tilde{\lambda}^{\tilde{d}} \lambda_b^{d_b}. \tag{5.10}$$

Similar to works like [Bog13; Fer16], the effective infection propagation rate is computed under the condition that the infection at the source i never recovers and the epidemic dynamics are tracked on the line graph between i and j. For every edge, the probability of propagation of infection through it is given by the corresponding infection spreading rate. This is due to the fact that for a node in the infected state, two events can occur: i) spontaneous recovery with rate 1, and ii) infection propagation to a susceptible neighbor via an edge with rate λ_a, λ_b or $\tilde{\lambda}$, depending on the type of the edge. Thus, the probability of infection propagation can be expressed as $\frac{\lambda}{1+\lambda}$, which at low infection rates can be approximated simply by λ. The probabilities of propagation through successive edges are independent of each other and thus, the probability that infection from i propagates via $d_a + d_b$ intra-layer edges and $\tilde{d}$ inter-layer edges is given by the above expression. The system of differential equations (5.1)-(5.2) can be simplified by using the vectorized infection densities $\boldsymbol{\rho}(t) \equiv [\rho_1^{(a)}(t) \cdots \rho_m^{(a)}(t) \rho_1^{(b)}(t) \cdots \rho_n^{(b)}(t)]^T$:

$$\frac{d\boldsymbol{\rho}(t)}{dt} = -\Delta \boldsymbol{\rho}(t) + (\mathbf{1} - \boldsymbol{\rho}(t)) \circ \mathbf{M} \boldsymbol{\rho}(t), \tag{5.11}$$

where $\Delta \equiv \text{diag}[\bar{\delta}_1^A \cdots \bar{\delta}_n^B]$ represents the diagonal matrix of the recovery rates, $\mathbf{M}$ represents the infection propagation matrix whose ijth element is the infection propagation rate between nodes i and

j, and $\circ$ denotes element-wise multiplication or the Hadamard product operator. The vectorized system equation (5.11) modelling the epidemic dynamics is a nonlinear differential equation of the first order for which, closed form solutions are not possible in the general case. This showcases the main roadblock preventing an exact analysis of epidemic dynamics in networks. For arbitrary network topologies, the matrices $\mathbf{M}$ and $\acute{}$ do not have a mathematically tractable structure. Furthermore, for most practical problems the size of the matrices is too large for numerical solutions.

To circumvent these issues, we analyze the epidemic dynamics on microscopic interlink subgraphs and characterize the condition under which the epidemics do not die out in the local neighborhood of the interlinks. The coarse-grained model for the system equations allows us to capture the effect of the local neighborhood of the end-points of the interlinks even when the matrices $\mathbf{M}$ and $\acute{}$ are defined as simple 2×2 matrices, representing the two end-points of an interlink. This is the simplest possible abstraction of the network topology and we show that even this simplistic characterization is able to capture non-trivial information about the local intra-layer neighborhoods of the endpoints. Experimenting with more sophisticated subgraphs is an obvious direction for future extensions of this work, which we are interested in pursuing.

For most practical problems, a single interlink subgraph will not be able to satisfy the infection density requirements of our problem. As a result, the desired metastable state is composed of different interlink subgraphs interacting with each other. Our interlink design strategy is to first identify the conditions under which an interlink subgraph can support a metastable infection state; thereafter the interlink structure is constructed in such a way that different interlinking subgraphs can reliably support other each other and lead to a composite metastable state spanning multiple interlinks. In the remainder of this section, we uncover several crucial properties of the infection dynamics on the interlink subgraphs, which are utilized in the next section for designing the optimal interlinking strategy.

5.3.1 Epidemics in interlink subgraphs

In this section, we quantify the conditions for the existence of metastable infection state in an interlink subgraph, comprising a single interlink between two nodes, $i\in V_a$ and $j\in V_b$. Thereafter, we estimate the infection size in the local neighborhood of active hubs. Finally, we approximate the probability with which hubs connected to each other via interlinks infect each other.

Lemma 5.3.3 *Consider SIS epidemics with parameters $\boldsymbol{\lambda}=\{\lambda_a,\lambda_b,\tilde{\lambda}\}$ on the interlink subgraph spanning nodes $i\in V_a$ and $j\in V_b$. A necessary and sufficient condition for the existence of a metastable infection state in this subgraph is:*

$$\bar{\delta}_a(i)\cdot\bar{\delta}_b(j)<\tilde{\lambda}^2, \tag{5.12}$$

where $\bar{\delta}_l(i)$ denotes the effective recovery rate for the node i in layer l.

The existence of a metastable infection state in the interlinking subgraph is contingent on the instability of the system equations (5.11), linearized around the absorbing state $\boldsymbol{\rho}=0$, which can be

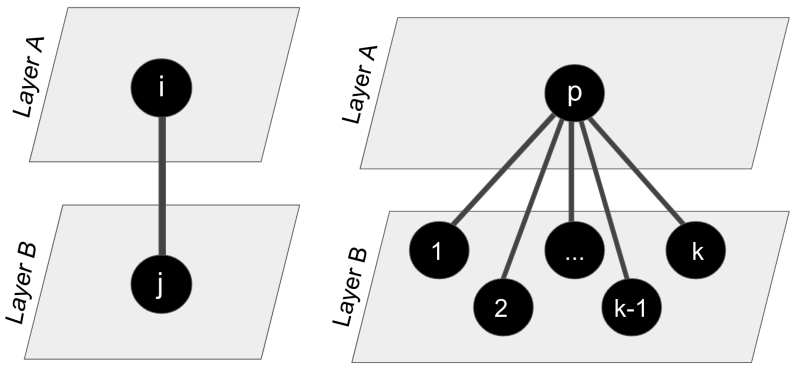

Figure 5.1 Instances of the microscopic subgraphs: a) Interlink subgraph with 1 interlink, b) Interlink subgraph with k interlinks.

written as:

$$\frac{d\boldsymbol{\rho}}{dt} = (\mathbf{M} - \acute{})\boldsymbol{\rho} = \mathbf{S}\boldsymbol{\rho}, \tag{5.13}$$

where $\mathbf{S}$ represents the interaction matrix comprising the effective recovery rates in the diagonal elements and the effective infection propagation rates in the off-diagonal terms. The instability of this fixed point is guaranteed if the interaction matrix $\mathbf{S}$ has a positive spectral radius. For the interlink subgraph as shown in Fig. 5.1, the interaction matrix $\mathbf{S} \equiv \mathbf{M} - \acute{}$ can be written as:

$$\mathbf{S} = \begin{bmatrix} -\bar{\delta}_a(i) & \tilde{\lambda} \\ \tilde{\lambda} & -\bar{\delta}_b(j) \end{bmatrix}$$

The eigenvalues of $\boldsymbol{S}$ can be computed as:

$$\mu = \frac{1}{2} \cdot \left[-\left(\bar{\delta}_a(i) + \bar{\delta}_b(j)\right) \pm \left[\left(\bar{\delta}_a(i) - \bar{\delta}_b(j)\right)^2 + 4\tilde{\lambda}^2\right]^{1/2} \right].$$

From the above expression, it is not difficult to prove that a positive eigenvalue of $\boldsymbol{S}$ exists if and only if the condition stated in lemma holds true. The above lemma characterizes the requirements for a node to be classified as a hub. Let us consider the simplification $\lambda_a = \lambda_b = \tilde{\lambda} = \lambda$, where the effective recovery rate can be approximated as $\bar{\delta}_l(i) \sim e^(-(k_i+1)\lambda^2)$, where i has k_i intra-layer and 1 inter-layer link. Plugging in $k_i = k_j = k$ into (5.12) reveals that the presence of hubs with degree in the order of $\frac{1}{\lambda^2}\log(\frac{1}{\lambda})$ and greater ensures the existence of a metastable state. This implies that metastable states can exist even for arbitrarily small infection rates as long as hubs of sufficiently high degrees exist. This insight allows us to appreciate the results in works like [Cha09; Mou13], which state that infinite sized power law graphs are always super-critical, i.e. metastable states exist for any infection rate. For the finite sized networks considered here, this condition calibrates the definition of “hubs" as a function of the infection rate. In the following, we consider a slightly more complicated topology where a node i has multiple inter-layer links and characterize the conditions for the existence of metastable infection states in that case.

Corollary 5.3.4 *Consider a subgraph comprising node $p \in V_a$ connected with k inter-layer neighbors*

denoted by the set $\sigma(p)$. The nodes in $\sigma(p)$ do not have any intra-layer links. Under SIS epidemics with parameters $\boldsymbol{\lambda}$, a sufficient condition for the existence of a metastable infection state around i is given by the expression:

$$\bar{\delta}_a(p) \leq 2k\tilde{\lambda} + k(k-1)\tilde{\lambda}^2 - ke^(-\tilde{\lambda}^2), \tag{5.14}$$

where $\bar{\delta}_a(p)$ denotes the effective recovery rate of p given by Lemma 5.3.1.

This case, shown in Fig. 5.1, is an extension of Lemma 5.3.3 with the difference that node i has multiple inter-layer neighbors. Thus, the subgraph under question comprises $1+k$ nodes with k inter-layer links. The interaction matrix $\boldsymbol{S}$ for this case is of dimension $(1+k)\times(1+k)$, whose elements can be written as:

$$s_{ij} = \begin{cases} -\bar{\delta}_a(i) & \text{if } i=1, j=1, \\ -\bar{\delta}_b(i) & \text{if } i\neq 1, j\neq 1, i=j, \\ \tilde{\lambda} & \text{if } i=1, j\neq 1 \text{ and } j=1, i\neq 1, \\ \tilde{\lambda}^2 & \text{if } i\neq 1, j\neq 1, i\neq j. \end{cases}$$

Note that the last two lines of the above definition are a consequence of Lemma 5.3.2. Note that the only path between two nodes in $\sigma(p)$ constitutes two inter-layer links. It should not be difficult to see that even for this simplistic construction of the subgraph, the eigendecomposition of $\boldsymbol{S}$ is considerably more complicated than the previous case. Due to this reason, we obtain conditions for the existence of positive eigenvalues instead of actually computing all the $k+1$ eigenvalues of $\boldsymbol{S}$. As a consequence, our result becomes weaker and only sufficient conditions for the existence of the metastable infection state can be characterized. Note that if there exists a $\mathbf{u}\in\mathbf{R}^{k+1}$, such that $\mathbf{u}^T\boldsymbol{S}\mathbf{u}>0$, we can guarantee that $\boldsymbol{S}$ has a positive eigenvalue. For simplicity, we choose $\mathbf{u}$ as the all-1 column vector such that the quadratic term can be easily computed as the sum of all elements of $\boldsymbol{S}$. The effective recovery rates for the inter-layer neighbors of p can be approximated by $\bar{\delta}(j)\sim e^(-\tilde{\lambda}^2)$, where j denotes the inter-layer neighbors. Plugging in the values of $\bar{\delta}(j)$ into the condition $\mathbf{u}^T\boldsymbol{S}\mathbf{u}>0$ yields the desired result. The above results gives us the condition under which metastable infection states can be induced around a node p, even in the extreme case that its inter-layer neighbors have no intra-layer links. This condition will be utilized to augment the metastable infection state with nodes which do not quality as hubs by themselves. Next, let us look at the expected infection size in the neighborhood of active hubs. For this case, we approximate the local neighborhood around hubs as an extended star as shown in Fig. 5.2, where all outgoing edges of the star are extended to form line graphs.

Lemma 5.3.5 *Consider a single-layered SIS dynamics with infection rate λ on an extended star topology, where the hub is permanently infected. The average number of infected nodes around the hub of intra-layer degree k can be approximated by $\frac{\lambda k}{1-\lambda}$.*

From Lemma 5.3.2, we know that the probability of a node at a distance of d from the hub to be infected is given by λ^d. Thus, the number of infected nodes at a distance d from the hub is just k

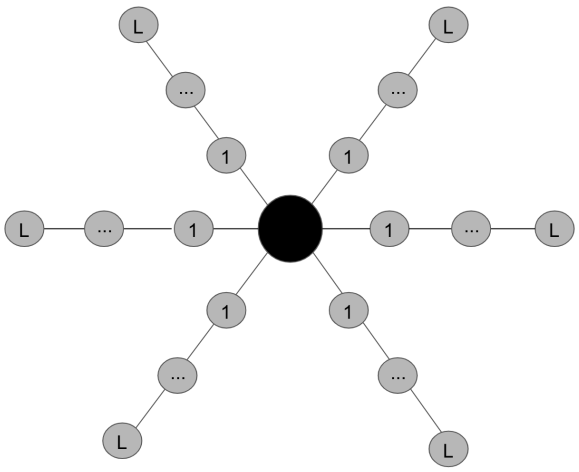

Figure 5.2 Extended star topology with infected centre with attached line graphs of length L.

times this probability. Let us represent the length of the path attached to the hub by l. Thus, the total number of infected nodes (T) in the local neighborhood of the hub can be computed as:

$$T(l) = \sum_{d=1}^{l} \lambda^d k = k\frac{\lambda - \lambda^{l+1}}{1-\lambda}. \tag{5.15}$$

As l tends to infinity, $T(l)$ converges to $\frac{\lambda k}{1-\lambda}$. As we mainly consider small infection rates near the epidemic threshold in this dissertation, the error of approximating $T(l)$ by $\frac{\lambda k}{1-\lambda}$ is very small even for finite values of l. The above results gives us an idea of the extent of the spread of infection around an active hub. Note that in reality, the estimated infection size around the hub can vary since the different paths emanating from it can interact with each other. However, we argue that under the low infection rate regime, the interaction between different paths is minimal and the infection size estimated by Lemma 5.3.5 provides a good approximation to the actual infection size observed in networks. We substantiate this argument via simulation experiments in Section 5.6. Lemma 5.3.5 states that hubs roughly infect $\frac{\lambda k}{1-\lambda}$ nodes in their vicinity, which will not be sufficient to satisfy the infection density requirements Γ for most practical problems. Thus, it is clear that although a single interlink directly connecting two nodes in the desired region of the network is capable of inducing a metastable state, the average number of infected nodes for this case is quite small. In order to induce a metastable state with more infected nodes, we need to consider multiple hubs; each of which will infect a small proportion of their respective neighborhoods, thereby satisfying the infection density requirements of our problem.

With the requirement of multiple hubs established, we turn our focus to the problem of reliably maintaining connectivity between the different hubs which can mutually re-infect each other, thereby sustaining activity in the composite metastable infection state for a long time.

Lemma 5.3.6 *Consider SIS epidemic dynamics with parameters $\boldsymbol{\lambda} = \{\lambda_a, \lambda_b, \tilde{\lambda}\}$ on an interlink subgraph spanning nodes $i \in V_a$ and $j \in V_b$. The probability (η_i) of the infection propagating from*

hub i to the interlinked neighbor j can be written as:

$$\eta_i = \frac{\tilde{p}}{\tilde{p} + (1-\tilde{p})(1-p_a^2)^{k_i}}, \tag{5.16}$$

where $\tilde{p} \equiv 1 - e^(-\tilde{\lambda})$, $p_a \equiv 1 - e^(-\lambda_a)$, and k_i represents the intra-layer degree of i.

The epidemics start at hub i. As discussed in Lemma 5.3.1, it should now be easy to see that nodes of high intra-layer degree are very likely to sustain infection for a long time via multiple re-infection cycles, where upon recovery, i is re-infected by one of its intra-layer neighbors. Node j interlinked to i can only be infected via propagation along the interlink, characterized by the probability $\tilde{\lambda}$. i can get multiple opportunities of propagating infection to j, since every time it recovers, i can get re-infected by its k_i intra-layer neighbors. By (5.6), we have that the probability that i is re-infected is given by $X \triangleq 1-(1-p_a^2)^{k_i}$, where $p_a = 1 - e^(-\lambda_a)$. Thus, the probability that j is not infected at the end of m rounds of re-infection is given by $X^m(1-\tilde{p})^m$. As a result, the total probability that i successfully propagates infection to its interlinked neighbor j is given by:

$$\eta_i = \sum_{m=0}^{\infty} \tilde{p}[1-(1-p_a^2)^{k_i}]^m (1-\tilde{p})^m, \tag{5.17}$$

which yields the desired expression.

Remark 2 *Note that we ignore the effects of the presence of additional inter-layer links of i in the computation of the re-infection probability. This is because the inherent problem setting is that construction of interlinks is a costly operation and the number of interlinks associated with a hub node is expected to be insignificant in comparison to the size of the intra-layer neighborhood. In the presence of additional inter-links, η_i represents a lower bound to the empirically observed probability.*

5.3.2 Estimation of infection size

As discussed in the previous section, a single interlink subgraph is generally not sufficient to satisfy the infection density requirements $\Gamma = (\gamma_a, \gamma_b)$ specified by Problem 5.2. This establishes the necessity of considering multiple hubs for designing the interlinking structure between the network layers. Let the set of hubs in the two desired regions in the network layers be denoted by H_a and H_b, respectively, where cardinality of the two sets is given by n_a and n_b. In this section, we estimate the average infection size resulting from a candidate interlinking structure $\sigma \equiv \{\sigma_a(1), \cdots, \sigma_a(n_a), \sigma_b(1), \cdots, \sigma_b(n_b)\}$, where $\sigma_a(i)$ (or $\sigma_b(i)$) represents the set of hubs in layer B (or A) interlinked to the ith hub in layer A (or B). In the next section, we optimize the interlinking structure σ so as to maximize the estimated infection size.

We focus on the intra-layer and inter-layer neighborhood of a particular hub i in network layer A. When the infection in the local intra-layer neighborhood of hub i dies out, hub i can be re-infected by one of its inter-layer neighbors, represented by the set $\sigma_a(i)$. The probability that a particular

hub $j \in \sigma_a(i)$propagates its infection to hub i via the inter-layer link is given by Lemma 5.3.6 to be:

$$\eta_j = \frac{\tilde{p}}{\tilde{p} + (1-\tilde{p})(1-p^2)^{k_j}}, \tag{5.18}$$

where k_j denotes the intra-layer degree of hub j. As i can get re-infected by any one of its $\sigma_a(i)$ inter-layer neighbors, the overall infection probability is given by the expression: $1 - \prod_{j \in \sigma(i)}(1-\eta_j)$. Combining this with the estimate for infection size given by Lemma 5.3.5, the average size of infection in the local intra-layer neighborhood around hub i is given by:

$$f(\sigma_a(i)) = \frac{\lambda_a k_i}{1-\lambda_a}\Big[1 - \prod_{j \in \sigma_a(i)} (1-\eta_j)\Big], \tag{5.19}$$

where $f(\sigma_a(i))$ denotes the average infection size around hub i in layer A, $\sigma_a(i)$ denotes the set of inter-layer neighbors of i, λ_a is the intra-layer infection propagation rate in layer A, $\tilde{\lambda}$ is the inter-layer infection propagation rate, k_i is the degree of node i and η_j is the infection propagation probability from j to i given by Lemma 5.3.6.

We remind the reader that even for a simplified epidemic model like the SIS model, an exact analysis of the epidemic dynamics is not possible in general. This necessitates the use of approximate analysis for characterizing the properties of epidemic dynamics on networks with arbitrary topology. Recall that we focus on the low infection rate regime, where the epidemics are localized around nodes of high degrees. Due to the localized nature of the infection patterns, the total infection size in the composite metastable infection state, spanning multiple hub nodes, can be approximated by the sum of the individual infection sizes around all hubs. This assumption makes sense since the infection patterns in the local neighborhood of the hubs do not significantly interact with each other due to the localized epidemics. Note that similar assumptions about the network topology are made in works like [Cha09; Mou13] examining the critical infection rates in infinite sized scale free networks. Although we focus on finite sized networks here, we verify via extensive simulation experiments that the estimates of infection sizes, computed in this dissertation under such assumptions, remain largely consistent with the simulations for extended ranges of parameters on both real world and synthetic network topologies. Thus, for an interlinking structure σ, the average infection size around the hubs, denoted by $f(\sigma)$, is given by the expression:

$$\begin{aligned} f(\sigma) = &\sum_{i \in H_a} \frac{\lambda_a k_i}{1-\lambda_a}\Big[1 - \prod_{j \in \sigma_a(i)} q_j\Big] + \\ &\sum_{i \in H_b} \frac{\lambda_b k_i}{1-\lambda_b}\Big[1 - \prod_{j \in \sigma_b(i)} q_j\Big], \end{aligned} \tag{5.20}$$

where the summations index over the hub nodes in the two network layers, and $q_j \triangleq (1-\eta_j)$. Note that the $\sigma(i)$'s in the first summation refer to hub nodes in layer B and vice versa.

5.4 Optimizing the Interlinking structure

In the previous section, we utilized the theoretical results developed in Lemmas to approximate the infection size corresponding to a specific interlinking structure σ. Recall that the fundamental purpose of the interlinking structure is to maintain interaction between different hubs so that if the infection in the local neighborhood around a hub dies out, it can get re-infected by one of the other hubs via an inter-layer link. Thus, it is easy to see that the hubs connected to each other via the inter-layer links should form a connected graph so that all hubs can re-infect each other to sustain the composite metastable infection state for a long time. Since the minimally connected graph spanning n vertices is a tree, the minimum number of interlinks required to maintain connectivity between $n_a + n_b$ hubs is $n_a + n_b - 1$, where n_a and n_b represent the cardinalities of the set of hubs H_a and H_b, respectively. The choice of the hubs constituting the sets H_a and H_b is discussed in the next section. In this section, we impose this minimum constraint on the interlinking structure σ and optimize it with the objective of maximizing the average infection size $f(\sigma)$ given by (5.20). The maximization of the infection size guarantees optimal utilization of the interlinks. The optimization problem for determining the interlinking structure connecting the hubs H_a and H_b is given by:

$$\max_{\sigma} \quad f(\sigma) \tag{5.21a}$$

$$\text{subject to} \quad \sum_{i \in H_a} |\sigma(i)| = \sum_{i \in H_b} |\sigma(i)| = n_a + n_b - 1, \tag{5.21b}$$

$$\bigcup_{i \in H_a} \sigma(i) = H_b, \ \bigcup_{i \in H_b} \sigma(i) = H_a. \tag{5.21c}$$

In the above optimization problem, the first constraint enforces that the minimum number of interlinks are used for constructing the interlinking structure, while the second one ensures that all hubs in H_a and H_b are supported via interlinks. As a first step towards obtaining the optimal interlinking structure, we impose the assumption that the hub nodes in the same layer of the network are of the same degree, i.e. $k_i = k_a, \ \forall i \in H_a$ and $k_i = k_b, \ \forall i \in H_b$. The reason behind this assumption is that the theoretically optimal interlinking structure can only be obtained under this assumption. For the general case, the optimization problem looses its structure and we need to resort to approximate greedy algorithms to design the interlinking structure.

5.4.1 Interlinking structure for identical hub degrees

In this section, we study the optimization problem (5.21) under the identical hub degree assumption, where k_a and k_b represent the intra-layer degrees of the hubs in sets H_a and H_b, respectively. Under this assumption, the interlinking structure σ can be simplified to the vectorized allocation of interlinks $\boldsymbol{b} \equiv [b_1 \cdots b_{n_a} \, b_{n_a+1} \cdots b_{n_a+n_b}]$, where b_i specifies the number of interlinks allocated to hub i. Note that the first n_a indices of $\boldsymbol{b}$ define the interlink allocation for the n_a hubs in H_a, while the last n_b indices define the allocations for H_b. The reason behind this simplification of the interlinking

structure is that the identical hub degree assumption obfuscates the identity of the nodes in H_a and H_b. As a result, the interlinking structure σ is completely specified by the information of the number of interlinks allocated to each hub. It is easy to see that this simplification does not hold in the general case where hubs in H_a and H_b have distinct intra-layer degrees. For identical hub degrees, the objective function in (5.21) can be written as:

$$f(\boldsymbol{b}) = \sum_{i \in H_a} \xi_a \left(1 - {q_a}^{b_i}\right) + \sum_{i \in H_b} \xi_b \left(1 - q_b^{b_i}\right), \tag{5.22}$$

where $\xi_a \triangleq \frac{\lambda_a k_i}{1-\lambda_a}$ and $\xi_b \triangleq \frac{\lambda_b k_i}{1-\lambda_b}$ are defined as the expected infection size around active hubs in both layers of the network, as specified by Lemma 5.3.5; q_a (or q_b) denotes the probability of infection not propagating from a hub in H_a (or H_b) to an inter-layer neighbor in H_b (or H_a); and $b_i \triangleq |\sigma(i)|$ denotes the number of inter-layer neighbors of hub i. According to the definition of $\boldsymbol{b}$, the first summation runs over the initial n_a indices representing hubs in H_a, while the second summation runs over the remaining n_b indices representing the hubs in H_b. Our objective in this section can be written as:

$$\max_{\boldsymbol{b}} \quad \sum_{i \in H_a} \xi_a \left(1 - {q_a}^{b_i}\right) + \sum_{i \in H_b} \xi_b \left(1 - q_b^{b_i}\right) \tag{5.23a}$$

$$\text{subject to} \quad \sum_{i \in H_a} b_i = \sum_{i \in H_b} b_i = n_a + n_b - 1, \tag{5.23b}$$

$$b_i \geq 1, \ \ \forall i \in H_a \cup H_b. \tag{5.23c}$$

Similar to (5.21), the first constraint in the above problem ensures that a minimum number of interlinks are used, while the second constraint ensures that all hubs are supported by interlinks. Let us separate the interlink allocation vector into two components $\boldsymbol{b}_{H_a}$ and $\boldsymbol{b}_{H_b}$, representing interlink allocation strategies for the hubs in H_a and H_b, respectively. It can be observed that the maximization of the objective $f(\boldsymbol{b})$ over the space of interlink allocation $\boldsymbol{b}$ is equivalent to independently maximizing the two summations in the objective function over the layer-wise interlink allocation structures $\boldsymbol{b}_{H_a}$ and $\boldsymbol{b}_{H_b}$. This is because the two summations in the objective function in (5.23) are only dependent on the layer-wise interlink allocations, i.e. variation in $\boldsymbol{b}_{H_a}$ does not affect the second term in the objective function (5.23a) and similarly, variation in $\boldsymbol{b}_{H_b}$ does not affect the first term. Note that the independence of the two summations in the objective function only holds true for the identical hub degree case. We will make use of the following result in determining the optimal interlinking structure maximizing the the objective in (5.23).

Lemma 5.4.1 *The function $f : \mathbb{R}^d \to \mathbb{R}$ defined by $f(\boldsymbol{x}) = \sum_i c_1(1 - c_2^{x_i})$ is Schur-concave (refer to) for $c_1 \geq 0$ and $0 \geq c_2 \geq 1$, where $\boldsymbol{x} = [x_1 \cdots x_d]^T$.*

By the Schur-Ostrowski criterion [Pea92], we have that f is symmetric and all partial derivatives of f exist, then f is Schur-concave if and only if the following condition holds for all $x \in \mathbb{R}^d$:

$$(x_i - x_j)\left(\frac{\partial f}{\partial x_i} - \frac{\partial f}{\partial x_j}\right) \leq 0,\ \forall 1 \leq i \neq j \leq d. \tag{5.24}$$

For our case, it is easy to see that f is symmetric and all its first partial derivatives exist. In order to prove to Schur-concavity of $f(\boldsymbol{x})$, we need to show that the above condition holds. The partial derivatives can be computed as:

$$\frac{\partial f}{\partial x_i} = -c_1 c_2^{x_i} \log c_2. \tag{5.25}$$

Let us assume without loss of generality that $x_i \geq x_j$. Plugging in the partial derivative computations into the Schur-concavity condition gives us:

$$\begin{aligned}&(x_i - x_j)\left(\frac{\partial f}{\partial x_i} - \frac{\partial f}{\partial x_j}\right)\\ &= (x_i - x_j) c_1 \log c_2 (c_2^{x_j} - c_2^{x_i}) \leq 0,\end{aligned}$$

where the final inequality holds because i) $c_2^{x_j} \geq c_2^{x_j}$, since $0 < c_2 < 1$ and $x_i \geq x_j$; and ii) $\log c_2 < 0$, since $0 < c_2 < 1$. This satisfies the Schur-Ostrowski criterion and thus, proves the lemma. Let us define the *maximally uniform* interlink allocation as follows: an interlink allocation strategy $\boldsymbol{b} \equiv [b_1 \cdots b_{n_a}\, b_{n_a+1} \cdots b_{n_a+n_b}]$ is maximally uniform, if for both $\boldsymbol{b}_{H_a} \equiv [b_1 \cdots b_{n_a}]$ and $\boldsymbol{b}_{H_b} \equiv [b_{n_a+1} \cdots b_{n_a+n_b}]$, the variance of the allocation strategies $\boldsymbol{b}_{H_a}$ and $\boldsymbol{b}_{H_b}$ is minimum. In other words, an interlink allocation strategy is defined to be maximally uniform, if no exchange of interlinks among two hubs in H_a or H_b can minimize the variance of $\boldsymbol{b}$. It should not be difficult to see that for a maximally uniform $\boldsymbol{b}$:

$$\max_{i \neq j} |b_i - b_j| \leq 1,\ \forall i, j \in H_a \text{ or } H_b. \tag{5.26}$$

This is because if two hubs in the same layer of the network have a difference of allocated interlinks, which is greater than 1, we can always re-allocate the interlinks among these hubs to further minimize the variance of $\boldsymbol{b}$. With the schur-concavity of the function f defined in Lemma 5.4.1 and the definition of maximally uniform interlink allocation in hand, we can state the result for the optimal interlinking structure.

Theorem 5.4.2 *If the hub nodes in each layer of the network, comprising the composite metastable infection state, have the same intra-layer degree, the maximally uniform interlink allocation strategy maximizes the expected infection size in the network.*

As discussed earlier, under the uniform degree assumption of the hub nodes in H_a and H_b, the maximization of the objective function in the optimization problem (5.23) is equivalent to two independent optimization problems, for each layer of the network, which for layer A can be written

as:

$$\max_{\boldsymbol{b}} \quad \sum_{i \in H_a} \xi_a \left(1 - {q_a}^{b_i}\right) \tag{5.27a}$$

$$\text{subject to} \quad \sum_{i \in H_a} b_i = n_a + n_b - 1, \tag{5.27b}$$

$$b_i \geq 1, \ \ \forall i \in H_a. \tag{5.27c}$$

Recall that $q_a \triangleq 1-\eta_a$, where η_a is defined in Lemma 5.3.6 as the probability of infection propagating from a hub node in layer A to an interlinked hub in layer B. ξ_a is defined as the average infection size in the local intra-layer neighborhood of an active hub in layer A and it can be expressed as $\xi_a = \frac{\lambda_a k_a}{1-\lambda_a}$, where k_a is the intra-layer degree of the hubs in layer A and λ_a is the intra-layer infection propagation rate in layer A. It is easy to verify that the objective function in the optimization problem (5.27) is of the same form as that in Lemma 5.4.1 and thus, it is Schur-concave. As a consequence of the definition of Schur-concavity, for all interlink allocation strategies $\boldsymbol{b}_x, \boldsymbol{b}_y \in \mathbb{R}^{n_a}$, where $\boldsymbol{b}_x$ is majorized by $\boldsymbol{b}_y$, the value of the objective function corresponding to $\boldsymbol{b}_x$ will be greater. Thus, as the interlink allocation strategy becomes more and more uniform, the value of the objective function increases.

Here, we are interested in obtaining the allocation strategy for $(n_a + n_b - 1)$ interlinks to n_a hubs in layer A. It is easy to see that depending on the values of n_a and n_b, a uniform allocation of interlinks, where the same number of interlinks is allocated to all n_a hubs, is not possible. However, as an outcome of the schur-concavity of the objective function, we can conclude that the maximally uniform allocation strategy optimizes the objective function. The same arguments can be made for the allocation of $(n_a + n_b - 1)$ interlinks to the n_b hubs in layer B, thus proving the theorem.

5.4.2 Interlinking structure for the general case

In the previous section, we showed that the optimal interlinking structure maximizing the average infection size in the network can be obtained for the case where the intra-layer degrees of the hubs in both layers of the network are the same. We utilized the Schur-concavity of the objective function to conclude that the maximally uniform allocation of interlinks optimizes our objective. Recall that the individual identities of the hub nodes are obfuscated under the identical degree assumption and as a result, the interlinking structure can be specified just by the allocation of the number of interlinks. In the general case with non-identical hub degrees, the Schur-concavity of the objective function is lost and a theoretically optimal interlinking structure cannot be obtained. However, we have been able to leverage certain conjectures about the interlink allocation strategy and the design of the interlinks, which can be shown via simulations to outperform other heuristic and randomized strategies. In particular, we propose a conjecture stating that the uniform allocation of interlinks continues to be a good strategy even for the general case. Thereafter, we propose a greedy strategy for the construction of the inter-layer links between the set of hubs H_a and H_b. Although both the interlink allocation strategy and the greedy design of the interlinks are suboptimal, the superiority in

performance of these strategies in comparison with randomized and heuristic interlinking strategies is clearly showcased via extensive simulation experiments. We present the details of the randomized and heuristic interlinking strategies along with the corresponding simulation experiments in Section 5.6.

Conjecture 5.4.3 *Consider an interlink allocation strategy, where two hubs y and z in the same layer of the network are interlinked to the set of hubs $\sigma(y)$ and $\sigma(z)$, respectively, where $b_y \triangleq |\sigma(y)|$ and $b_z \triangleq |\sigma(z)|$. If $b_y > b_z + 1$, allocating an interlink from $\sigma(y)$ to $\sigma(z)$, to make the interlink allocation more uniform, leads to an improvement in the objective function $f(\sigma)$ in (5.21) with high probability.*

We focus on the limiting case, where $b_y = b_z + 2$. For a larger difference in the allocation of the interlinks, similar arguments can be applied recursively. Let the sets of nodes interlinked to u and v before the exchange be given by $\sigma(y) = \{h_1, \cdots, h_{b_y}\}$ and $\sigma(z) = \{h_{b_y+1}, \cdots, h_{b_y+b_z}\}$. We are interested in examining the change in the value of the objective function when the interlink allocation is made more uniform, i.e. when a hub from $\sigma(y)$ is moved to $\sigma(z)$. Let $f(\sigma)$ and $f(\sigma')$ denote the average infection sizes around the two hubs y and z before and after the exchange of the interlinks. Thus, we can write:

$$f(\sigma) = \xi_y \left(1 - \prod_{j=1}^{b_y} q_j\right) + \xi_z \left(1 - \prod_{j=b_y+1}^{b_y+b_z} q_j\right), \tag{5.28}$$

$$f(\sigma') = \xi_y \left(1 - \prod_{j=1}^{b_y-1} q_j\right) + \xi_z \left(1 - \prod_{j=b_y}^{b_y+b_z} q_j\right), \tag{5.29}$$

where we assume that the hub h_{b_y} is interlinked to z after the exchange; and $q_j = 1 - \eta_j$, as defined previously. The difference between the infection sizes after the exchange, $\Delta f \triangleq f(\sigma') - f(\sigma)$ can be written as:

$$\Delta f = (1 - q_{b_y}) \left(\xi_z \prod_{j=b_y+1}^{b_y+b_z} q_j - \xi_y \prod_{j=1}^{b_y-1} q_j\right). \tag{5.30}$$

The two products in the second term contain b_z and $b_z + 1$ elements, respectively. Recall that the q_j's define the probability that an infection from hub j does not propagate to an interlinked neighbor. For nodes of high intra-layer degrees (hubs), the q_j's are expected to be small values near 0. As a result, the product of b_z terms is significantly higher than the product of $b_z + 1$ terms. In comparison, the variation in the $\xi \triangleq \frac{\lambda k}{1-\lambda}$ values are expected to be much lower since only nodes of high intra-layer degrees qualify as hubs according to the constraints specified in Lemma 5.3.3. Thus, although Conjecture 5.4.3 cannot be rigorously proved, using the above arguments we can see how it holds in practice. Furthermore, this result is verified by extensive simulation experiments presented in Section 5.6.

Under the general case of non-identical intra-layer degrees of the hubs in H_a and H_b, the interlink allocation strategy cannot solely determine the interlinking structure between the two network layers. Unlike the previous case, here we need to devise an interlinking strategy in addition to the allocation

of interlinks. Thus, we are interested in looking at the problem of optimizing the interlinking structure given a maximally uniform interlink allocation, which was shown to be a good strategy by the arguments in Conjecture 5.4.3. Unfortunately, even for this case a mathematically rigorous optimal interlink structure design cannot be obtained. Interestingly, for a maximally uniform interlink allocation we can rigorously obtain the interlinking structure *minimizing* the objective function in (5.21) but a strategy for maximizing the objective cannot be obtained. This stems from the peculiar result arising from the Generalized Rearrangement Inequality, which we developed in a previous work [Cha17]. We present the statement of the inequality here without the proof for ease of reference.

Lemma 5.4.4 (Generalized Rearrangement Inequality) *Given any two sequences of positive real numbers, $x = \{x_1, x_2, \cdots, x_{cn}\}$ and $y = \{y_1, y_2, \cdots, y_n\}$ and any arbitrary permutation $\rho = \{\rho_1, \cdots, \rho_{cn}\}$ of the sequence $\{1, 2, \cdots, cn\}$ where ρ_i denotes the i th element of ρ, let us define the summations:*

$$\Phi_1 = \sum_{i=1}^{n} y_i \prod_{j=1}^{cn} x_{cn-j+1}, \Phi_2 = \sum_{i=1}^{n} y_i \prod_{j=1}^{cn} x_{\rho_j}, \Phi_3 = \sum_{i=1}^{n} y_i \prod_{j=1}^{cn} x_j. \tag{5.31}$$

If the sequences $\{x\}$ and $\{y\}$ are both non-increasing or both non-decreasing,

$$(\Phi_1, \Phi_2) \leq \Phi_3. \tag{5.32}$$

We re-iterate the estimation of the infection size from (5.20) here for reference:

$$f(\sigma) = \sum_{i \in H_a} \frac{\lambda_a k_i}{1-\lambda_a} + \sum_{i \in H_b} \frac{\lambda_b k_i}{1-\lambda_b} \tag{5.33}$$

$$-\Big(\sum_{i \in H_a} \frac{\lambda_a k_i}{1-\lambda_a} \prod_{j \in \sigma_a(i)} q_j + \sum_{i \in H_b} \frac{\lambda_b k_i}{1-\lambda_b} \prod_{j \in \sigma_b(i)} q_j \Big). \tag{5.34}$$

It is easy from the expression above that the summations in Lemma 5.4.4 are similar in structure to the terms inside the parenthesis. As a consequence of the result in Lemma 5.4.4, we can show that the interlinking structure maximizing the average infection size cannot be obtained. In this dissertation, we propose the construction of the interlinks based on the anti-monotonic arrangement, wherein the hubs with the highest intra-layer degree in layer A are coupled to the hubs with the lowest intra-layer degree in layer B. Although this interlinking strategy is provably sub-optimal due to the result in Lemma 5.4.4, simulation results show that it outperforms other randomized interlinking strategies. However, a surprising result revealed in our simulation experiments is that if a uniform interlink allocation constraint is imposed, the variation of the interlinking structure does not have a major impact on the average size of infection realized in the network. Thus, we can conclude that for the general case of non-identical hub degrees, the interlink allocation strategy plays a more important role than the specific interlinking structure. We plan to examine this observation in detail in future works.

5.5 Engineering the metastable state

The analysis of the epidemic dynamics on interlink subgraphs revealed that under certain conditions, specified by Lemma 5.3.3, a single interlink connecting two hubs can sustain a metastable infection state in the local intra-layer neighborhood around the hubs. However, we show via Lemma 5.3.5 that the average infection size in the local neighborhood of each hub is approximately given by $\frac{\lambda k}{1-\lambda}$, where k denotes the intra-layer degree of the hub and λ indicates the intra-layer infection propagation rate. We remind the reader that since our fundamental objective is to achieve controlled infection spreading in networks, we are primarily interested in the regime of low infection propagation rates, where the epidemics are localized in the desired region of the network. It should not be difficult to see that for low values of λ, the average infection size resulting from a single interlink will usually be insufficient for most practical problems. In this section, we discuss the scheme of engineering composite metastable infection states utilizing a viable number of interlinks, significantly lower than the size of the desired region of the network.

5.5.1 The core and supplementary groups

We start our discussion about the construction of the composite metastable infection state by defining two groups of nodes: the *core* group and the *supplementary* group. A group is nothing but the set of hubs in both layers of the desired region of the network, around which a metastable infection state can be sustained. More specifically, these two groups define the set of nodes in the desired region of the network which can support a metastable infection state by using a single interlink. Thus, the core and the supplementary groups define the nodes in the network which can sustain metastable infection state utilizing minimum number of interlinks. A core group is defined as a set of nodes $\chi_a^0 \cup \chi_b^0$, where any interlink subgraph between two nodes from χ_a^0 and χ_b^0 can sustain a metastable infection state in its neighborhood. In other words, χ_a^0 and χ_b^0 are defined as the set of nodes in D_a and D_b, respectively, such that an interlink between any $a \in \chi_a^0$ and any $b \in \chi_b^0$ satisfies Lemma 5.3.3. On the other hand, the supplementary group, represented by $\chi_a^1 \cup \chi_b^1$, is defined as the set of nodes in D_a and D_b which need the support of specific nodes from the core group for sustaining long lasting infections. The core group provides us with increased flexibility with respect to the design of the interlinking structure since by definition, any interlink between two constituents can support long lasting infections. Using the supplementary group for engineering the composite metastable state puts additional constraints on the interlinking structure, as any interlink between the constituents cannot sustain a metastable infection state as the requirements specified in Lemma 5.3.3 are not satisfied for all pairs.

Let us represent the nodes with the highest intra-layer degree in D_a and D_b by a_1 and b_1, respectively. Let ϕ_a (ϕ_b) denote the set of nodes in D_a (D_b), which satisfy the constraints in Lemma 5.3.3

when interlinked to $b_1 \in D_b$ ($a_1 \in D_a$). Mathematically, this can be written as:

$$\phi_a = \{v \in D_a | \bar{\delta}_a(v) \cdot \bar{\delta}_b(b_1) < \tilde{\lambda}^2\}, \tag{5.35}$$

$$\phi_b = \{v \in D_b | \bar{\delta}_b(v) \cdot \bar{\delta}_a(a_1) < \tilde{\lambda}^2\}. \tag{5.36}$$

where $\bar{\delta}_l(i)$ denotes the effective recovery rate for node i in layer l as defined by Lemma 5.3.3. Since we are defining ϕ_a and ϕ_b with respect to the highest degree node in the other layer, these two sets specify the nodes in the desired network region D_a and D_b, which can sustain a metastable infection state in their neighborhood by using a minimum number of interlinks. Recall that by Lemma 5.3.1, the effective recovery rate $\bar{\delta}(i)$ decreases with the infection propagation rates. Thus, for a low enough infection parameter $\boldsymbol{\lambda} = (\lambda_a, \lambda_b, \tilde{\lambda})$, the sets ϕ_a and ϕ_b can be empty. ϕ_a and ϕ_b can also be empty if the desired subgraphs comprises nodes of low intra-layer degrees. The emptiness of the ϕ's imply that the network parameters in Problem 5.2 are not sufficient to induce long lasting metastable infection states by using a minimum number of interlinks. Although we discuss some techniques to augment the infection state resulting from the hubs in ϕ_a and ϕ_b in later sections of this dissertation, relying solely on the augmentation techniques leads to unstable infection states. For this dissertation, we consider network parameters leading to empty sets for ϕ_a and ϕ_b to be infeasible regions, where the interlinking design strategies proposed here cannot be utilized to solve Problem 5.2.

Assuming non-empty ϕ_a and ϕ_b, which constitutes the feasible region for interlink construction, the core hub group can be defined as:

$$\chi_a^0 = \{v \in D_a | \bar{\delta}_a(v) < \tilde{\lambda}\}, \tag{5.37}$$

$$\chi_b^0 = \{v \in D_b | \bar{\delta}_b(v) < \tilde{\lambda}\}. \tag{5.38}$$

It can be easily verified that an interlink between any two nodes, $i \in \chi_a^0$ and $j \in \chi_b^0$, satisfies Lemma 5.3.3 and as a consequence, can support a metastable infection state in the intra-layer neighborhood of i and j. As a consequence of the definition of ϕ_a and ϕ_b in (5.35)-(5.36), the following relations hold:

$$\chi_a^0 \cup \chi_a^1 = \phi_a, \chi_b^0 \cup \chi_b^1 = \phi_b. \tag{5.39}$$

Thus, the supplementary group of hubs can be simply defined as: $\chi_a^1 = \phi_a - \chi_a^0$ and $\chi_b^1 = \phi_b - \chi_b^0$. Unlike the core group, constituents of the supplementary group cannot be interlinked arbitrarily to each other. By the definition of the ϕ's, we can see that any node in the supplementary group can be interlinked to the highest degree node in the other network layer. However, we showed in the previous section that a uniform allocation of interlinks maximizes the average infection size. Thus, interlinking all nodes in the supplementary group to the highest degree nodes in the other layer is not a good interlinking strategy. Note that the subset of nodes from the supplementary group, which can be interlinked reliably to nodes of the core group, progressively shrinks as we try to interlink them to nodes of lower intra-layer degree. This complicates the design of the interlinking structure

for the supplementary group of hubs, as will be seen in later sections.

5.5.2 Augmenting the metastable state

The core and the supplementary group of hubs define the set of nodes, in the desired region of the network, which can sustain a composite metastable infection state in their intra-layer neighborhoods using minimum number of interlinks. The role played by the inter-layer connections in this case is to maintain a reliable interaction among the different hubs so that if the infection in the local neighborhood of any hub dies out, it can be re-infected by an interlinked hub. However, for some practical problems the infection size achievable from the core and the supplementary group may be insufficient. In this section, we discuss strategies of augmenting the metastable infection state so as to increase the average infection size.

Contrary to the case of the core and the supplementary groups, the interlinks play a dual role during the augmentation of the metastable state. In addition to maintaining a reliable interaction between different hubs, the interlinks also need to enhance the inter-layer degree of the nodes so as to qualify them as hubs. Note that all nodes which qualify as “hubs" using a single interlink, by satisfying the constraints specified in Lemma 5.3.3, are included in the definition of ϕ_a and ϕ_b in (5.35)-(5.36). As a result, any node used to augment the metastable infection state necessarily requires multiple inter-layer links, where the required number of inter-layer links can be estimated from Corollary 5.3.4. A natural question arises whether the multiple interlinks should be used either to enhance the interaction with other hubs or to increment the average infection size by expanding the neighborhood of these new hubs to include nodes beyond ϕ_a and ϕ_b. We take a deeper look into this trade-off below. It will be evident from the following discussion that the mathematics governing the augmentation of the metastable infection state is significantly more complex than the previous analysis presented here and a rigorous treatment is not possible. As a part of future extensions to this work, we plan to explore whether other mathematical models can allow us to develop more rigorous arguments for constructing the composite metastable infection state.

Let us discuss the impact of augmenting the composite metastable state, comprising the core and the supplementary groups, with the node i. We assume without loss of generality that $i \in D_a$. Let c_i be the total number of interlinks required for i to qualify as a hub. Recall that c_i can be computed from Corollary 5.3.4. As discussed above, the interlinks of i have two goals: i) maintaining interaction with hubs in the metastable state, and ii) expanding the metastable state by including additional nodes. For satisfying the first goal, the interlinks should be connected to existing hubs. Recall that Corollary 5.3.4 is obtained under the assumption that the hub is interlinked to nodes of minimal degree. Thus, i can sustain a metastable infection state in its neighborhood if it is interlinked to any node in the core or the supplementary group. The coupling to the core or the supplementary group is necessary so that augmented hubs can be re-infected by other hubs. Let us assume that among the c_i interlinks added to i, d_i links are connected to hubs in the core and the supplementary group, while the remaining are connected to the un-interlinked nodes from $D_b - \phi_b$ with the highest intra-layer degrees. The reason behind choosing the nodes with the highest intra-layer degrees is

to maximize the infection size resulting from the augmentation of the metastable state. Let Δf denote the increment in the average infection size resulting from augmenting the metastable state by including node i. We can write:

$$\Delta f = \frac{\lambda_a k_i}{1-\lambda_a}\left(1-\prod_{j=1}^{d_i} q_j^{(b)}\right) + \sum_{j=1}^{c_i-d_i} \frac{\lambda_b k_j}{1-\lambda_b}(1-q_i^{(a)}), \tag{5.40}$$

where $q_j^{(b)}$represents the probability that the infection from node j in layer B does not propagate to i and $q_i^{(a)}$ denotes the probability that infection from $i \in D_a$ does not propagate to the $c_i - d_i$ interlinked nodes in layer B. It can be observed from the above expression that as d_i increases, the first term increases whereas the second one decreases. However, the gain in the first term progressively diminishes are more terms are added where it finally converges to $\frac{\lambda_a k_i}{1-\lambda_a}$. For the second term, the growth is almost linear in the number of terms. Although a rigorous maximization is not possible owing to the non-convexity of the problem, it is not difficult to see that an optimal interlinking strategy would be to use a few interlinks to maintain the interaction with other hub nodes in the core and the supplementary group, while the remaining interlinks should be connected so as to include new nodes in the metastable infection state. We performed some experiments to observe the impact of different values of d_i and observed that $d_i = 2$ works well for most cases.

5.5.3 Algorithms for interlinking design

In the following, we present the algorithms for designing the interlinking structure for the three cases: i) the core group of hubs, ii) the supplementary group of hubs, and iii) the augmentation of the metastable infection state formed by the core and the supplementary hub groups. Obtaining the set of hubs necessary for satisfying the infection density requirements in Problem 5.2 is presented in the next section. Here, we present the interlinking strategies under the assumption that the set of hubs is already known.

The design of the interlinking structure for the core group of hubs is presented in Algorithm 4. Our objective is to design the interlinking structure between two set of hubs $H_a^0 \subseteq \chi_a^0$ and $H_b^0 \subseteq \chi_b^0$, where the core groups χ_a^0 and χ_b^0 are defined by the equations (5.37)-(5.38). We design the interlinking structure from the perspective of the layer with the lesser number of nodes; if H_a^0 and H_b^0 have the same number of nodes Algorithm 4 holds for both perspectives. Without loss of generality, we assume that $|H_a| \leq |H_b|$. Let us index the hubs in H_a^0 in the decreasing order of the intra-layer degrees and the hubs in H_b^0 in the increasing order of the intra-layer degrees. Algorithm 4 starts with the computation of the required number of interlinks $l_{\text{tot}} \triangleq n_a^0 + n_b^0 - 1$, where n_a^0 and n_b^0 represent the number of nodes in H_a^0 and H_b^0, respectively. In Section 5.4, we show that the maximally uniform allocation of interlinks is a good strategy, although its optimality can be rigorously proved only for the case of identical hub degrees. Furthermore, we show that the anti-monotonic interlinking of

Algorithm 4 Interlinking the core group

procedure CORESTRAT(H_a^0, H_b^0)
  $(n_a^0, n_b^0) \leftarrow (|H_a^0|, |H_b^0|)$.
  $l_{\text{tot}} \leftarrow (n_a^0 + n_b^0 - 1)$, $i_b \leftarrow 0$.
  $r \leftarrow l_{\text{tot}} (\text{mod } n_a^0)$, $q \leftarrow \lfloor \frac{l_{\text{tot}}}{n_a^0} \rfloor$
  $\sigma \equiv \{\sigma(i) = \emptyset,\ \forall 1 \leq i \leq n_a\}$, defining the
  interlinks for $i \in H_a$.
  for $i_a = 1, \cdots, n_a$ **do**
    if $i_a \leq r$ **then**
      $\sigma(i_a) \leftarrow H_b^0[i_b : i_b + q + 1]$
      $i_b = i_b + q$
    else
      $\sigma(i_a) \leftarrow H_b^0[i_b : i_b + q]$
      $i_b = i_b + q - 1$
  return $H_a^0 \longleftrightarrow H_b^0$

hubs based on their intra-layer degrees is expected to perform better. Utilizing these two ideas, we device a greedy strategy for designing the interlinking structure for the core group of hubs. Let the quotient and remainder resulting from dividing l_{tot} by n_a^0 be denoted by q and r, respectively, where $l_{\text{tot}} = q \cdot n_a^0 + r$. The interlinking structure is described by $\sigma \equiv \{\sigma_a(1), \cdots, \sigma_a(n_a)\}$, where $\sigma_a(i)$ denotes the set of nodes in layer B interlinked to the ith node in H_a^0. Let i_b denote the index of the hubs in layer B. To satisfy the maximally uniform interlink allocation, we greedily couple the first r hubs in H_a^0 to $q+1$ nodes in H_b^0, where $H_b^0[i_b : i_b + q + 1]$ represents the $q+1$ nodes with indices running from i_b through $i_b + q + 1$. Each of the remaining $n_a - r$ nodes in H_a^0 are interlinked to q nodes in H_b^0. Note that adjacent $\sigma_a(i)$'s share one element ensuring the connectivity of the network of hubs in H_a^0 and H_b^0. An instance of the interlinking strategy is presented in Fig. 5.3. Algorithm 4 returns the interlinking structure σ between the set of hubs H_a^0 and H_b^0 denoted by the expression $H_a^0 \longleftrightarrow H_b^0$, where the superscript indicates that these hubs are a subset of the core group of hubs.

Next, let us discuss the design of the interlinking structure for the supplementary group. The procedure for this is detailed in Algorithm 5. Our objective here is to interlink the two supplementary groups H_a^1 and H_b^1 with the interlinked core group $H_a^0 \longleftrightarrow H_b^0$. Let us index the nodes in H_a^1 and H_b^1 in the decreasing order of their intra-layer degree. For each node $i \in \chi_a^1$, we can define the candidate sets:

$$\kappa_i = \{j \in \chi_b^0 | \bar{\delta}_a(i) \bar{\delta}_b(j) < \tilde{\lambda}^2\}. \tag{5.41}$$

By Lemma 5.3.3, we know that any interlink between i and an element of the candidate set is able to sustain a metastable infection state. Note that χ_b^0 is the candidate set for nodes in χ_a^0 and vice versa, which is why all interlinks between members of the core group are valid. This difference in the candidate sets complicates the design of the interlinks for the supplementary hubs. Starting from the node in H_a^1 with the highest intra-layer degree, we interlink it to a node in its candidate set with the minimum degree. It should not be difficult to see that this strategy biases the allocation

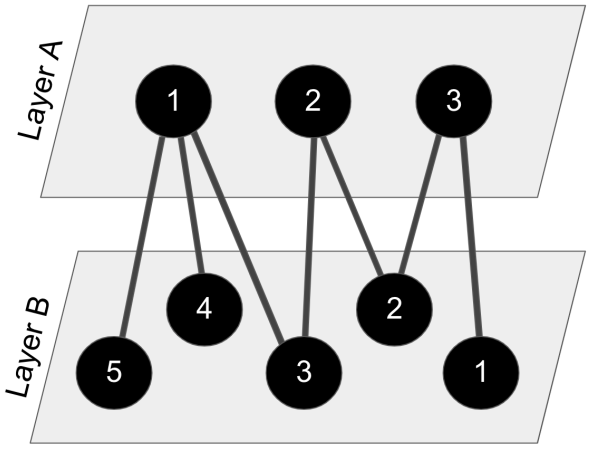

Figure 5.3 Instance of interlinking structure between two subsets of the core group, with $H_a^0 = \{1,2,3\}$ and $H_b^0 = \{1,2,3,4,5\}$. The maximally uniform interlink allocation to H_a^0 following Algorithm 4 is 3, 2, 2, respectively

of interlinks towards low degree hubs in the candidate set. However, the size of the candidate sets κ_i progressively reduces as we move towards nodes i with smaller intra-layer degrees, since $\bar{\delta}(i)$ varies inversely with the node degree of i. As a result, nodes of lower intra-layer degrees in H_a^1 are by default interlinked to the higher degree nodes in H_b^0as the candidate sets shrink in size. Due to these competing factors, the simple interlinking strategy in Algorithm 5 works quite well in practice.

Finally, Algorithm 6 presents the interlink design strategy for further augmenting the metastable infection state beyond the core and the supplementary groups; the infection state resulting from $H_a^0 \cup H_a^1 \longleftrightarrow H_b^0 \cup H_b^1$ is augmented with the sets H_a^2 and H_b^2. For this case, we utilize the result in Corollary 5.3.4, establishing the sufficient condition for the existence of a metastable infection state in the neighborhood of a node. The augmentation of the metastable state by including node $i \in D_a - \phi_a$ is done via connecting i to the core or the supplementary group of nodes via two interlinks, while the remaining interlinks are coupled to nodes of the highest intra-layer degree in $D_b - \phi_b$. The design strategy for the core and the supplementary group of hubs as well as the augmentation of the metastable state will be further clarified when we look at specific case studies in Section 5.6.

5.5.4 Estimating the hub sets

The scheme of achieving controlled infection spreading in the network is to incrementally assemble a composite metastable infection state in the desired region of the network by interlinking different hubs in the network to each other. Each hub, owing to the size of its neighborhood, is capable of sustaining a long lasting infection in its immediate neighborhood. Thus, by interlinking different hubs, we ensure a reliable interaction between them so that they can re-infect each other and thereby sustain long lasting infections in their neighborhood. In the previous section, we presented the algorithms for interlinking the core and the supplementary group of hubs. Furthermore, we also

Algorithm 5 Interlinking the supplementary group

procedure SUPPSTRAT($H_a^1, H_b^1, H_a^0 \longleftrightarrow H_b^0$)
  $(n_a^1, n_b^1) \leftarrow (|H_a^1|, |H_b^1|)$.
  ###Generating interlinks between H_a^1 and H_b^0
  $\sigma \equiv \{\sigma(i) = \emptyset,\ \forall 1 \leq i \leq n_a^1\}$, defining the
  supplementary interlinks for $i \in H_a^1$.
  for $i = 1, \cdots, n_a^1$ **do**
    $\kappa_i = \{j \in H_b^0 | \bar{\delta}_a(i)\bar{\delta}_b(j) < \tilde{\lambda}^2\}$.
    $\sigma(i) \leftarrow$ minimum degree node in κ_i.
  ###Generating interlinks between H_b^1 and H_a^0
  $\sigma \equiv \{\sigma(i) = \emptyset,\ \forall 1 \leq i \leq n_b^1\}$, defining the
  supplementary interlinks for $i \in H_b^1$.
  for $i = 1, \cdots, n_b^1$ **do**
    $\kappa_i = \{j \in H_a^0 | \bar{\delta}_a(j)\bar{\delta}_b(i) < \tilde{\lambda}^2\}$.
    $\sigma(i) \leftarrow$ minimum degree node in κ_i.
  return $H_a^0 \cup H_a^1 \longleftrightarrow H_b^0 \cup H_b^1$

discussed the scheme of augmenting the infection state to include additional nodes, though the augmentation necessitates the use of additional interlinks. However, the design of the interlinking structure was done under the context where the different hub sets H_a^i and H_b^i are known, where $i = 0, 1, 2$ denote the core, the supplementary and the augmented group of nodes, respectively. It is important to note that the specific design of the interlinking structure is dependent on the desired infection density $\Gamma = (\gamma_a, \gamma_b)$ in the desired region of the network denoted by D_a and D_b. Here γ_a and γ_b denote the desired average fraction of infected nodes in the network region. In this section, we discuss the estimation of the hub sets necessary to compose the metastable infection state satisfying the infection density requirements. Recall that our main interest lies in cases where a controlled infection can be induced in the desired region using significantly lower number of interlinks than the size of the regions.

The basic idea behind the estimation of the number of hubs is to progressively “grow" the metastable infection state by interlinking additional hubs to expand the metastable state, until the infection density requirements are satisfied. It can be observed from (5.20) that the estimation of the infection size is dependent on the hub sets H_a and H_b and the specific interlinking structure between these sets. However, we saw in the previous section that the design of the interlinking structure is different for the core, the supplementary or the augmented group. Furthermore, it is important to note that the definitions of the different groups are dependent on the infection spreading parameter $\boldsymbol{\lambda} \equiv (\lambda_a, \lambda_b, \tilde{\lambda})$, i.e. $\boldsymbol{\lambda}$ determines whether H_a and H_b can be composed of solely with nodes in the core group, or whether supplementary and augmented group of nodes are necessary.

In order to develop the method for estimation of the hub sets H_a and H_b required for constructing the desired metastable infection state satisfying the infection density requirements of our problem,

Algorithm 6 Augmenting the metastable state

t

procedure AUGSTRAT($H_a^2, H_b^2, H_a^0 \cup H_a^1 \longleftrightarrow H_b^0 \cup H_b^1$)
  $(n_a^2, n_b^2) \leftarrow (|H_a^2|, |H_b^2|)$.
  ###Generating interlinks between H_a^2 and D_b
  $\sigma \equiv \{\sigma(i) = \emptyset,\ \forall 1 \le i \le n_a^2\}$, defining the
  supplementary interlinks for $i \in H_a^2$.
  for $v \in H_a^2$ **do**
    $c_v \leftarrow$ compute using Corollary 5.3.4.
    $\sigma(i) \leftarrow 2$ random nodes in $H_b^0 \cup H_b^1$.
    $\sigma(i) \leftarrow$ top $c_v - 2$ nodes in $D_b - H_b^0 \cup H_b^1$.
  ###Generating interlinks between H_b^1 and H_a^0
  Repeat Steps 4 - 9 with layer roles reversed.
  return $H_a^0 \cup H_a^1 \cup H_a^2 \longleftrightarrow H_b^0 \cup H_b^1 \cup H_b^2$

we formulate a sub-routine that identifies the distribution of the three groups (core, supplementary and augmented) in H_a and H_b, and interlinks the hubs accordingly. Algorithm 7 starts with the computation of the core and the supplementary groups in the desired region of the network D_a and D_b with respect to $\boldsymbol{\lambda}$. Thereafter, the sets H_a and H_b are compared with the core and the supplementary groups to determine whether augmentation is necessary. The flags c_l's and s_l's, respectively denote whether the core and the supplementary groups in layer l have been exhausted by H_a and H_b, indicating the necessity of augmentation of these groups to engineer the required metastable infection state. Finally, the interlinking structure between H_a and H_b is designed utilizing the three methods developed in the previous section.

With this sub-routine in hand, we are ready to describe the method for the estimation of the hub sets H_a and H_b that can satisfy the infection density requirements of our problem. It should be clear from the above discussion that the problem of estimating the number of hubs cannot be decoupled from the problem of designing of the interlinking structure. Due to this reason, the only way to ensure the use of a minimum number of interlinks is to sequentially grow the metastable infection state by considering additional hubs in H_a and H_b, until the infection density requirements are satisfied. Thus, the algorithm for the estimation of the hubs Algorithm 8 essentially gives us the desired metastable infection state. The input to Algorithm 8 is the desired infection sizes $\xi_{\text{des}}^a \triangleq \gamma_a |D_a|$ and $\xi_{\text{des}}^b \triangleq \gamma_b |D_b|$. The algorithm first computes the core and the supplementary node groups and then populates the sets H_a^∞ and H_b^∞in the decreasing order of the intra-layer degrees. H_l^∞ comprises the core group, the supplementary group and the rest of the nodes in the desired region D_l. Thus, the ordered sets H_a^∞ and H_b^∞describe the order of the nodes from the desired region which are to be used to grow the metastable infection state that can satisfy the infection density requirements of our problem. The intermediate infection densities, given by ξ_{curr}^a and ξ_{curr}^b in Algorithm 8, are computed from (5.20), representing the estimated infection sizes in both layers of the network. Thus, we can see that Algorithm 8 essentially achieves the controlled infection spreading parameterized

Algorithm 7 Generating optimal interlinks

procedure GENOPTINTER($H_a, H_b, \boldsymbol{\lambda}$)
  Compute $\chi_a^0, \chi_a^1, \chi_b^0, \chi_b^1$ for $\boldsymbol{\lambda}$.
  ###Checking core and supplementary groups in D_a.
  (c_a, s_a) = (False, False).
  if $H_a \subseteq \chi_a^0$ **then**
    Do nothing.
  else
    if $H_a \subseteq \chi_a^0 \cup \chi_a^1$ **then**
      c_a = True, s_a = False.
    else
      c_a = True, s_a = True.
  ###Checking core and supplementary groups in D_b.
  (c_b, s_b) = (False, False).
  if $H_b \subseteq \chi_b^0$ **then**
    Do nothing.
  else
    if $H_b \subseteq \chi_b^0 \cup \chi_b^1$ **then**
      c_b = True,s_b = False.
    else
      c_b = True, s_b = True.
  ###Constructing the interlinks.
  $\sigma \leftarrow \{\}$.
  if c_a is False **then**
    if c_b is False **then**
      σ = CORESTRAT(H_a, H_b)
    else if c_b is True and s_b is False **then**
      σ =CORESTRAT(H_a, χ_b^0)
      σ =SUPPSTRAT($\{\}, H_b - \chi_b^0, \sigma$)
    else
      σ =CORESTRAT(H_a, χ_b^0)
      σ =SUPPSTRAT($\{\}, \chi_b^1, \sigma$)
      σ =AUGSTRAT($\{\}, H_b - (\chi_b^0 \cup \chi_b^1), \sigma$)
  else if c_a is True and s_a is False **then**
    if c_b is False **then**
      σ = CORESTRAT(χ_a^0, H_b)
      σ =SUPPSTRAT($H_a - \chi_a^0, \{\}, \sigma$)
    else if c_b is True and s_b is False **then**
      σ =CORESTRAT(χ_a^0, χ_b^0)
      σ =SUPPSTRAT($H_a - \chi_a^0, H_b - \chi_b^0, \sigma$)
    else
      σ =CORESTRAT(χ_a^0, χ_b^0)
      σ =SUPPSTRAT($H_a - \chi_a^0, \chi_b^1, \sigma$)
      σ =AUGSTRAT($\{\}, H_b - (\chi_b^0 \cup \chi_b^1), \sigma$)
  else
    if c_b is False **then**
      σ = CORESTRAT(χ_a^0, H_b)
      σ =SUPPSTRAT($\chi_a^1, \{\}, \sigma$)
      σ =AUGSTRAT($H_a - (\chi_a^0 \cup \chi_a^1), \{\}, \sigma$)
    else if c_b is True and s_b is False **then**
      σ =CORESTRAT(χ_a^0, χ_b^0)
      σ =SUPPSTRAT($\chi_a^1, H_b - \chi_b^0, \sigma$)
      σ =AUGSTRAT($H_a - (\chi_a^0 \cup \chi_a^1), \{\}, \sigma$)
    else
      σ =CORESTRAT(χ_a^0, χ_b^0)
      σ =SUPPSTRAT($\chi_a^1, \chi_b^1, \sigma$)
      σ =AUGSTRAT($H_a - (\chi_a^0 \cup \chi_a^1), H_b - (\chi_b^0 \cup \chi_b^1), \sigma$)
  return σ

Algorithm 8 Constructing the metastable infection state

procedure CONSTRUCTMETA($\xi^a_{\text{des}}, \xi^b_{\text{des}}, \boldsymbol{\lambda}$)
  Compute $\chi^0_a, \chi^1_a, \chi^0_b, \chi^1_b$ for $\boldsymbol{\lambda}$
  $H^\infty_a \leftarrow \{\chi^0_a, \chi^1_a, D_a - (\chi^0_a \cup \chi^1_a)\}$ indexed by degrees.
  $H^\infty_b \leftarrow \{\chi^0_b, \chi^1_b, D_b - (\chi^0_b \cup \chi^1_b)\}$ indexed by degrees.
  $(i_a, i_b) \leftarrow (1,1)$.
  $H_a \leftarrow \{\chi^0_a[i_a]\}$, $H_b \leftarrow \{\chi^0_b[i_b]\}$.
  $\sigma \leftarrow$GENOPTINTER($H_a, H_b, \boldsymbol{\lambda}$)
  $(\xi^a_{\text{curr}}, \xi^b_{\text{curr}}) = f(\sigma)$ computed using (5.20).
  while $\xi^a_{\text{curr}} < \xi^a_{\text{des}}$ or $\xi^b_{\text{curr}} < \xi^b_{\text{des}}$ **do**
    if $\xi^a_{\text{curr}} < \xi^a_{\text{des}}$ **then**
      $H_a = H_a + H^\infty_a[i_a]$
      $\sigma =$GETOPTINTER(H_a, H_b)
      $\xi^a_{\text{curr}} = f_a(\sigma)$ computed using (5.20)
      $i_a = i_a + 1$
    if $\xi^b_{\text{curr}} < \xi^b_{\text{des}}$ **then**
      $H_b = H_b + H^\infty_b[i_b]$
      $\sigma =$GETOPTINTER(H_a, H_b)
      $\xi^b_{\text{curr}} = f_b(\sigma)$ computed using (5.20)
      $i_b = i_b + 1$
  return σ

by γ_a and γ_b in the desired region D_a and D_b of the network. It is important to note that the control of the infection density is discrete in nature. As additional nodes are progressively interlinked to the metastable infection state, a fraction of their neighborhoods, parameterized by the corresponding intra-layer infection rate λ_a or λ_b, continues to remain infected. The discrete variation in the achievable infection density is dependent on the specific intra-layer degrees of the hubs in D_a and D_b. Thus, this discrete control of the infection size describes an important limitation of the solution to Problem 5.2.

5.5.5 Limits of achievable infection densities

We end this section by discussing the limits of the achievable infection densities in the desired subgraphs $D_a \subseteq G_a$ and $D_b \subseteq G_b$, where G_a and G_b are the isolated network layers given in Problem 5.2. It should be intuitive that any desired infection density $0 \leq \gamma_a, \gamma_b \leq 1$ is not achievable in the desired subgraphs. Here, we discuss the limits of the achievable infection densities which can be realized using a small number of interlinks.

It should be clear from the discussion in the previous section that the composite metastable infection state comprising the core and the supplementary group of hubs, represents the case where the design of the interlinking structure utilizes the minimum number of inter-layer links. This is because the construction of the interlinking structure between $\chi^0_a \cup \chi^1_a$ and $\chi^0_b \cup \chi^1_b$ is realized by interlinking the hubs in the core and the supplementary groups to form a minimally connected

graph: a tree. The exact computation of the infection size achievable by these two groups of hubs is given by (5.20), which is dependent on the interlinking structure σ. To avoid the dependence on σ, a simple upper bound can be obtained by neglecting the q_j terms:

$$\gamma_a^{\text{cs}} = \frac{\lambda_a}{1-\lambda_a} \sum_{i \in \chi_a^0 \cup \chi_a^1} k_i, \tag{5.42}$$

$$\gamma_b^{\text{cs}} = \frac{\lambda_b}{1-\lambda_b} \sum_{i \in \chi_b^0 \cup \chi_b^1} k_i. \tag{5.43}$$

In the above equations, γ_l^{cs} represents the infection density in layer l of the network achievable by using the nodes in the core and the supplementary group of hubs. Thus, $\Gamma^{\text{cs}} = (\gamma_a^{\text{cs}}, \gamma_b^{\text{cs}})$ is nothing but the sum of the intra-layer degrees of the nodes in the core and the supplementary group, scaled by a function of the infection propagation rate in the network layers. Γ^{cs} is an important threshold as it indicates the approximate limits of infection sizes, which can be induced by utilizing a minimum number of interlinks. Although we discuss techniques for augmenting the metastable infection state formed by the core and the supplementary group of hubs, these techniques are not very reliable in pushing the achievable infection density far beyond Γ^{cs}. Thus, for cases where the desirable infection density (Γ) is much higher than that achievable by the core and the supplementary hubs (Γ^{cs}), a sensible strategy is to strive for increasing the infection propagation rate $\boldsymbol{\lambda} = (\lambda_a, \lambda_b, \tilde{\lambda})$ so as to include more nodes in ϕ_a and ϕ_b which can lead to an increment in the achievable infection density Γ^{cs}.

5.6 Simulation Results

The basic idea behind our work is to estimate the epidemic dynamics in complex networks utilizing approximate methods, since the exact mathematical model is not tractable in the general case. In this section, we discuss our simulation experiments validating our approximate theoretical results on both synthetic and real world networks. We start this section by discussing the details of the simulation framework for studying the epidemic dynamics in networks. We proceed by verifying the theoretical results presented in the Lemmas by testing them on complex network topologies. Recall that the theoretical results obtained in Section 5.3 are based on various simplifications of the topology and thus, examining their validity on complex network topologies is an important step. Thereafter, we compare our interlinking design strategy with other heuristics to observe the variation in performance. To the best of our knowledge, ours is one of the first works in optimizing the network structure to achieve a desired infection density and we have not been able to find other strategies in literature against which our proposed strategy can be compared. Due to this reason, we compare the performance of our proposed method with variations of our strategy to portray the impact the interlinking design on the properties of localized infection states. Finally, we present two case studies involving real world networks, where we showcase our algorithm for designing the interlinking structure to satisfy the infection density requirements. The real world

networks have been chosen to serve as examples of practical network design problems, where the ideas presented in our dissertation can be utilized. The infection density requirements in the two case studies showcase the interlinking design problem under two regimes: i) the sufficient case, where the core group of hubs present in the network are sufficient to achieve the desirable infection state, ii) the augmented case, where the core and the supplementary groups in the network are not sufficient and we need to augment the resulting metastable infection state to satisfy the infection density requirements.

5.6.1 Details of the Simulation Framework

The SIS epidemics on networks are simulated with a continuous time dynamics using the Gillespie algorithm [Gil77] which is popularly used in most works in this area. We use Python and its associated libraries (NetworkX, NumPy) to build our simulation framework. In particular, we extend the simulation framework presented in [Bog13] to a multilayer scenario. For all the simulation experiments, the infection seeds are taken to be the different hubs in the network. During the course of the simulations, we track three quantities: i) the number of infected nodes in each layer of the network, denoted by $N_I(t)$, ii) the number of active intra-layer links, denoted by $E_A(t)$, and iii) the number of active inter-layer links, denoted by $\tilde{E}_A(t)$. Here active links are the network edges originating from infected nodes. At each step of the simulation by the Gillespie algorithm, one of three events occur: i) a randomly chosen infected node is cured with probability $p_r = N_I(t)/[N_I(t)+\lambda E_A(t)+\tilde{\lambda}\tilde{E}_A(t)]$, ii) an active intra-layer link is randomly chosen with probability $p_i = \lambda E_A(t)/[N_I(t)+\lambda E_A(t)+\tilde{\lambda}\tilde{E}_A(t)]$ and the susceptible node attached to this active link (if present) is infected, and iii) an active inter-layer link is randomly chosen with probability $p_{\tilde{i}} = \tilde{\lambda}\tilde{E}_A(t)/[N_I(t)+\lambda E_A(t)+\tilde{\lambda}\tilde{E}_A(t)]$ and its susceptible end point is infected. Note that for cases where the intra-layer infection propagation rate is different for both layers, the active links in each layer need to be tracked individually. It is easy to see that $p_r + p_i + p_{\tilde{i}} = 1$ and thus, one of these three events occurs at each time step. Thereafter, the system time is updated as $t \to t + 1/[N_I(t)+\lambda E_A(t)+\tilde{\lambda}\tilde{E}_A(t)]$ and the infected nodes and active links are recomputed. Due to the stochastic nature of the epidemic dynamics, we plot the averaged results over multiple independent Monte Carlo (MC) runs for all the figures.

5.6.2 Verification of the Lemmas

The fundamental contribution of this dissertation is to approximate the epidemic dynamics in complex networks by studying epidemics in microscopic subgraphs. In particular, the dynamics are characterized by localized metastable infection states in the local neighborhood of high degree nodes (hubs) and the relative interaction between different hubs. For the verification of Lemma 5.3.3, we simulated the extinction times of epidemics on different interlink sub-graphs, where the intra-layer degree of the end-point of the interlink in layer B is kept fixed, while the intra-degree of the end-point in layer A is varied in the x-axis. To achieve the setting of this experiment, we generate the layer B of the network as a Barabasi-Albert (BA) graph with parameter $m = 1$ of size 5000. A node of degree 100, chosen from layer B, is taken to be one of the fixed end-points of the

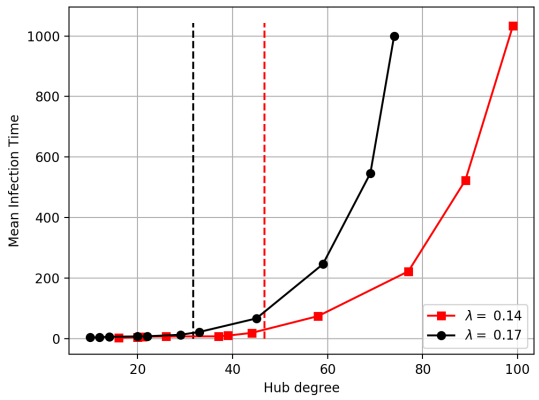

Figure 5.4 Variation of extinction time in interlink subgraphs with the intra-layer degrees of the constituent hubs.

interlink subgraph. For the other end-point of the interlink subgraph, nodes of desired intra-layer degrees are chosen from layer A, generated as another BA graph with the same parameters. For cases where a node with a particular intra-layer degree is not available, we regenerate the network layer with the same or a larger size depending on the necessity. Starting from the initial configuration of both hub nodes infected, we compute the duration of the metastable infection state until the absorbing state configuration is reached and plot in the y axis. For each construction of the interlink subgraph, the average infection lifetime over 500 MC runs is plotted. In Figure 5.4, we observe a sharp increase in the extinction times as the intra-layer degrees of the hub nodes exceed the threshold as predicted by Lemma 5.3.3. This marks the onset of "long" infection times, where metastable infection states are sustained in the interlink subgraph for times exponential in the hub degree. As we can see from Figure5.4, the predicted thresholds accurately predict the onset of metastable infection states for both synthetic and real world networks. This supports a key approximation in our mathematical analysis of the epidemics: the epidemic dynamics in complex networks can be accurately approximated by characterizing the dynamics in the local neighborhood of hubs.

In Figure 5.5, we verify the predictions in Lemma 5.3.6 by simulating epidemic dynamics in interlink subgraphs spanning $i \in V_a$ and $j \in V_b$ with the initial infection configuration $\{i\}$, i.e. only the hub in layer A is infected. We are interested in simulating the probability of propagation of infection to hub j via the interlink and comparing it with our theoretical predictions. We consider the same setting as the previous experiment, wherein the intra-layer degree of node j is kept fixed while the intra-layer degree of i is varied. We simulate the epidemic dynamics in this scenario and the probability with which the infection from i propagates to j is plotted with respect to the hub degree of i. It can be observed from Figure 5.5 that the simulated probabilities closely follow the theoretical predictions for different network classes.

Finally, in Figure 5.6, we compare the theoretical estimation of the infection size presented in (5.20) with the simulated values, for the simplest case of an interlink subgraph. For an interlink

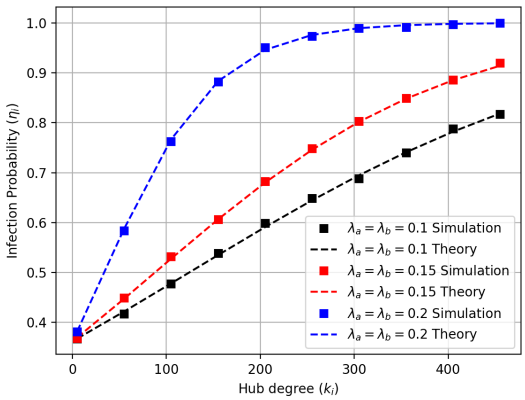

Figure 5.5 Variation of η_i with hub degree k_i for different infection propagation rates.

subgraph spanning $i \in V_a$ and $j \in V_b$, the infection size in layer A is given by $\frac{\lambda_a k_i}{1-\lambda_a}\eta_j$, where η_j denotes the probability of the infection propagating to i from j given by Lemma 5.3.6, k_i denotes the intra-layer degree of i and λ_a is the intra-layer infection propagation rate in layer A. To test the validity of the above expression, we simulate the epidemic dynamics on an interlink subgraph where the intra-layer degrees of both endpoints are 100. In Figure 5.6, we plot the intra-layer infection rate for layer A, i.e. λ_a in the x-axis, while the normalized average infection size $\frac{\lambda_a}{1-\lambda_a}\eta_j$ is plotted in layer A, where $k_i = 100$. This figure illustrates the basic idea behind our claim of the achievement of controlled infection spreading in networks over extended parameter settings. It can be observed from Figure 5.6 that the infection densities closely follow the theoretical predictions for an extended range of the infection rates. At high infection propagation rates, the simulated infection size blows up due to the divergent epidemic dynamics in the network that spreads throughout the network instead of being contained in the desired region. As discussed earlier, most works in literature focus on studying the epidemic dynamics in this regime, where a finite fraction of the entire network is infected. In this dissertation, we show that tuning the epidemic dynamics below the divergent regime allows us to realize controlled infection spreading in complex networks.

5.6.3 Comparison of different strategies

A significant contribution of this dissertation is to theoretically prove the optimality of the maximally uniform interlink allocation strategy under the assumption that the chosen hubs in each network layer have identical intra-layer degrees. In addition, we conjecture that the uniform allocation of interlinks continues to be a good albeit sub-optimal strategy for the general case of non-identical hub degrees. In this section, our objective is to verify the validity of these results via simulation experiments. We consider two isolated network layers represented by G_a and G_b, generated as BA graphs of size 10000 with $m = 1$. The desired regions in these layers (D_a and D_b) are specified by the four hop neighborhood around two randomly chosen points a_{rdn} and b_{rdn}. We construct the interlinking structure between D_a and D_b following different strategies and plot the average

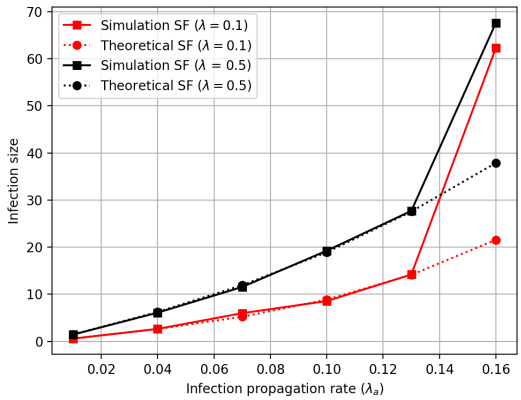

Figure 5.6 Variation of average size of localized infection around hubs with infection propagation rate.

infection density over 500 MC runs for layer A of the network as a function of the intra-layer infection propagation rate $\lambda_a = \lambda_b = \lambda$. The inter-layer infection propagation rate $\tilde{\lambda}$ is fixed at 0.2.

In Figure 5.7, we generate the interlinks using the following four strategies: i) one-to-one interlinking, where the nodes in D_a are coupled to nodes in D_b in the decreasing order of their intra-layer degrees, ii) one-to-many interlinking, where the highest degree nodes in D_a are coupled to four random nodes in D_b, iii) skewed interlink allocation, where different non-uniform interlink allocation strategies are used and the average performance is plotted, and iv) uniform interlink allocation, where four hubs in D_a and six hubs in D_b are interlinked following the uniform allocation strategy described in Theorem 5.4.2 with randomized interlinking structure. The first two of these four strategies are constructed so that they involve around 100 interlinks, while the last two strategies utilize $(6+4-1)=9$ interlinks. It can be observed from Figure 5.7 that the performance of the last two strategies is strikingly higher than the first two strategies although they utilize only a fraction of the interlinks. This clearly shows that enforcing interaction between different hubs is a very good strategy and naive heuristics for interlink design can perform extremely poorly. Furthermore, the difference between the uniform and the non-uniform allocation of the interlinks is also significant showing that a uniform allocation is clearly superior to non-uniform strategies.

In Figure 5.8, we want to observe the impact of different designs of the interlinking structure while adhering to the uniform allocation of interlinks. For reference, we include the plots corresponding to the first two strategies as well. Recall that we indicated the superiority of the anti-monotonic interlinking structure in Conjecture 5.4.3, although we were not able to obtain a rigorous proof. However, we can observe from Figure 5.8 that the specific interlinking scheme has a limited effect on the infection size realized in the network, as long as the uniform interlink allocation strategy is satisfied.

In the above sections, we presented the simulation experiments for verifying the theoretical results presented here. The experiments largely validated our results showing that the properties of epidemics revealed in Section 5.3 hold true even for complex network topologies. This confirms

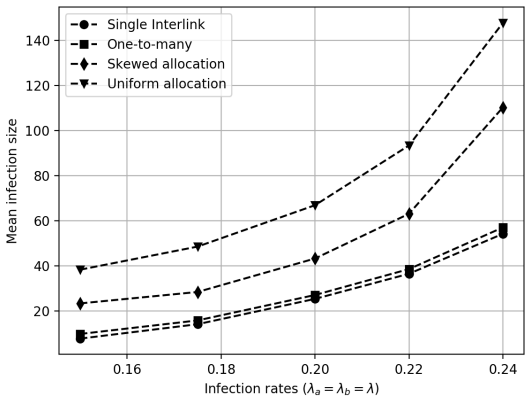

Figure 5.7 Comparison of infection sizes under the following interlinking strategies: i) one-to-one interlinking, ii) one-to-many interlinking, iii) Skewed interlink allocation, and iv) Uniform interlink allocation.

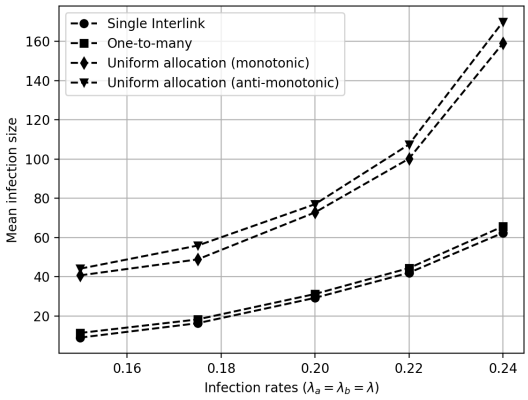

Figure 5.8 Comparison of infection sizes under the following interlinking strategies: i) one-to-one interlinking, ii) one-to-many interlinking, iii) Uniform interlink allocation following monotonic structure, and iv) Uniform interlink allocation following anti-monotonic arrangement.

the fundamental claim of this dissertation that epidemic dynamics on complex networks can be approximated by studying the dynamics on simplistic network topologies based on hubs and inter-relationships. Furthermore, the simulation experiments also showed the comparison among the infection sizes achieved by different interlinking strategies. In particular, we showed that a uniform allocation of interlinks has a significant impact on the infection size, whereas a scrambling of the interlinking structure design shows limited impact as long as the uniform allocation criteria is satisfied.

5.6.4 Case Studies

In this section, we apply the ideas developed here to two real world scenarios involving the design of the interlinking structure in multi-layer networks to achieve a desired infection density in a desired region of the network. The two case studies are chosen to exhibit interlinking structure design under the sufficient and the augmented regimes.

5.6.4.1 Case Study 1

For our first case, we consider the example of promoting inter-disciplinary research among two groups of researchers, representing the isolated network layers. We consider the specific case, where the two network layers represent the collaboration network [Les07] between researchers in the areas of Condensed Matter Physics (G_a) and Astrophysics (G_b), where $|G_a| = 23312$ and $|G_b| = 18872$. An intra-layer link between two nodes i and j indicate that the two researchers (nodes) have co-authored a paper. The infection in this case can be thought of as inter-disciplinary publications, while the inter-layer links can represent funding on inter-disciplinary proposals that will encourage the end-points of the interlinks, i.e. the authors in the respective fields, to publish papers with their intra-layer peers. We should remind the reader at this point that a practical model for this problem would obviously involve much more intricate details and variations than those considered in this dissertation. However, we feel that these case studies are important as they exhibit the diverse application of our dissertation and network science research in general. The network designer can be thought of as a funding agency, which is interested in obtaining a design strategy for allocating funds to specific researchers in a desired region of the network, say in North America ($D_a \cup D_b$), so as to ensure that inter-disciplinary papers continue to get published by researchers in the desired region for a "long" time.

Defining the problem more specifically, the network designer is interested in designing the inter-layer links between $D_a \subset G_a$ and $D_b \subset G_b$ so as to ensure that $\gamma_a = 0.05$ fraction of Condensed Matter Physicists and $\gamma_b = 0.1$ fraction of Astrophysicists continue to remain infected. Let the infection parameters be given by $\boldsymbol{\lambda} = \{0.1, 0.1, 0.2\}$. For our case, the desired regions are specified by the three hop neighborhood around two points $a_{\text{pos}} \in G_a$ and $b_{\text{pos}} \in G_b$. We chose these two points randomly and obtained the desired regions D_a and D_b with sizes 3842 and 2799, respectively. The desired infection densities yield: $\xi^a_{\text{des}} \approx 193$ and $\xi^b_{\text{des}} \approx 280$. The required design of the interlinking structure can be obtained by Algorithm 8 by calling the method ConstructMeta with the required arguments.

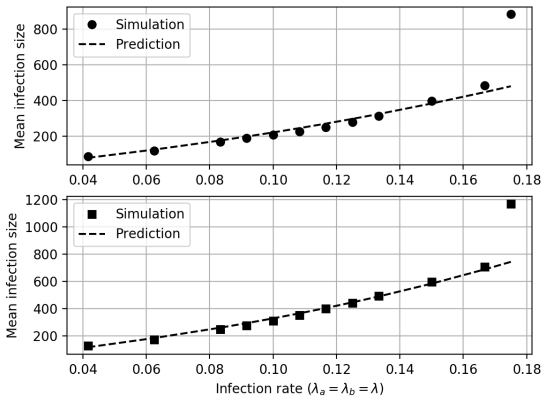

Figure 5.9 Predicted vs simulated infection size in the two network layers, D_a (top) and D_b (bottom), with varying infection propagation rate for Case 1.

Algorithm 8 sequentially grows the metastable infection state by constructing interlinks to hubs from D_a and D_b until the desired infection sizes are achieved. Note that the optimal interlinking structure constituting the metastable infection state is recomputed every time additional hubs are included in the metastable state. This is done to ensure the optimality of the interlinking structure at each intermediate step. The simulation experiments in the previous section revealed that the dependence of the infection size on the design of the interlinking structure is not pronounced as long as the uniform interlink allocation criteria is satisfied. In future extensions of this work, we are exploring the possibility of utilizing this idea to optimize the design of the algorithm so as to update the interlinking structure only in intermediate steps. However, such optimizations are beyond the scope of the current dissertation. For this case, we find out that the desired infection density requirements are satisfied by considering 5 hubs in D_a and 7 hubs in D_b, all of which belong to the core group of hubs in the desired region of the network. Thus, in this case the design of the interlinking structure is quite simple and only 11 $(=5+7-1)$ are required. The interlinking structure is designed by following Algorithm 4. In Fig. 5.9, we plot the average infection size corresponding to the proposed interlinking structure comprising 11 interlinks for different intra-layer infection propagation rates $(\lambda_a = \lambda_b = \lambda)$ and a fixed inter-layer rate $\tilde{\lambda} = 0.2$. The specific infection rate specification for this case is $\boldsymbol{\lambda} = \{0.1, 0.1, 0.2\}$ and the corresponding average infection sizes are $(\xi^a, \xi^b) = (210.2, 311.1)$, which satisfies the infection density requirements. Furthermore, it can be clearly observed from the figure that the theoretically predicted infection sizes agree very well with the simulations for an extended range of λ. This clearly shows that controlled infection spreading has been achieved in the two network layers and the proposed interlinking strategy is able to achieve the infection density requirements.

5.6.4.2 Case Study 2

For our second case, we consider the example of the spread of the COVID-19 disease via face-to-face interaction among two groups of essential workers, say, nurses and delivery workers, where the contact network of the two groups of workers represents the two network layers. We could not find relevant datasets documenting the contact among essential workers and as a proxy, we use the contact data collected in an exhibition at a science gallery [Ise11] as the two network layers, where the data for the first half of the exhibition is taken as G_a, while the remainder of the data is taken as G_b, where $|G_a| = 3046$ and $|G_b| = 4311$. An intra-layer link between agents i and j indicate that they have been in close contact with each other for over 20 seconds. The objective of the network designer is to develop a planning strategy for the interaction of the agents in the two networks. In this dissertation, our objective is to achieve the maximum possible infection size in the desired region of the network using the minimum number of interlinks. For developing planning to prevent disease spreading, a more practical problem would be to maximize the interaction among the two groups of agents while minimizing the spread of the disease. However, the problem of maximizing the infection size using a minimum number of interlinks is also a valid problem as it reveals the extent to which infection can sustain the multi-layer network even when a relatively small number of inter-layer links are constructed in the network.

The values for the desired infection densities in this case are taken as $\gamma_a = 0.1$ and $\gamma_b = 0.2$, whereas the infection spreading rates are taken to be the same as before $\boldsymbol{\lambda} = \{0.1, 0.1, 0.2\}$. Similar to the previous case, the desired region in the network layers are defined with respect to the three hop neighborhoods around two randomly chosen nodes, which yields $|D_a| = 245$ and $|D_b| = 380$. For this case, however, the core and the supplementary group of hubs in D_a and D_b are not sufficient to satisfy the infection density requirements. In particular, the number of hub in the core and the supplementary groups in the two desired region is given by $(\chi_a^0, \chi_a^1) = (3, 5)$ and $(\chi_b^0, \chi_b^1) = (4, 5)$, respectively. Algorithm 8 reveals that an additional 23 interlinks are necessary to augment the composite metastable state to satisfy the density requirements of this problem. In particular, the metastable state formed by the core and the supplementary hub groups have to be augmented with 2 hubs in layer A and 3 hubs in layer B, which require $4, 5, 3, 5$, and 6, inter-layer links, respectively. Although the design of the interlinking structure for this case is considerably more complicated than the previous one, the total number of interlinks used 39, with 16 links interlinking the core and the supplementary group and 23 interlinks in the augmented group, is significantly lower than the total number of interlinks possible $|D_a| \cdot |D_b|$. The simulated infection size corresponding to this interlinking structure is presented in Fig. 5.10 for a varying infection rate. It can be observed that the achievable infection sizes closely follow the theoretical predictions for extended ranges of λ before eventually blowing up in the regime corresponding to global epidemics. These cases clearly exhibit that following the interlinking design proposed here enables us to realize the fundamental objective of this dissertation: a controlled spreading of infection in a desired region of the multi-layer network.

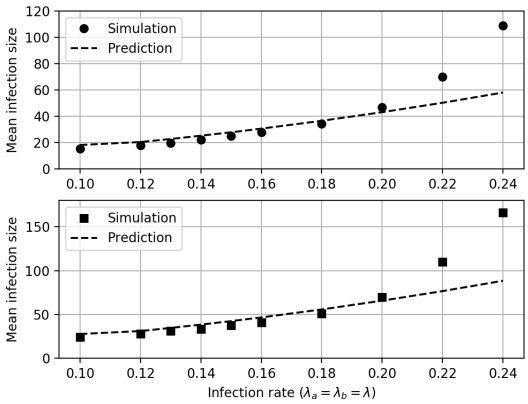

Figure 5.10 Predicted vs simulated infection size in the two network layers, D_a (top) and D_b (bottom), with varying infection propagation rate for Case 2.

5.7 Conclusion

Recent works in probability and statistics [Cha09; Mou13; VH18] as well as network science [Bog13; Fer16] study epidemic dynamics on complex networks by approximating the epidemics on microscopic subgraphs, capturing the network hubs and the inter-relationship among different hubs. In this dissertation, we extend this approach to investigate the properties of epidemic dynamics on multilayer networks. We show that the interlink structure between different isolated network topologies can be designed to sustain metastable infection states in a desired region of the network. Under extended parameter ranges, we show that the density of the infection states can be approximated by considering the epidemic dynamics on the interlink subgraphs. For a known network topology and parameters governing the epidemic dynamics, we can design the interlinking structure to realized a long lasting controlled infection state with a desired infection density, subject to certain feasibility conditions.

To the best of our knowledge, ours is one of the first works investigating the impact of the interlinking structure on epidemic dynamics on multilayer networks. Although the ideas presented here can be applied with certain modifications to single layer networks, we adhere to the multi-layered model since it provides a clean distinction between the existing network (intra-layer topology) and the additional manipulations (inter-layer topology), thereby allowing us to better unravel our contributions. Generalization of the framework to a cost constrained setting or considering cases involving multiple (>2) network layers constitute relatively straightforward extensions of our current work. A fundamental yet crucial idea that is verified through our study is that the dynamics of infection spreading processes on finite multilayer networks can be reliably approximated by investigating the dynamics on subgraphs capturing effectively the first order information about the network topology. An interesting direction of future work which we are currently exploring is to quantify the impact of considering higher order topological information from the network. Such studies will

help us to accurately characterize the error of studying epidemic dynamics on approximate network topologies.

CHAPTER

6

CONCLUSION

Our goal in this dissertation is to develop a better understanding of the propagation of spreading processes through multilayer interdependent networks. The work presented in this dissertation also showcases the enormous impact of the inter-layer link structure on the dynamics of these phenomena.

6.1 Contributions

Under certain conditions, we are able to obtain theoretically optimal interlinking structures to optimize the propagation in multi-layer networks. We show that the practical applications of such theoretically optimal interlinking structures are limited, because these can be derived only when the topology of the network layers follow well-behaved theoretical graph generation models. These graph generation models are undoubtedly vital towards development of a higher level understanding of the network structure and the dynamics of various phenomena over them. However, real world networks can drastically vary in topology in comparison to these theoretical models. Due to this reason, we try to assert the importance of posing network design problems considering arbitrary network topologies through the work presented here. In the general case of arbitrary topologies, the theoretical optimality of the developed interlinking strategies is lost. However, we argue that such sub-optimal strategies provide vital guidelines in developing network design principles which are applicable to real world problems.

An interesting finding of our dissertation is that the optimal interlinking structure for distinct mechanisms of propagation vary widely. This illustrates a key contribution of this dissertation that a universal metric is incapable of measuring the robustness of multi-layer networks against

distinct models of failure spreading processes. We argue against the approach considered by some researchers wherein the optimization of the network structure is performed via optimization of such universal metrics. We show that the network design strategies developed by optimizing universal metrics are not guaranteed to perform well under different mechanisms of spreading processes. Through the work presented in this dissertation, we advocate that network design principles should be dependent on the underlying mechanisms of processes that we are trying to optimize.

In the later stages of our dissertation, we study one of the earliest and classical models of spreading processes on networks: infectious disease spreading through contact networks. The main motivation towards focusing on such simplistic phenomena is to illustrate the wide gaps in the current scientific understanding of propagation processes on networks. Classical research on epidemic spreading on networks have looked at the epidemic dynamics from the point of view of a dichotomy between healthy and infectious phases, where an initial infection in the network either dies down or propagates throughout the network affecting a finite fraction of networks in the steady state. Looking closer at the threshold of this dichotomy reveals rich information about the epidemic dynamics, which a steady state analysis fails to portray. In the regime close to the threshold, we show that an intelligent design of the interlinking structure allows us to *control* the spread of phenomena.

6.2 Future directions of research

A fascinating feature of the work presented in this dissertation is that as we dove deeper into the study of phenomena propagation in multi-layer networks, we progressively shifted our focus to simpler models. This is due to the fact that there are a plethora of unexplored territories in research on network science and we strongly believe that the scientific community is far from developing a deep understanding of this area. Network science research in many ways is in its nascent stages. We expect that the work presented in this dissertation clearly illustrates the fact that our research constitutes the initial steps towards the solution of the different problems and significant advances can be made in each of them.

Due to these reasons, we envisage several directions in which the work presented here can be extended. Posing the network design problem in a truly multi-layer setting is an interesting avenue; most of the work presented here consider two network layers and designs the inter-linking strategies among these layers. We expect that a more sophisticated modeling of the interlink construction cost, to emulate real-world constraints, will greatly enhance the applicability of the proposed network design guidelines to real-world problems. Incorporation of geographic constraints in the interlink construction problem, modeling the propensity of individual nodes to accept a change in their neighborhood topology, among many others, are important steps in that direction. Another important avenue of future directions of work is to consider a pre-existing interlinking structure in the network and developing strategies to modify the structure to yield desired effects. For all the problems considered in this dissertation, we pose the problem from the perspective of designing from scratch. It should not be difficult to see that such an assumption is rarely expected to hold in

practice.

Although the analysis presented in this work imposes several constraints on the network structure for some cases and approximations on the mechanism of propagation for others, we feel that our results would still enable researchers to gain a better understanding of spreading processes on multi-layer interdependent networks. Furthermore, the interlink optimization principles developed in this work can aid network practitioners to design better multilayer networks from the perspective of controlling various spreading processes on these networks. We hope that our work will motivate further research in the burgeoning area of multi-layer network science.

BIBLIOGRAPHY

[Alb02] Albert, R. & Barabási, A.-L. "Statistical mechanics of complex networks". *Reviews of modern physics* **74**.1 (2002), p. 47.

[Arr17] Arruda, G. F. de, Cozzo, E., Peixoto, T. P., Rodrigues, F. A. & Moreno, Y. "Disease localization in multilayer networks". *Physical Review X* **7**.1 (2017), p. 011014.

[Ber05] Berger, N., Borgs, C., Chayes, J. T. & Saberi, A. "On the spread of viruses on the internet". *Soda*. Vol. 5. 2005, pp. 301–310.

[Bog13] Boguná, M., Castellano, C. & Pastor-Satorras, R. "Nature of the epidemic threshold for the susceptible infected susceptible dynamics in networks". *Physical review letters* **111**.6 (2013), p. 068701.

[Bov14] Bovenkamp, R. van de & Van Mieghem, P. "Time to metastable state in SIS epidemics on graphs". *2014 Tenth International Conference on Signal-Image Technology and Internet-Based Systems*. IEEE. 2014, pp. 347–354.

[Boy04] Boyd, S. & Vandenberghe, L. *Convex optimization*. Cambridge university press, 2004.

[Bra07] Braunstein, L. A., Wu, Z., Chen, Y., Buldyrev, S. V., Kalisky, T., Sreenivasan, S., Cohen, R., Lopez, E., Havlin, S. & Stanley, H. E. "Optimal path and minimal spanning trees in random weighted networks". *International Journal of Bifurcation and Chaos* **17**.07 (2007), pp. 2215–2255.

[Bru12] Brummitt, C. D., D'Souza, R. M. & Leicht, E. A. "Suppressing cascades of load in interdependent networks". *Proceedings of the National Academy of Sciences* **109**.12 (2012), E680–E689.

[Bul10] Buldyrev, S. V., Parshani, R., Paul, G., Stanley, H. E. & Havlin, S. "Catastrophic cascade of failures in interdependent networks". *Nature* **464**.7291 (2010), pp. 1025–1028.

[Buz06] Buzna, L., Peters, K. & Helbing, D. "Modelling the dynamics of disaster spreading in networks". *Physica A: Statistical Mechanics and its Applications* **363**.1 (2006), pp. 132–140.

[Cal00] Callaway, D. S., Newman, M. E., Strogatz, S. H. & Watts, D. J. "Network robustness and fragility: Percolation on random graphs". *Physical review letters* **85**.25 (2000), p. 5468.

[Cas10] Castellano, C. & Pastor-Satorras, R. "Thresholds for epidemic spreading in networks". *Physical review letters* **105**.21 (2010), p. 218701.

[Cat13] Cator, E. & Van Mieghem, P. "Susceptible-infected-susceptible epidemics on the complete graph and the star graph: Exact analysis". *Physical Review E* **87**.1 (2013), p. 012811.

[Cha16] Chan, H. & Akoglu, L. "Optimizing network robustness by edge rewiring: a general framework". *Data Mining and Knowledge Discovery* **30**.5 (2016), pp. 1395–1425.

[Cha09] Chatterjee, S., Durrett, R., et al. “Contact processes on random graphs with power law degree distributions have critical value 0”. *The Annals of Probability* **37**.6 (2009), pp. 2332–2356.

[Cha17] Chattopadhyay, S., Dai, H., Hosseinalipour, S. & Eun, D. Y. “Designing Optimal Interlink Patterns to Maximize Robustness of Interdependent Networks against Cascading Failures”. *IEEE Transactions on Communications* (2017).

[Che15] Chen, Z., Du, W.-B., Cao, X.-B. & Zhou, X.-L. “Cascading failure of interdependent networks with different coupling preference under targeted attack”. *Chaos, Solitons & Fractals* **80** (2015), pp. 7–12.

[Col07] Colizza, V., Pastor-Satorras, R. & Vespignani, A. “Reaction–diffusion processes and metapopulation models in heterogeneous networks”. *Nature Physics* **3**.4 (2007), p. 276.

[Cun15] Cunha, B. R. da, González-Avella, J. C. & Gonçalves, S. “Fast fragmentation of networks using module-based attacks”. *PloS one* **10**.11 (2015), e0142824.

[Dur10] Durrett, R. “Some features of the spread of epidemics and information on a random graph”. *Proceedings of the National Academy of Sciences* **107**.10 (2010), pp. 4491–4498.

[Edw01] Edwards, H. M. *Riemann's zeta function*. Vol. 58. Courier Corporation, 2001.

[Fer16] Ferreira, S. C., Sander, R. S. & Pastor-Satorras, R. “Collective versus hub activation of epidemic phases on networks”. *Physical Review E* **93**.3 (2016), p. 032314.

[Gan05] Ganesh, A., Massoulié, L. & Towsley, D. “The effect of network topology on the spread of epidemics”. *Proceedings IEEE 24th Annual Joint Conference of the IEEE Computer and Communications Societies.* Vol. 2. IEEE. 2005, pp. 1455–1466.

[Gho06] Ghosh, A. & Boyd, S. “Growing well-connected graphs”. *Decision and Control, 2006 45th IEEE Conference on*. IEEE. 2006, pp. 6605–6611.

[Gil77] Gillespie, D. T. “Exact stochastic simulation of coupled chemical reactions”. *The journal of physical chemistry* **81**.25 (1977), pp. 2340–2361.

[Gol12] Goltsev, A. V., Dorogovtsev, S. N., Oliveira, J. G. & Mendes, J. F. “Localization and spreading of diseases in complex networks”. *Physical review letters* **109**.12 (2012), p. 128702.

[Har52] Hardy, G. H., Littlewood, J. E. & Pólya, G. *Inequalities*. Cambridge university press, 1952.

[Hon15] Hong, S., Wang, B., Ma, X., Wang, J. & Zhao, T. “Failure cascade in interdependent network with traffic loads”. *Journal of Physics A: Mathematical and Theoretical* **48**.48 (2015), p. 485101.

[Hua11] Huang, X., Gao, J., Buldyrev, S. V., Havlin, S. & Stanley, H. E. “Robustness of interdependent networks under targeted attack”. *Physical Review E* **83**.6 (2011), p. 065101.

[Hua13a] Huang, X., Vodenska, I., Havlin, S. & Stanley, H. E. “Cascading failures in bi-partite graphs: model for systemic risk propagation”. *Scientific reports* **3** (2013).

[Hua13b] Huang, Z., Wang, C., Stojmenovic, M. & Nayak, A. “Balancing system survivability and cost of smart grid via modeling cascading failures”. *IEEE Transactions on Emerging Topics in Computing* **1**.1 (2013), pp. 45–56.

[Ise11] Isella, L., Stehlé, J., Barrat, A., Cattuto, C., Pinton, J.-F. & Broeck, W. Van den. “What’s in a crowd? Analysis of face-to-face behavioral networks”. *Journal of theoretical biology* **271**.1 (2011), pp. 166–180.

[Jam07] Jamakovic, A & Uhlig, S. “On the relationship between the algebraic connectivity and graph’s robustness to node and link failures”. *Next Generation Internet Networks, 3rd EuroNGI Conference on*. IEEE. 2007, pp. 96–102.

[Lee13] Lee, H. K., Shim, P.-S. & Noh, J. D. “Epidemic threshold of the susceptible-infected-susceptible model on complex networks”. *Physical Review E* **87**.6 (2013), p. 062812.

[Les07] Leskovec, J., Kleinberg, J. & Faloutsos, C. “Graph evolution: Densification and shrinking diameters”. *ACM Transactions on Knowledge Discovery from Data (TKDD)* **1**.1 (2007), p. 2.

[Liu11] Liu, D. & Chen, X. “Rumor propagation in online social networks like twitter–a simulation study”. *2011 Third International Conference on Multimedia Information Networking and Security*. IEEE. 2011, pp. 278–282.

[Liu18] Liu, Q. & Van Mieghem, P. “Network localization is unalterable by infections in bursts”. *IEEE Transactions on Network Science and Engineering* **6**.4 (2018), pp. 983–989.

[Lv17] Lv, D., Eslami, A. & Cui, S. “Load-Dependent Cascading Failures in Finite-Size Erdös-Rényi Random Networks”. *IEEE Transactions on Network Science and Engineering* (2017).

[Mat14] Mata, A. S., Ferreira, R. S. & Ferreira, S. C. “Heterogeneous pair-approximation for the contact process on complex networks”. *New Journal of Physics* **16**.5 (2014), p. 053006.

[Men16] Meng, D., Fazel, M. & Mesbahi, M. “Online algorithms for network formation”. *Decision and Control (CDC), 2016 IEEE 55th Conference on*. IEEE. 2016, pp. 135–140.

[Min14a] Min, B., Do Yi, S., Lee, K.-M. & Goh, K.-I. “Network robustness of multiplex networks with interlayer degree correlations”. *Physical Review E* **89**.4 (2014), p. 042811.

[Min14b] Min, B., Do Yi, S., Lee, K.-M. & Goh, K.-I. “Network robustness of multiplex networks with interlayer degree correlations”. *Physical Review E* **89**.4 (2014), p. 042811.

[Mou16a] Mountford, T., Mourrat, J.-C., Valesin, D. & Yao, Q. “Exponential extinction time of the contact process on finite graphs”. *Stochastic Processes and their Applications* **126**.7 (2016), pp. 1974–2013.

[Mou13] Mountford, T., Valesin, D., Yao, Q., et al. “Metastable densities for the contact process on power law random graphs”. *Electronic Journal of Probability* **18** (2013).

[Mou16b] Mourrat, J.-C., Valesin, D., et al. “Phase transition of the contact process on random regular graphs”. *Electronic Journal of Probability* **21** (2016).

[New18] Newman, M. *Networks*. Oxford university press, 2018.

[Ops11] Opsahl, T. “Why anchorage is not (that) important: Binary ties and sample selection”. *http://toreopsahl.com/2011/08/12/why-anchorage-is-not-that-important-binary-ties-and-sample-selection (accessed September 2013)* (2011).

[Oro10] Orosz, G., Wilson, R. E. & Stépán, G. *Traffic jams: dynamics and control*. 2010.

[Owe] Owen, G. *Game theory. 1995*.

[Par13] Parandehgheibi, M. & Modiano, E. “Robustness of interdependent networks: The case of communication networks and the power grid”. *Global Communications Conference (GLOBECOM), 2013 IEEE*. IEEE. 2013, pp. 2164–2169.

[PS01] Pastor-Satorras, R. & Vespignani, A. “Epidemic dynamics and endemic states in complex networks”. *Physical Review E* **63**.6 (2001), p. 066117.

[Pea92] Peajcariaac, J. E. & Tong, Y. L. *Convex functions, partial orderings, and statistical applications*. Academic Press, 1992.

[Pen15] Peng, X., Yao, H., Du, J., Wang, Z. & Ding, C. “Load-induced cascading failures in interconnected networks”. *Nonlinear Dynamics* **82**.1-2 (2015), pp. 97–105.

[Rad16] Radicchi, F. & Castellano, C. “Beyond the locally treelike approximation for percolation on real networks”. *Physical Review E* **93**.3 (2016), p. 030302.

[Ran11] Ranjan, G. & Zhang, Z.-L. “How to glue a robust smart-grid?: a finite-network theory for interdependent network robustness”. *Proceedings of the Seventh Annual Workshop on Cyber Security and Information Intelligence Research*. ACM. 2011, p. 22.

[Rue16] Rueda, D. F., Calle, E., Maldonado-Lopez, F. A. & Donoso, Y. “Reducing the impact of targeted attacks in interdependent telecommunication networks”. *Telecommunications (ICT), 2016 23rd International Conference on*. IEEE. 2016, pp. 1–5.

[SM12] Saumell-Mendiola, A., Serrano, M. Á. & Boguná, M. “Epidemic spreading on interconnected networks”. *Physical Review E* **86**.2 (2012), p. 026106.

[Sch13] Schneider, C. M., Yazdani, N., Araújo, N. A., Havlin, S. & Herrmann, H. J. “Towards designing robust coupled networks”. *Scientific reports* **3** (2013).

[Sch85] Schonmann, R. H. “Metastability for the contact process”. *Journal of statistical physics* **41**.3 (1985), pp. 445–464.

[Sha16] Shakeri, H., Albin, N., Sahneh, F. D., Poggi-Corradini, P. & Scoglio, C. “Maximizing algebraic connectivity in interconnected networks”. *Physical Review E* **93**.3 (2016), p. 030301.

[Sha10] Shao, J., Buldyrev, S. V., Havlin, S. & Stanley, H. E. "Cascade of failures in coupled network systems with multiple support-dependent relations". *arXiv preprint arXiv:1011.0234* (2010).

[She18] Sherborne, N., Miller, J. C., Blyuss, K. B. & Kiss, I. Z. "Mean-field models for non-Markovian epidemics on networks". *Journal of mathematical biology* **76**.3 (2018), pp. 755–778.

[Tan13] Tan, F., Xia, Y., Zhang, W. & Jin, X. "Cascading failures of loads in interconnected networks under intentional attack". *EPL (Europhysics Letters)* **102**.2 (2013), p. 28009.

[Val13] Valdez, L., Macri, P., Stanley, H. & Braunstein, L. "Triple point in correlated interdependent networks". *Physical Review E* **88**.5 (2013), p. 050803.

[VH18] VAN HAO, C. "Super-exponential extinction time of the contact process on random geometric graphs". *Combinatorics, Probability and Computing* **27**.2 (2018), pp. 162–185.

[VM08] Van Mieghem, P., Omic, J. & Kooij, R. "Virus spread in networks". *IEEE/ACM Transactions On Networking* **17**.1 (2008), pp. 1–14.

[Vid11] Vidal, M., Cusick, M. E. & Barabási, A.-L. "Interactome networks and human disease". *Cell* **144**.6 (2011), pp. 986–998.

[Wat98] Watts, D. J. & Strogatz, S. H. "Collective dynamics of 'small-world'networks". *nature* **393**.6684 (1998), p. 440.

[Wei17] Wei, Z.-W., Liao, H., Zhang, H.-F., Xie, J.-R., Wang, B.-H. & Chen, G.-L. "Localized endemic state transition in the SIS model on networks". *arXiv preprint arXiv:1704.02925* (2017).

[Wu18] Wu, Q. & Hadzibeganovic, T. "Pair quenched mean-field approach to epidemic spreading in multiplex networks". *Applied Mathematical Modelling* **60** (2018), pp. 244–254.

[Yag12] Yagan, O., Qian, D., Zhang, J. & Cochran, D. "Optimal allocation of interconnecting links in cyber-physical systems: Interdependence, cascading failures, and robustness". *IEEE Transactions on Parallel and Distributed Systems* **23**.9 (2012), pp. 1708–1720.

[Yağ12] Yağan, O., Qian, D., Zhang, J. & Cochran, D. "Optimal allocation of interconnecting links in cyber-physical systems: Interdependence, cascading failures, and robustness". *Parallel and Distributed Systems, IEEE Transactions on* **23**.9 (2012), pp. 1708–1720.

[Zav11] Zavlanos, M. M., Egerstedt, M. B. & Pappas, G. J. "Graph-theoretic connectivity control of mobile robot networks". *Proceedings of the IEEE* **99**.9 (2011), pp. 1525–1540.

[Zha18] Zhang, J. & Modiano, E. "Connectivity in Interdependent Networks". *IEEE/ACM Transactions on Networking* **26**.5 (2018), pp. 2090–2103.

[Zha17] Zhang, Y., Arenas, A. & Yağan, O. "Cascading failures in interdependent systems under a flow redistribution model". *arXiv preprint arXiv:1709.01651* (2017).

[Zhe18] Zheng, M., Wang, W., Tang, M., Zhou, J., Boccaletti, S & Liu, Z. “Multiple peaks patterns of epidemic spreading in multi-layer networks”. *Chaos, Solitons & Fractals* **107** (2018), pp. 135–142.

[Zhe17] Zheng, Y., Zhao, S., Liu, Y., Li, Y., Tan, Q. & Xin, N. “Weighted Algebraic Connectivity Maximization for Optical Satellite Networks”. *IEEE Access* **5** (2017), pp. 6885–6893.